

Coherent Imaging Methods with XFELs

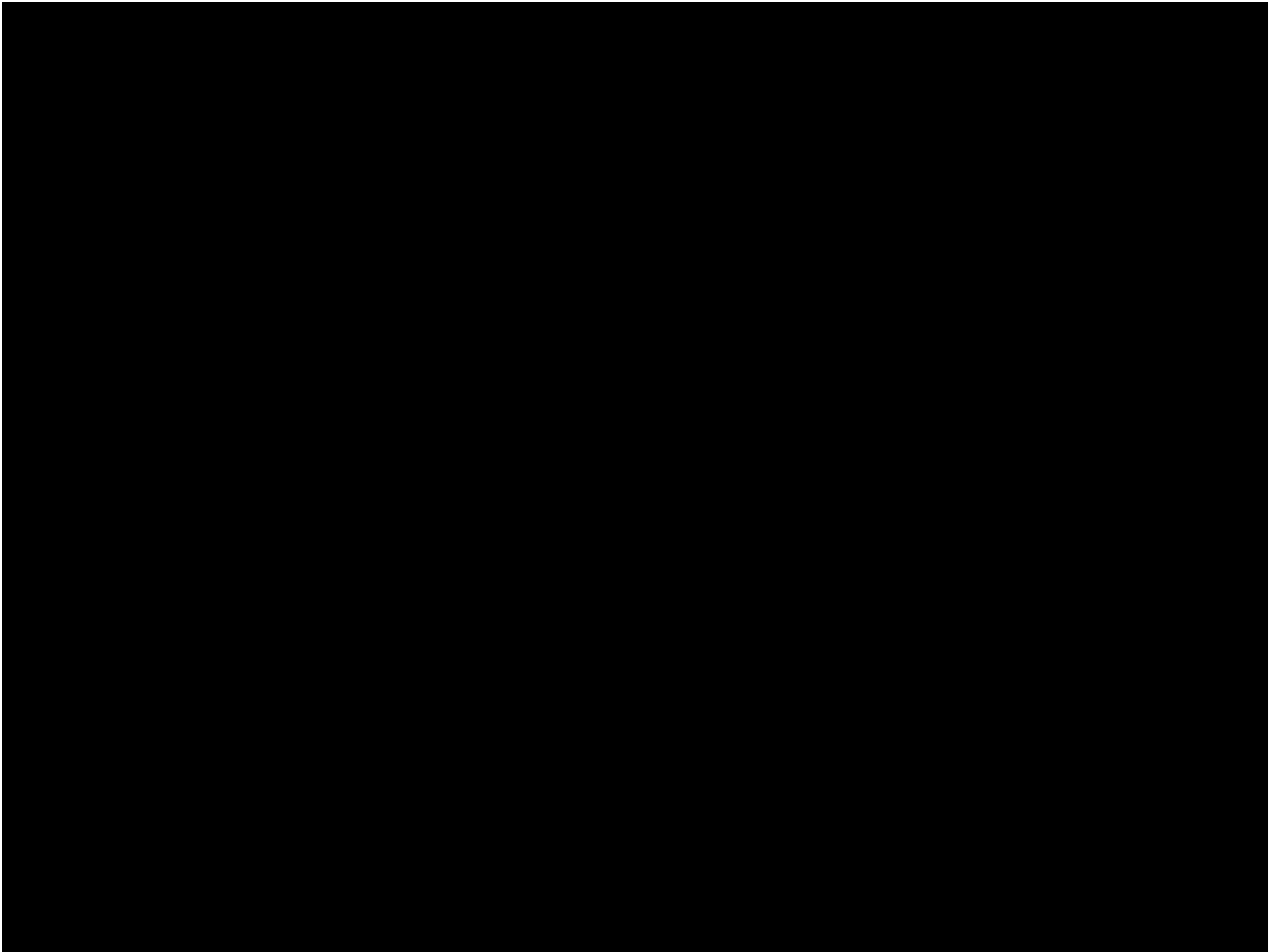
- Ian Robinson
- Loren Beitra
- Moyu Watari
- Ross Harder
- Marcus Newton
- Richard Bean
- Nicolas Burdet
- Xiaowen Shi
- Felisa Berenguer
- Fucai Zhang
- Jesse Clark

London Centre for Nanotechnology
University College, London
Brookhaven National Lab

School on X-ray and Neutron
Diffraction Techniques
Ghent, May 2018

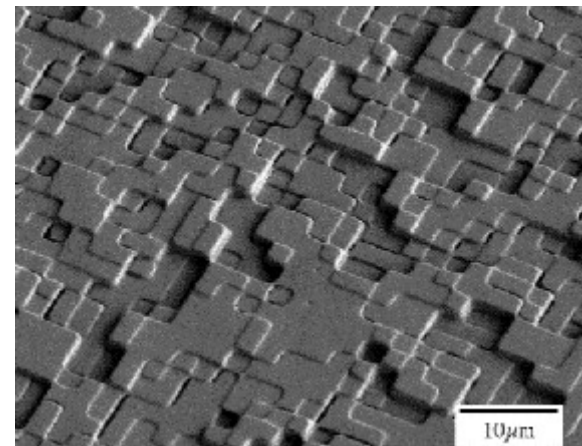
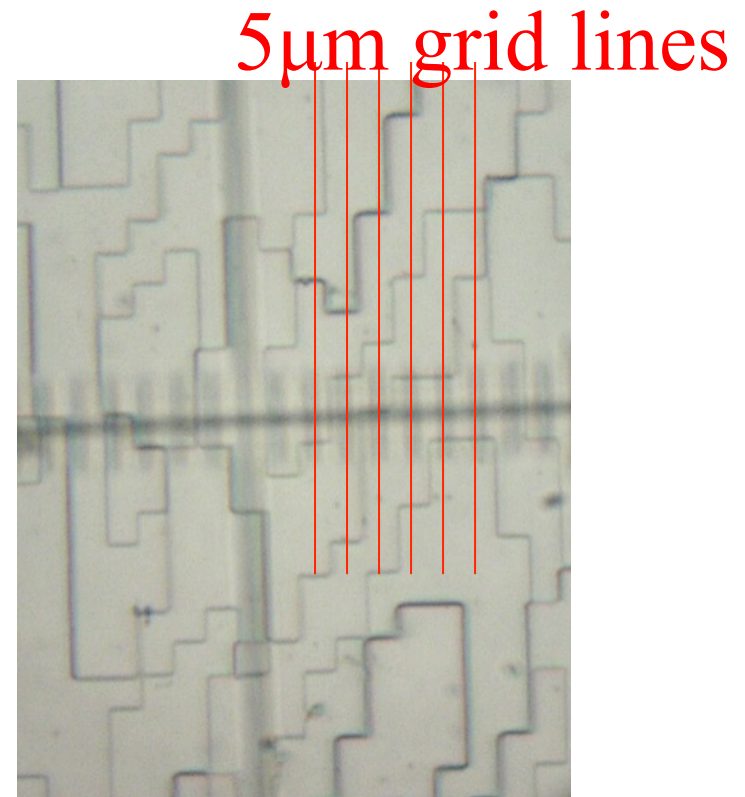
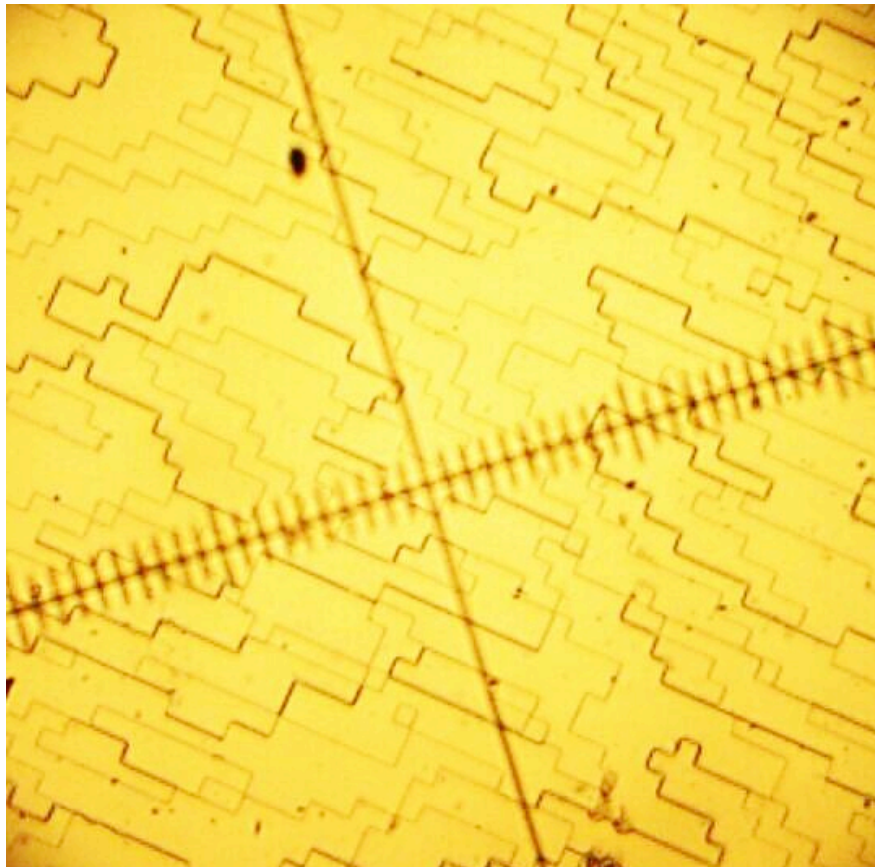
Coherent X-ray Scattering

- I. Coherence
- II. Measuring Coherence
- III. Coherent Imaging Modes
- IV. Ptychography
- V. Experimental methods

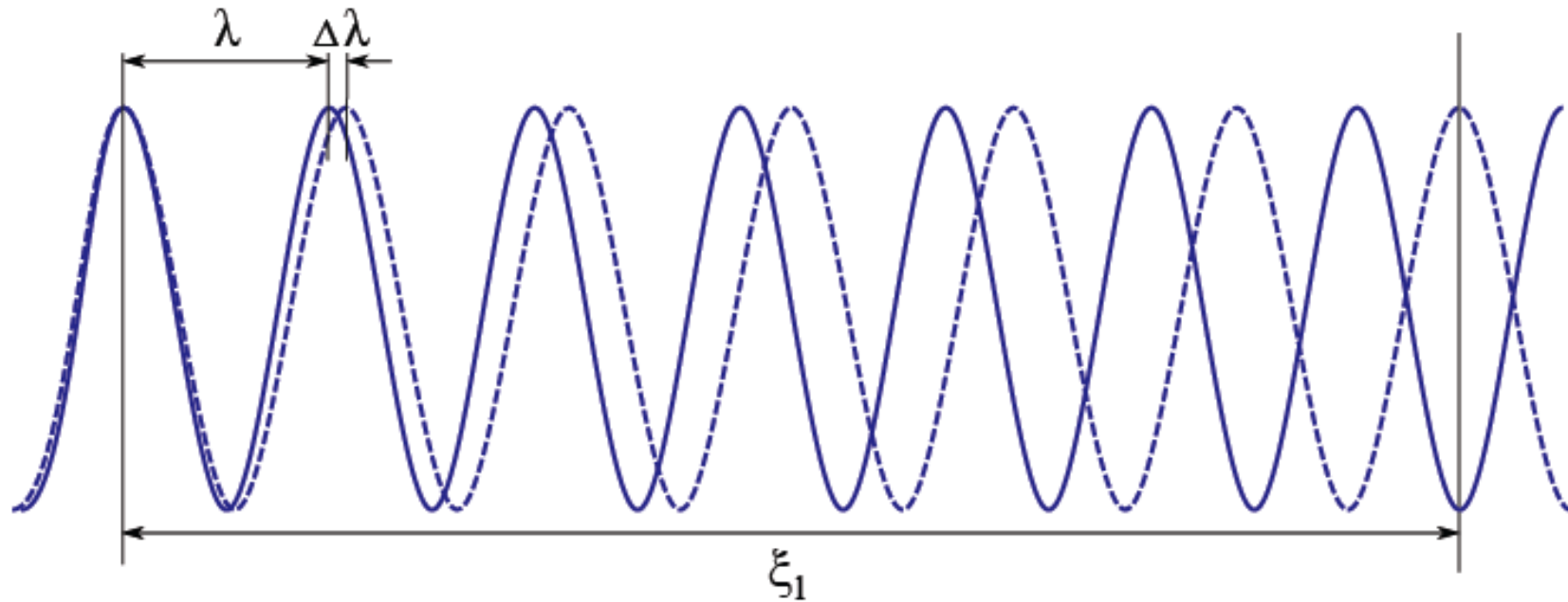


Microscope Images of Gratings

Digital Optics Corp: phase grating

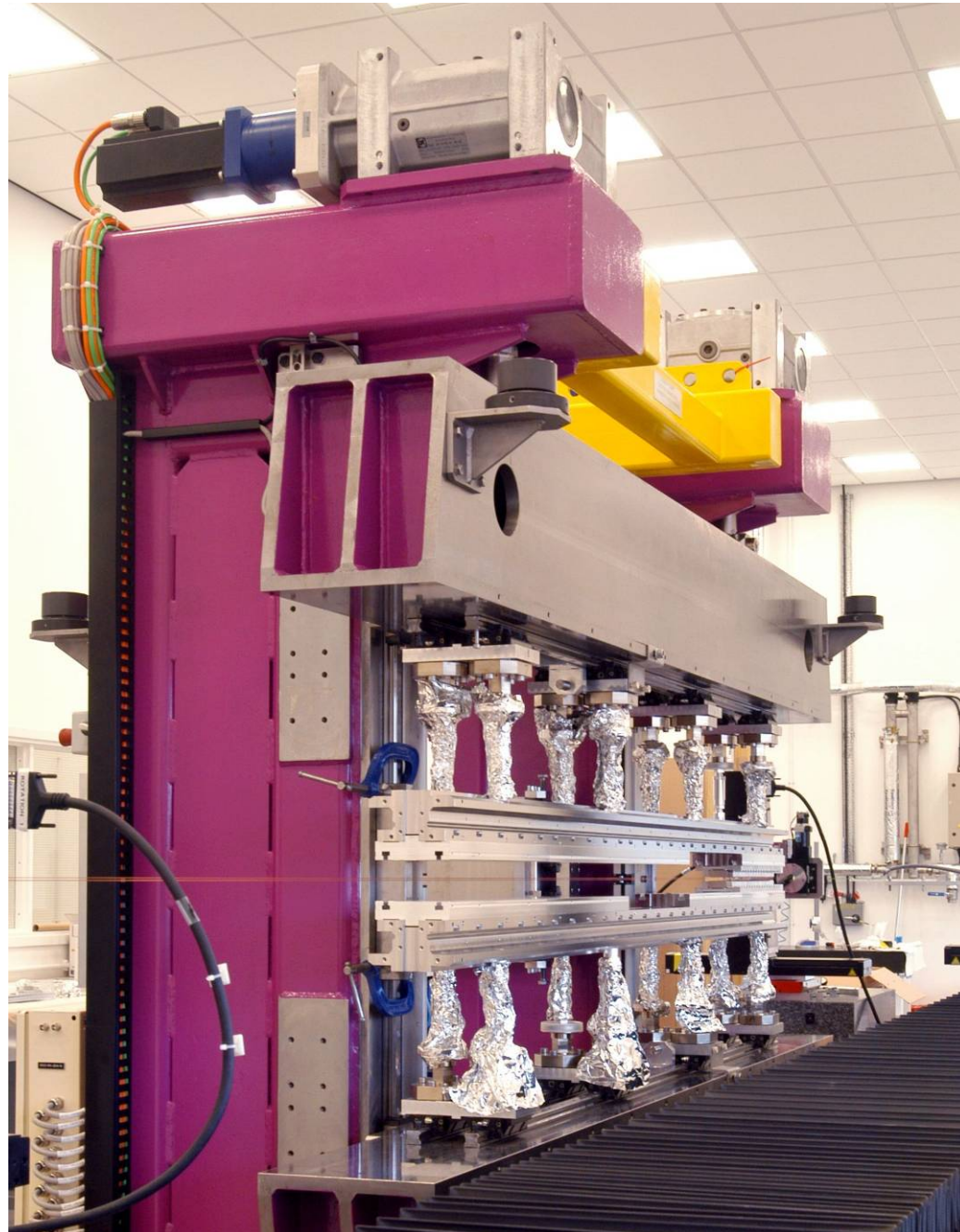


Longitudinal Coherence



$$\xi_L = \frac{1}{2} \frac{\lambda^2}{\Delta\lambda}$$

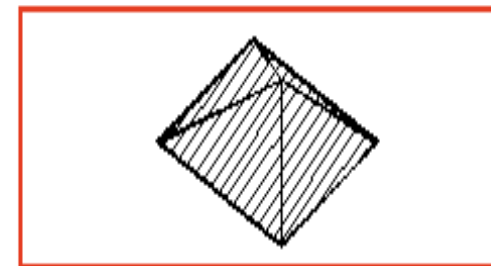
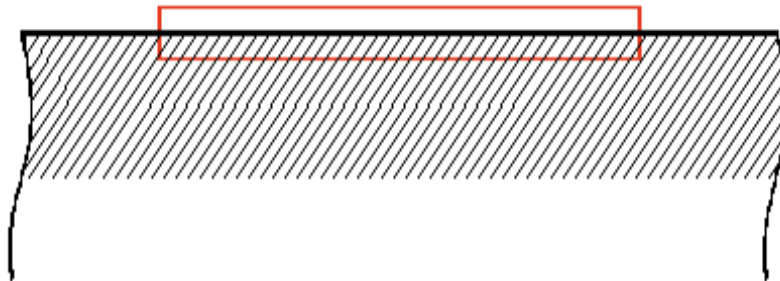
Diamond
in-vacuum
X-ray
Undulator



Coherence at 3rd Generation (undulator) Synchrotron Sources

Coherence of	ξ_{VER}	ξ_{HORIZ}	ξ_{LONG}	Flux
Raw Undulator	$35\mu\text{m}$	$9\mu\text{m}$	$0.004\mu\text{m}$	2×10^{12}
Si(111) Monochromator	$35\mu\text{m}$	$9\mu\text{m}$	$1\mu\text{m}$	1×10^{10}
C(111) Monochromator	$35\mu\text{m}$	$9\mu\text{m}$	$3\mu\text{m}$	3×10^9

Coherent region defined by slits

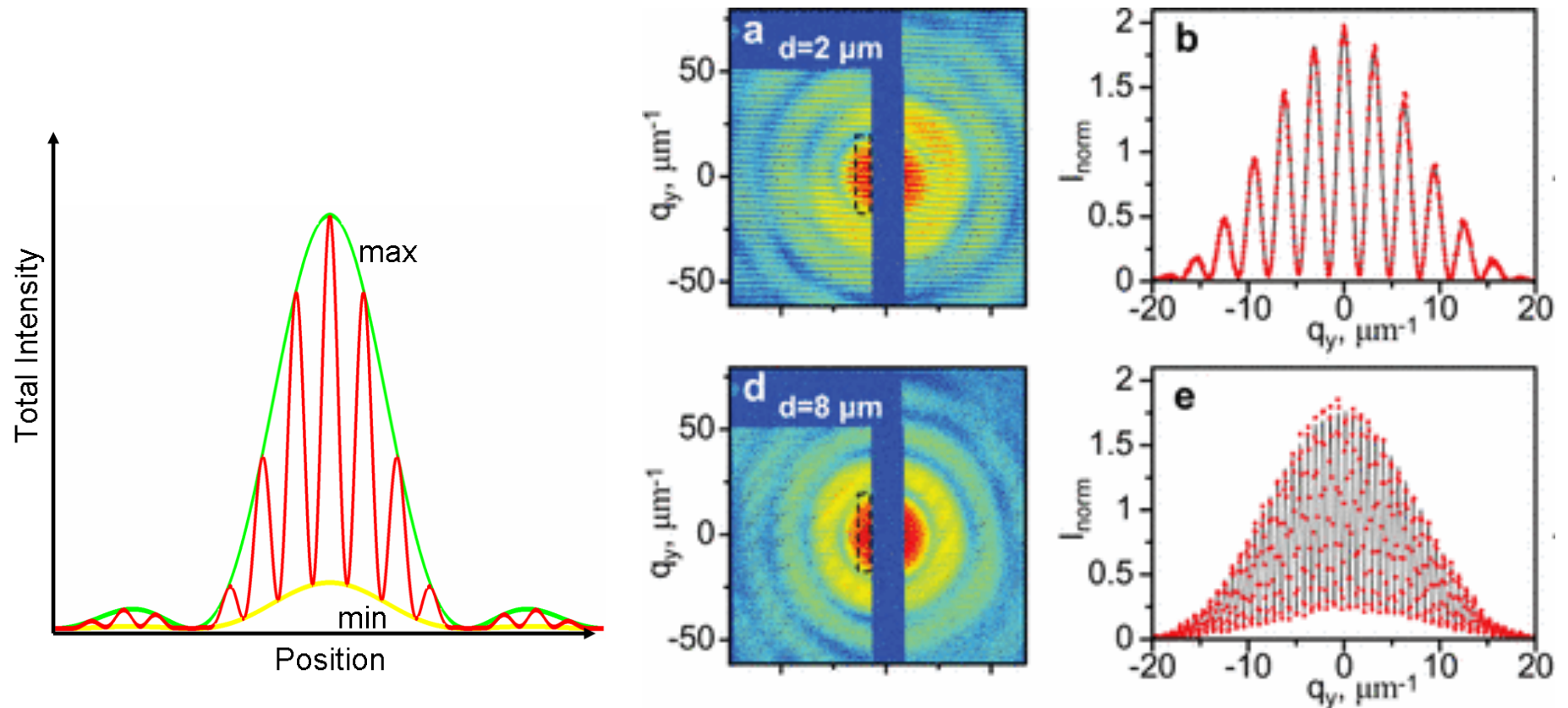


Coherent X-ray Scattering

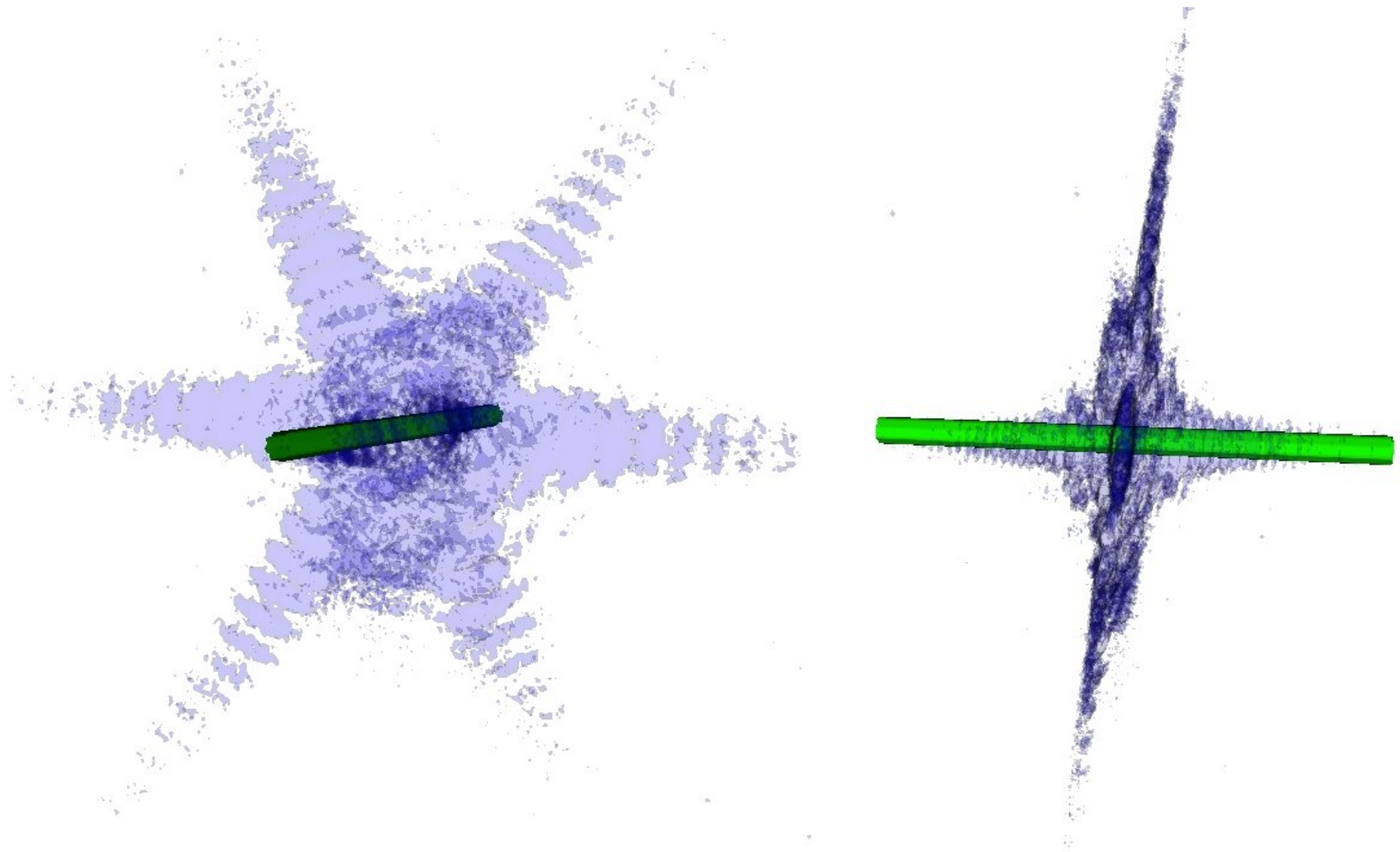
- I. Coherence
- II. Measuring Coherence**
- III. Coherent Imaging Modes
- IV. Ptychography
- V. Experimental methods

Fringe Visibility measures Coherence

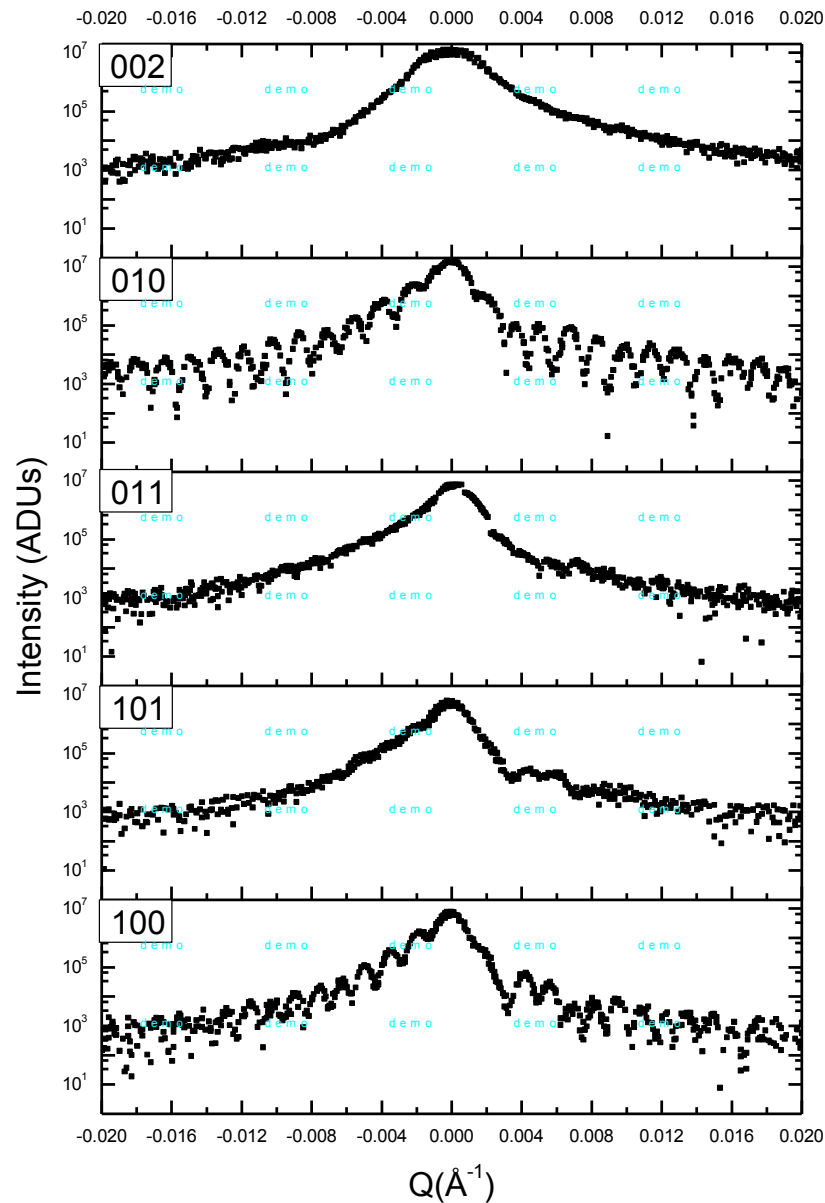
Coherence Properties of ... XFEL, I. A. Vartanyants et al PRL 107 144801 (2011)



How to extract the contrast data



Five Bragg peaks



002 no fringe visibility

010 & 100 good fringe visibility

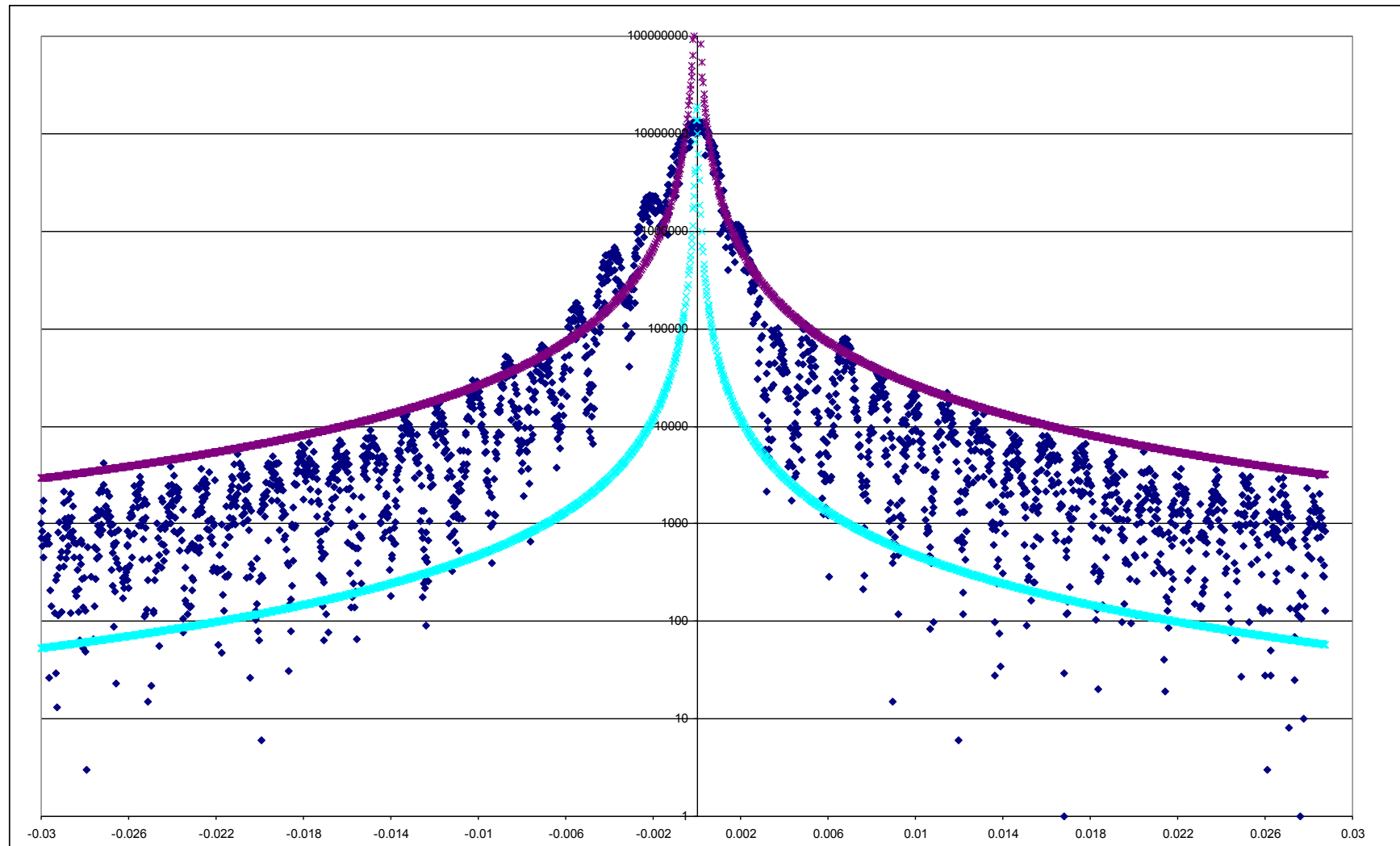
101 & 011 diminished fringe visibility
but fringes still evident

010:011 & 101:100
show complementary fringes
but not between each other

Error in coordinate transform ruled out

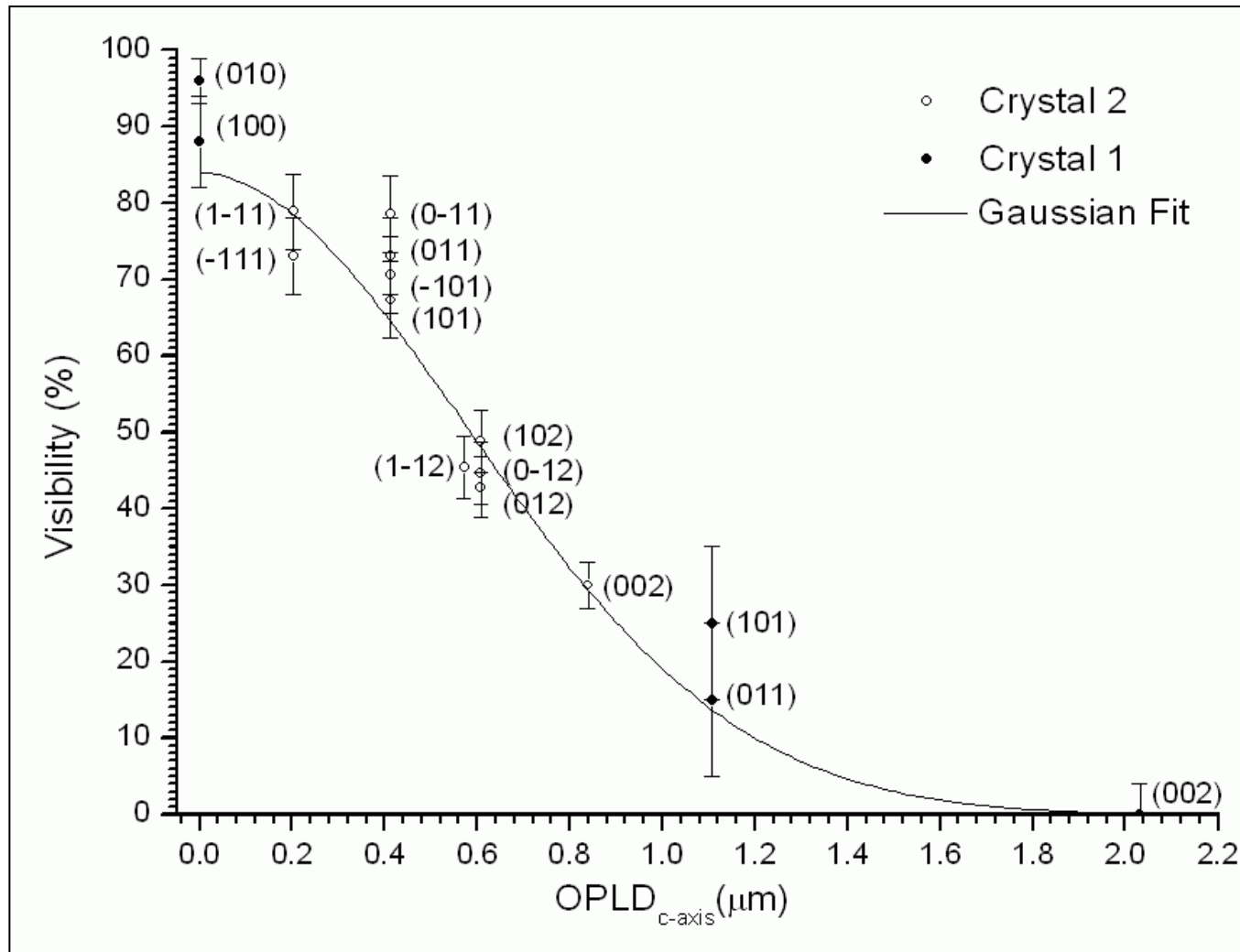
010 and 100 reflections fringe spacing
difference $\sim 20\%$

Fringe Visibility $96 \pm 2\%$ @010



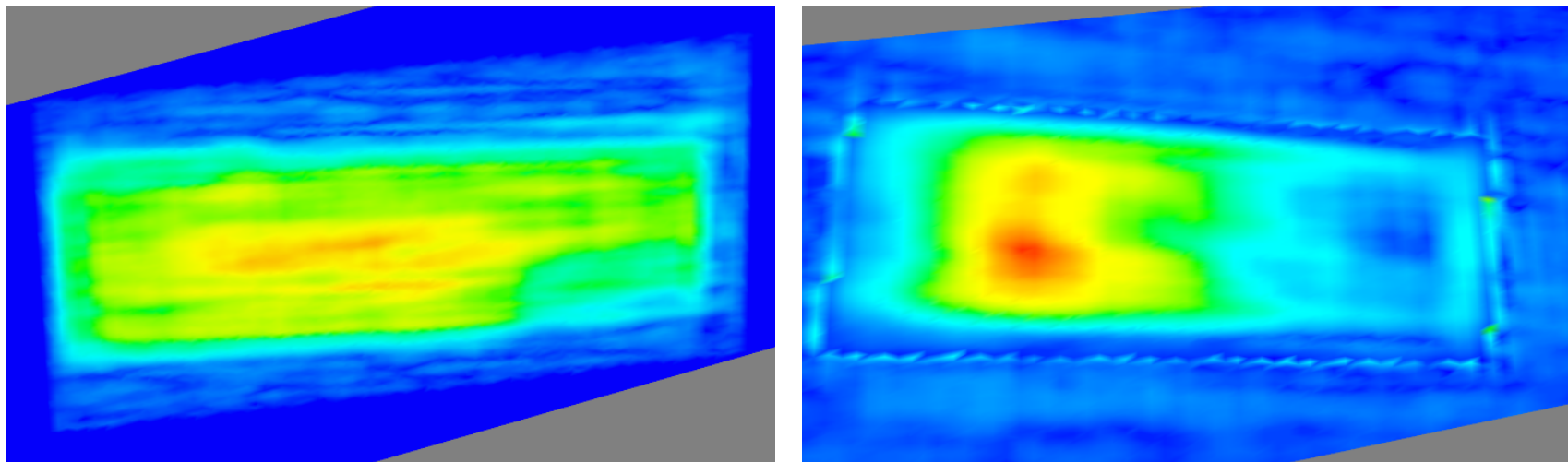
Measured Longitudinal Coherence

Steven Leake et al, Optics Express 17 15853 (2009)



Density Section of Reconstruction using 100 and 101 reflections

“hot spot” more developed for limited coherence
Steven Leake et al, Optics Express 17 15853 (2009)



Vary transverse coherence

using horizontal entrance slit settings

$12\mu m$

High coherence



Assuming perfect
coherence

$50\mu m$

Low coherence

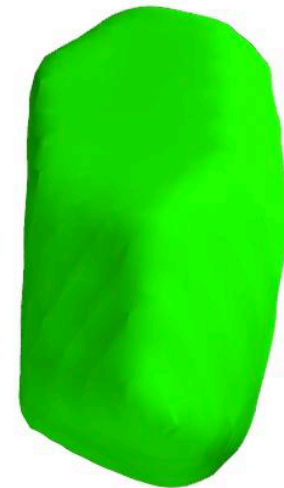


Assuming perfect
coherence

I. K. Robinson, Ghent 2018

$50\mu m$

Low coherence



Correcting for partial
coherence

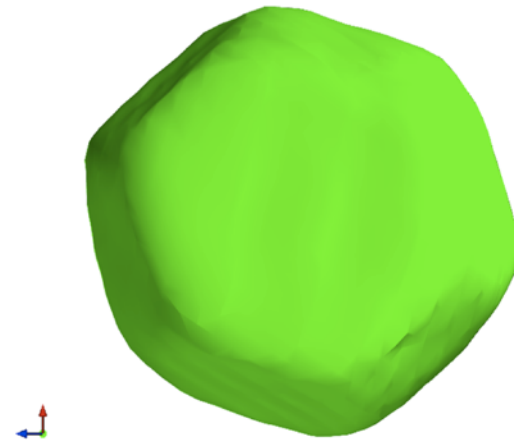
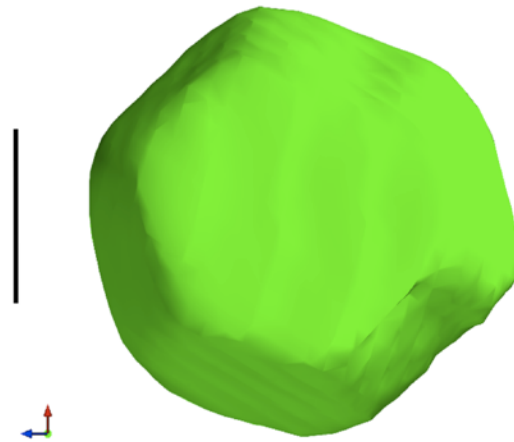
Top view of crystal

Jesse Clark et al, Nature Comms, 3 993 (2012)

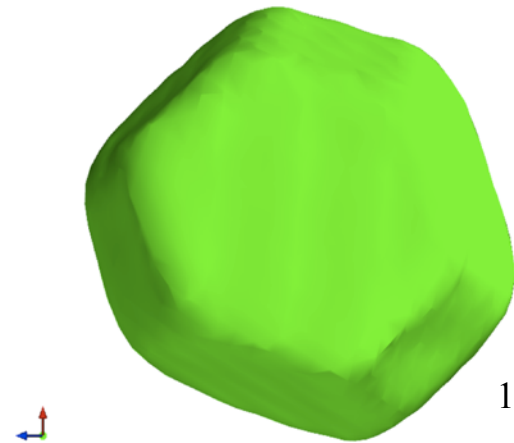
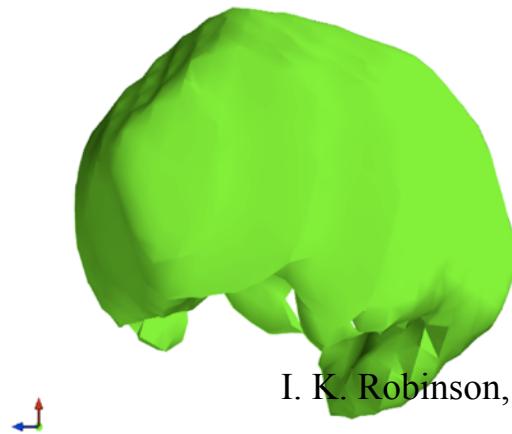
Assuming full
coherence

Correcting for partial
coherence

'High' coherence

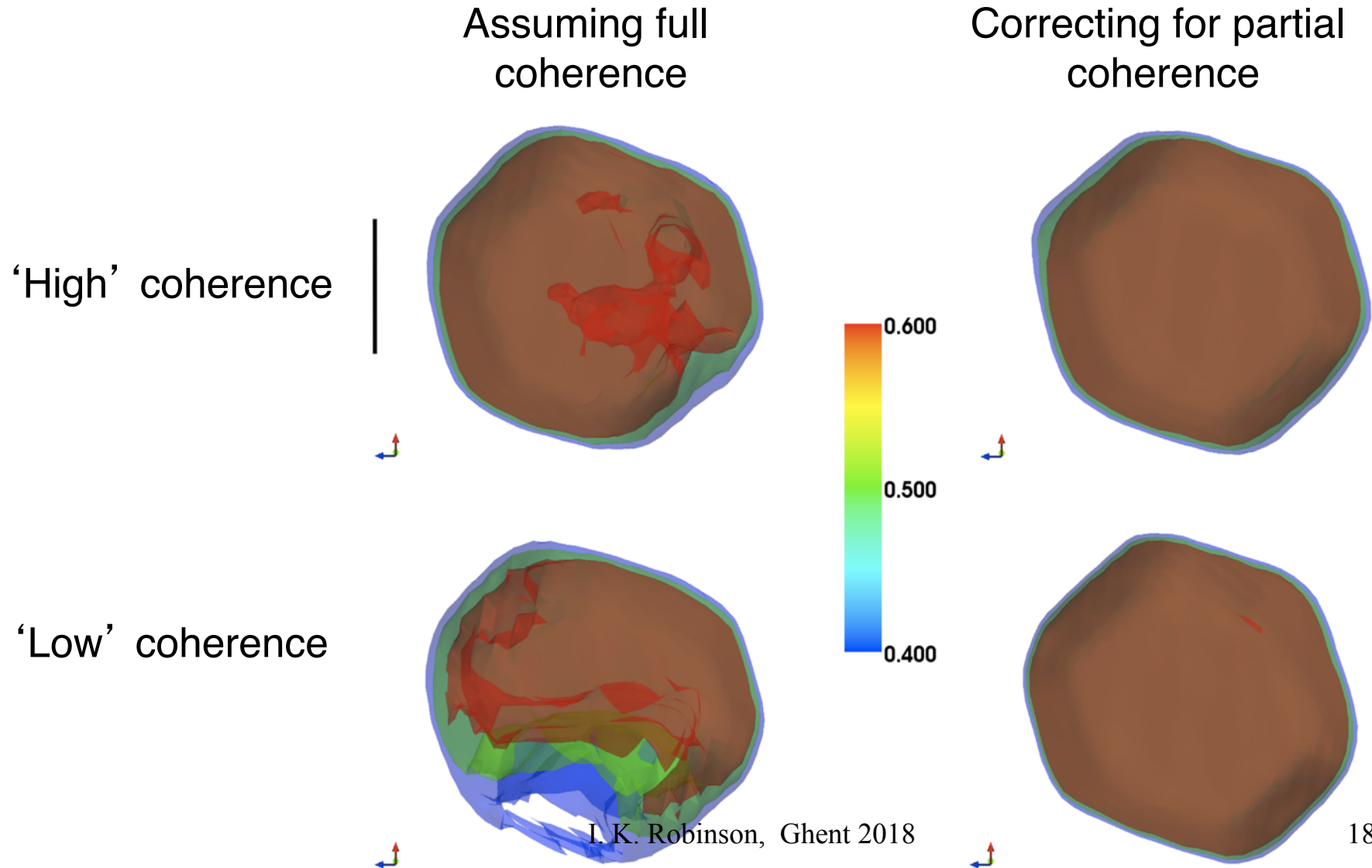


'Low' coherence



Top view of crystal

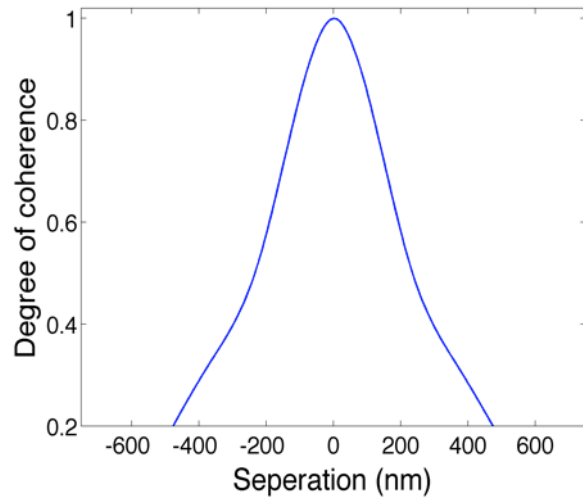
Jesse Clark et al, Nature Comms, 3 993 (2012)



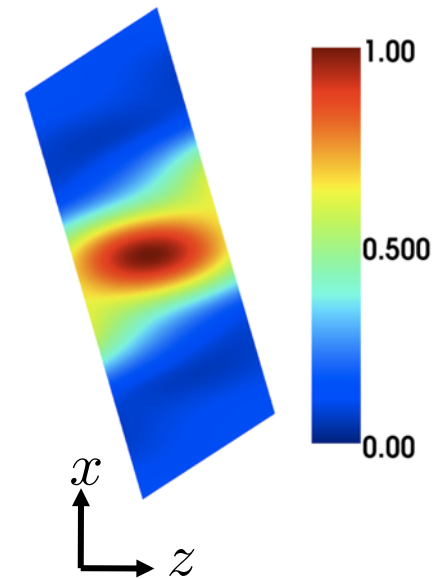
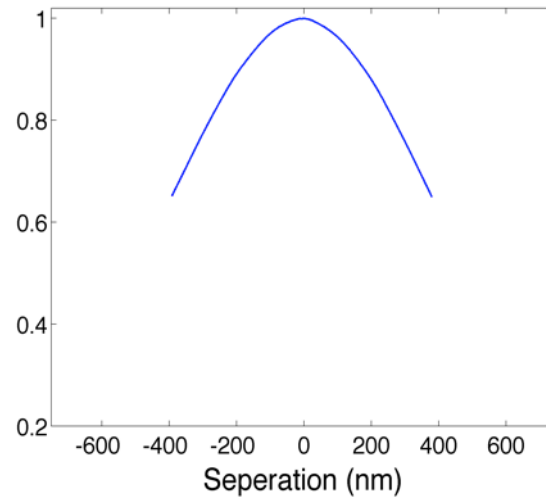
Derived coherence parameters

Jesse Clark et al, Nature Comms, 3 993 (2012)

x



z



Recovered
(HWHM)

$$l_x = 220 \text{ nm}$$

$$l_z = 485 \text{ nm}$$

Measured/
Estimated

$$l_x = 250 \text{ nm}$$

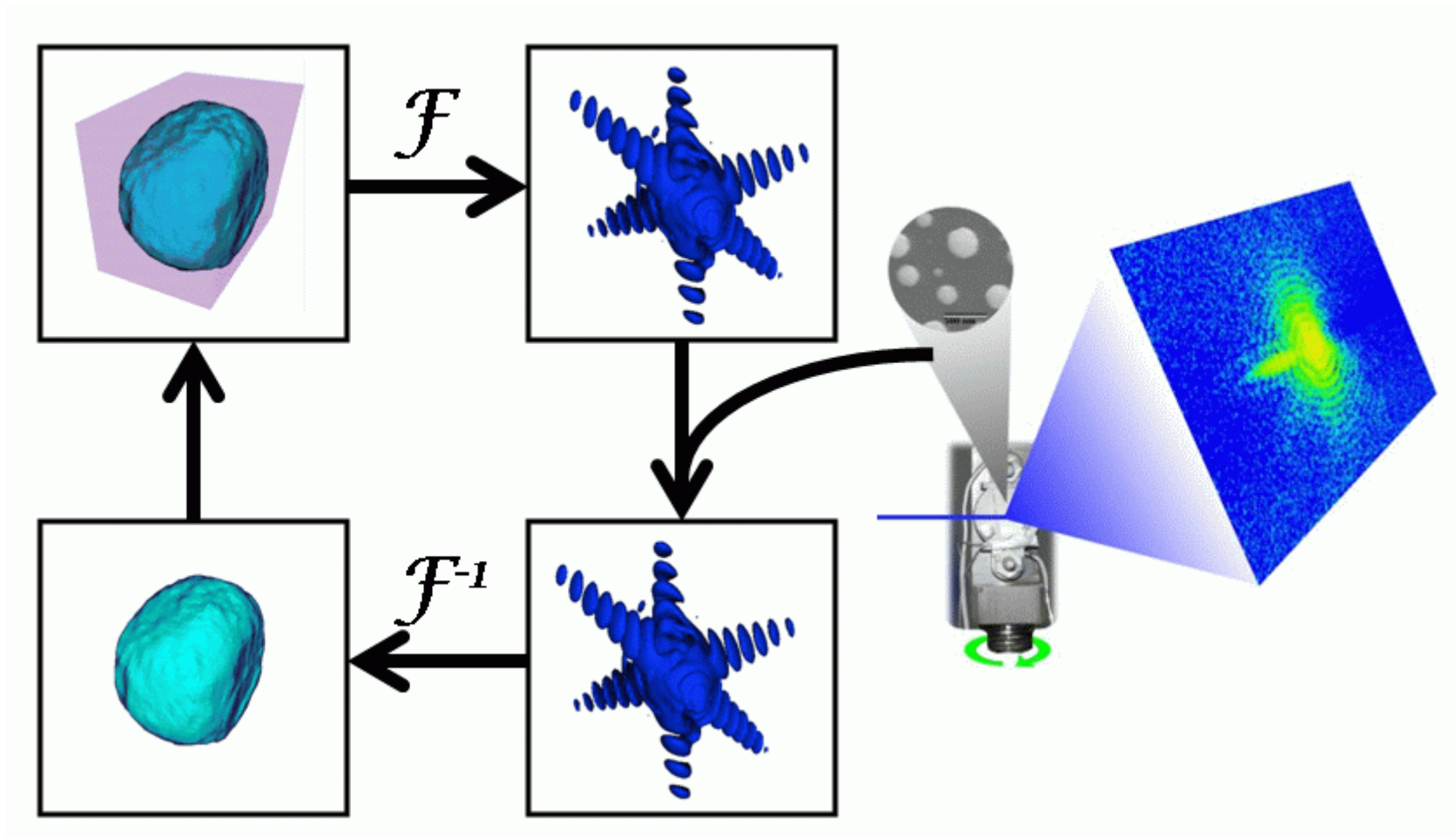
$$l_z = 660 \text{ nm}$$

I. K. Robinson, Ghent 2018

Coherent X-ray Scattering

- I. Coherence
- II. Measuring Coherence
- III. Coherent Imaging Modes**
- IV. Ptychography
- V. Experimental methods

Generic “Error Reduction” method



J. R. Fienup *Appl. Opt.* 21 2758 (1982)

R. W. Gerchberg and W. O. Saxton *Optik* 35 237 (1972)

I. K. Robinson, Ghent 2018

Free-space propagation

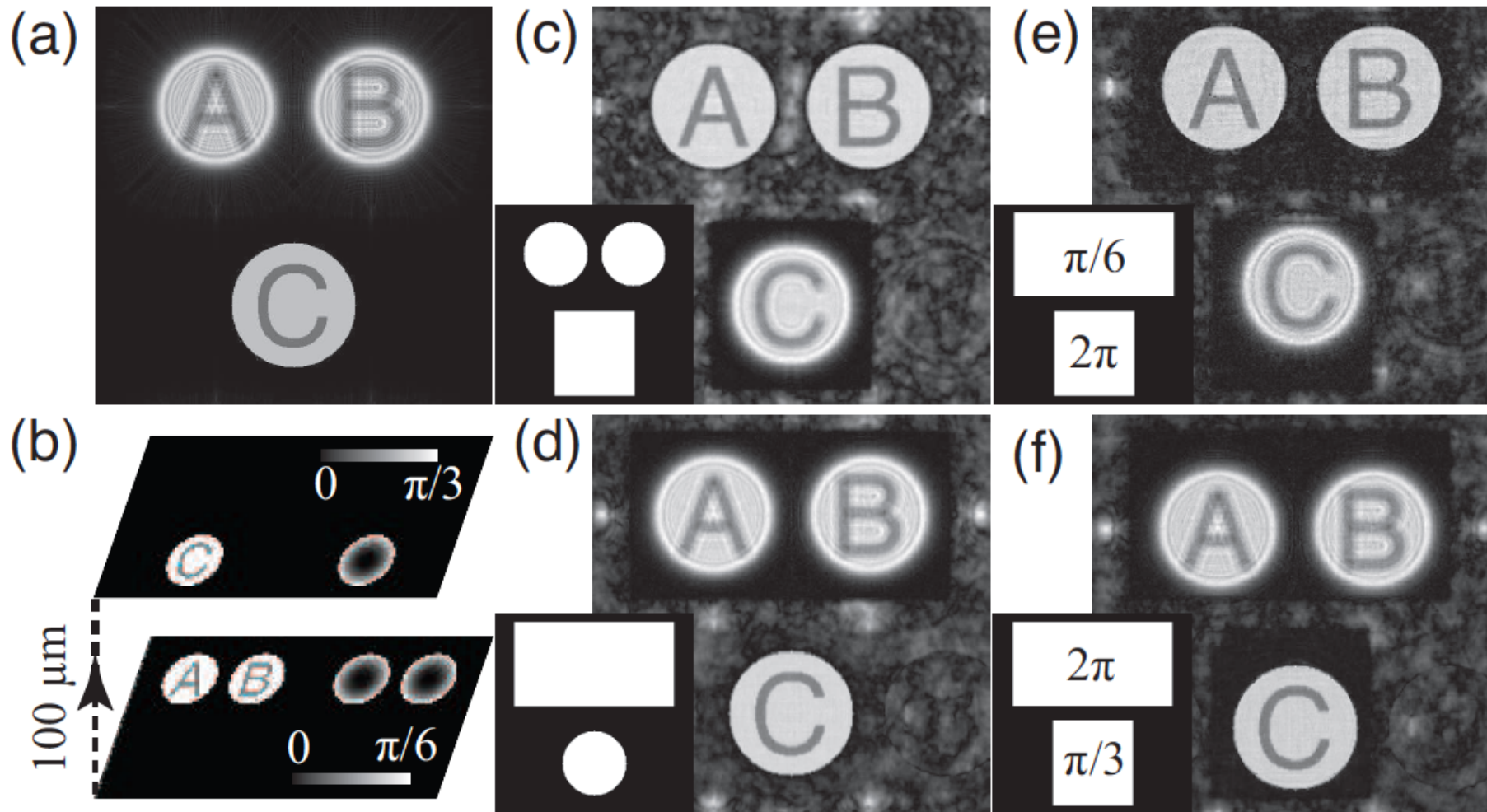
$$t'(\mathbf{r}') = \int t(\mathbf{r}) e^{ik(\mathbf{r}-\mathbf{r}')^2/2d} d\mathbf{r},$$

- Box \rightarrow box with fringes
- Real Gaussian \rightarrow complex *wider* Gaussian
- Real sharp object \rightarrow defocused complex object
- Propagated objects all have the same Fourier transform
- Inversion of far-field diffraction is **non-unique**

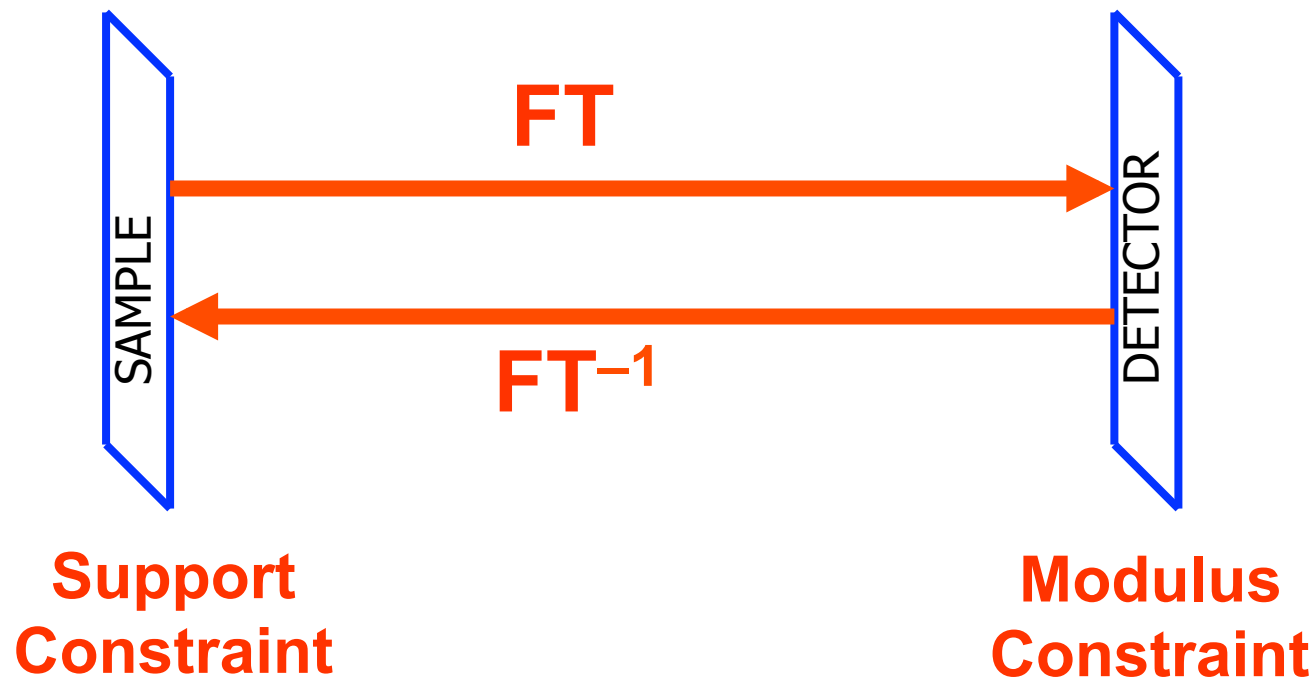
2D reconstruction support tests

J. C. H. Spence, U. Weierstall and M. Howells, Phil. Trans. 360, 875 (2002)

Xiaojing Huang, et al, Physical Review B 83 224109 (2011)



Coherent Diffractive Imaging General 2-plane Method



Curvature cures Stagnation

Image and its twin have same Fourier transform

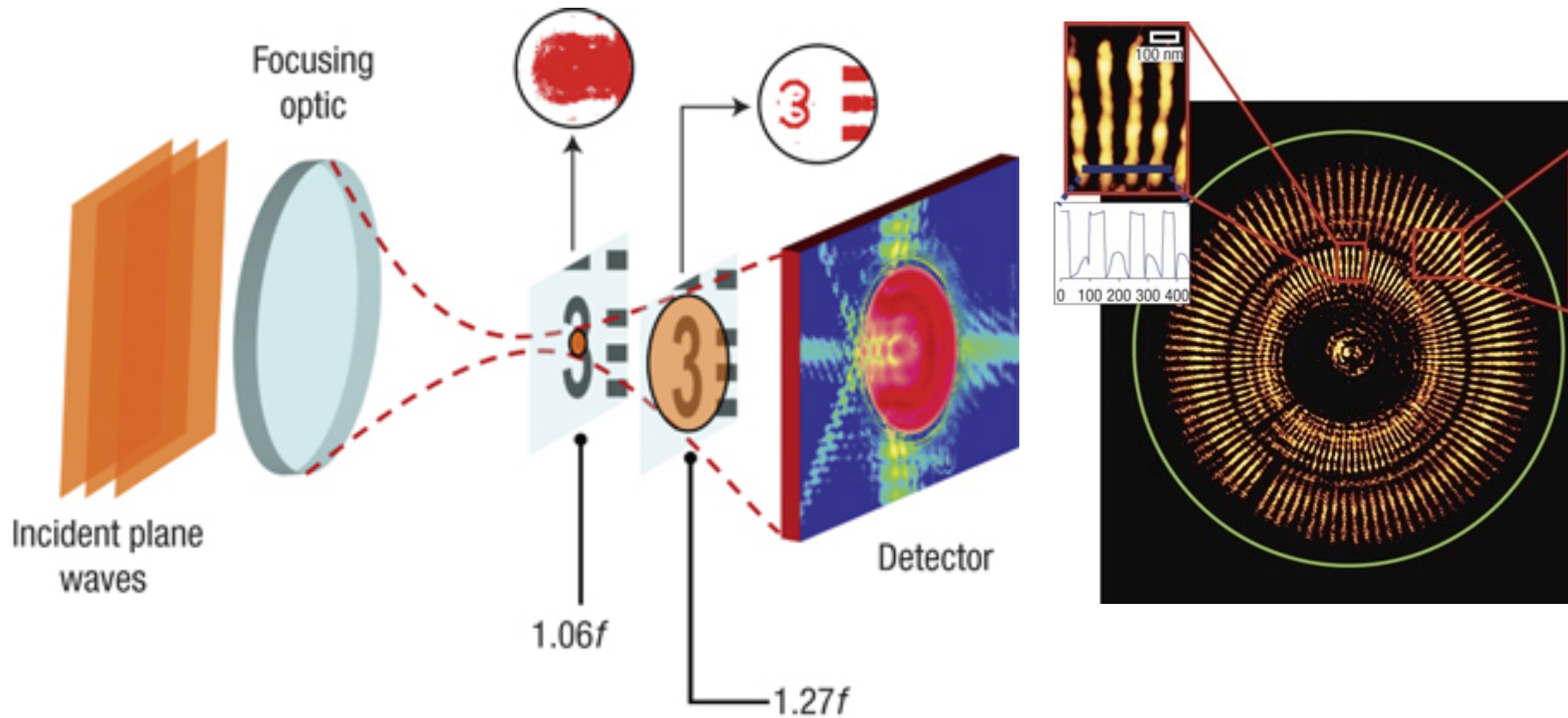
$$\rho(x) \quad \rho^*(-x)$$

$$\rho(x) \exp\left(\frac{i\pi x^2}{\lambda D}\right) \quad \rho^*(-x) \exp\left(\frac{-i\pi x^2}{\lambda D}\right)$$

Known modulation (phase curvature) allows twins to be discriminated using support

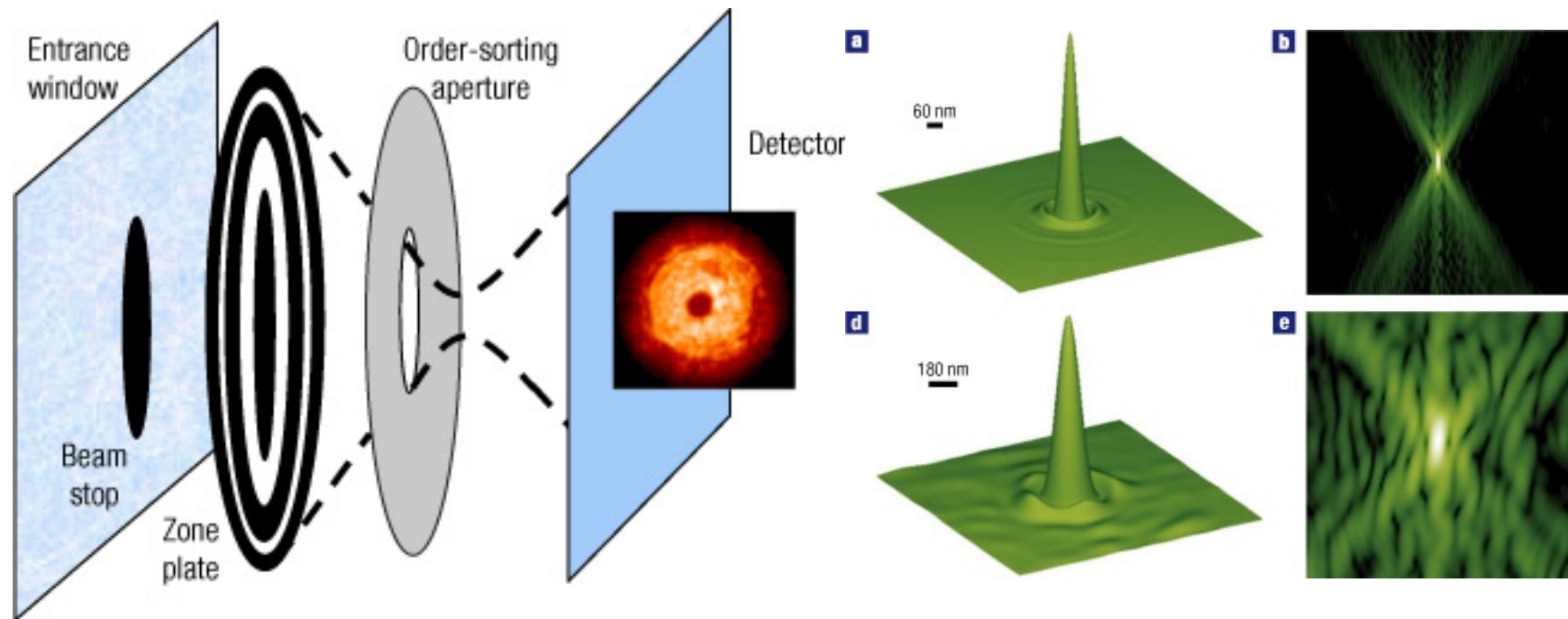
Keyhole coherent diffractive imaging

B. Abbey, K. A. Nugent, G. J. Williams, J. N. Clark, A. G. Peele, M. A. Pfeifer, M. de Jonge & I. McNulty, Nature Physics 4, 394 - 398 (2008)

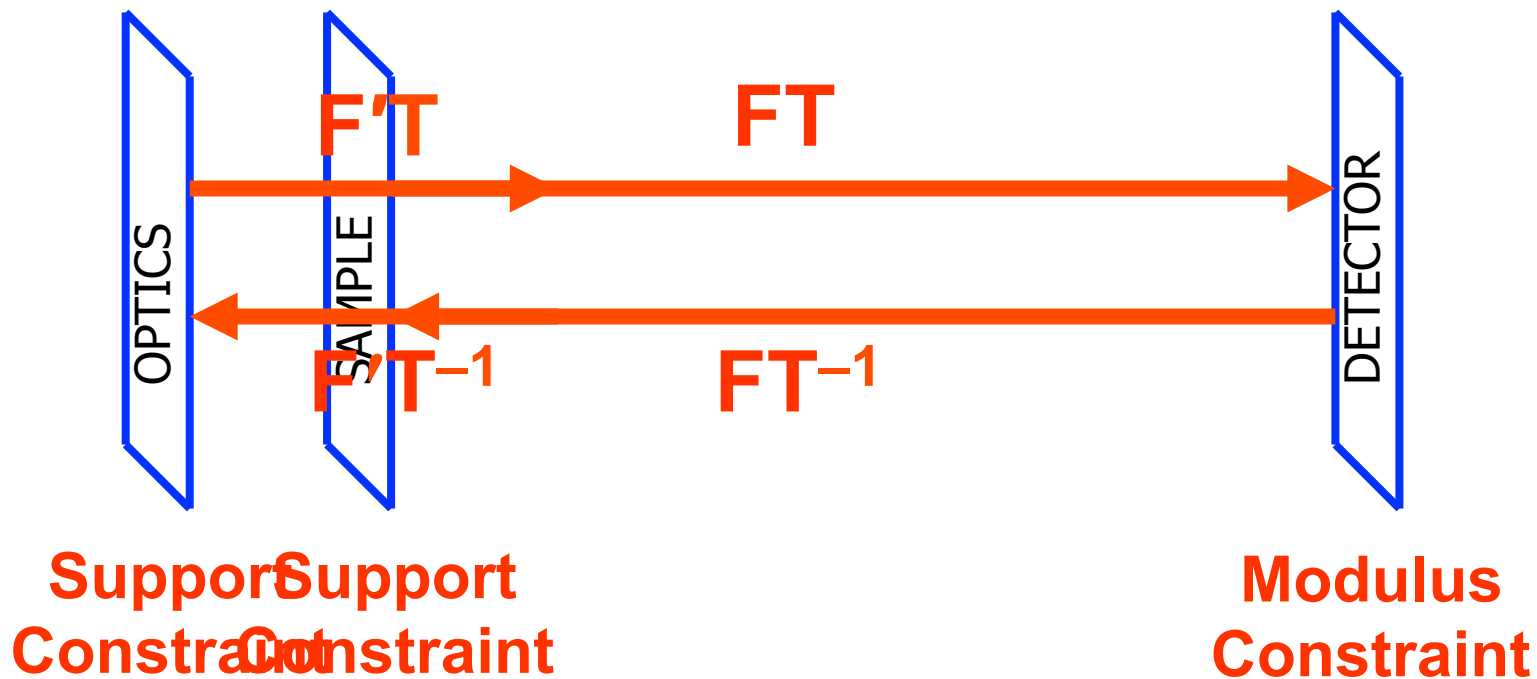


Diffractive imaging of highly focused X-ray fields

H. M. Quiney, A. G. Peele, Z. Cai, D. Paterson and
K. A. Nugent, Nature Physics 2, 101 - 104 (2006)



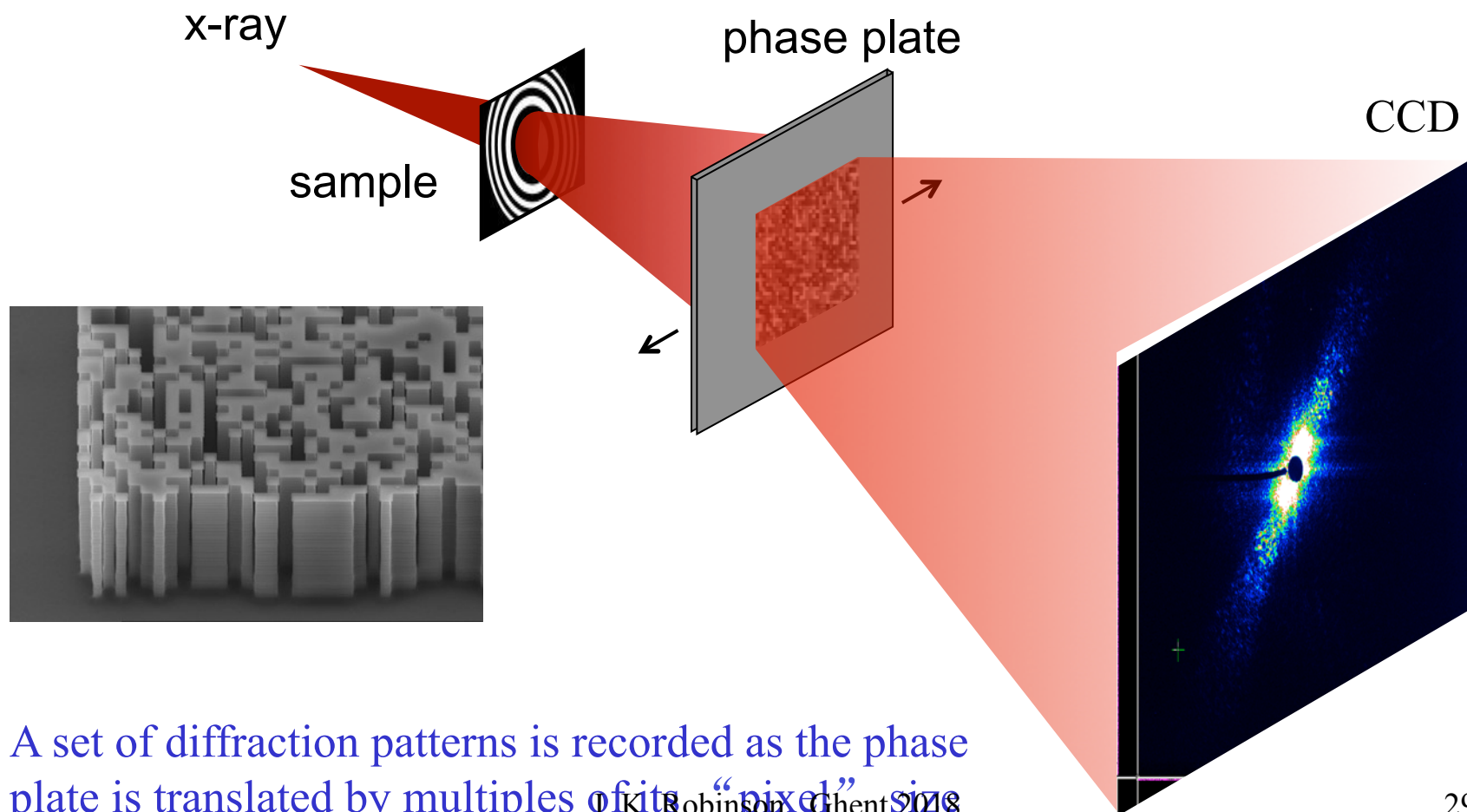
Coherent Diffractive Imaging General 3-plane Method



Imaging by Wavefront Modification

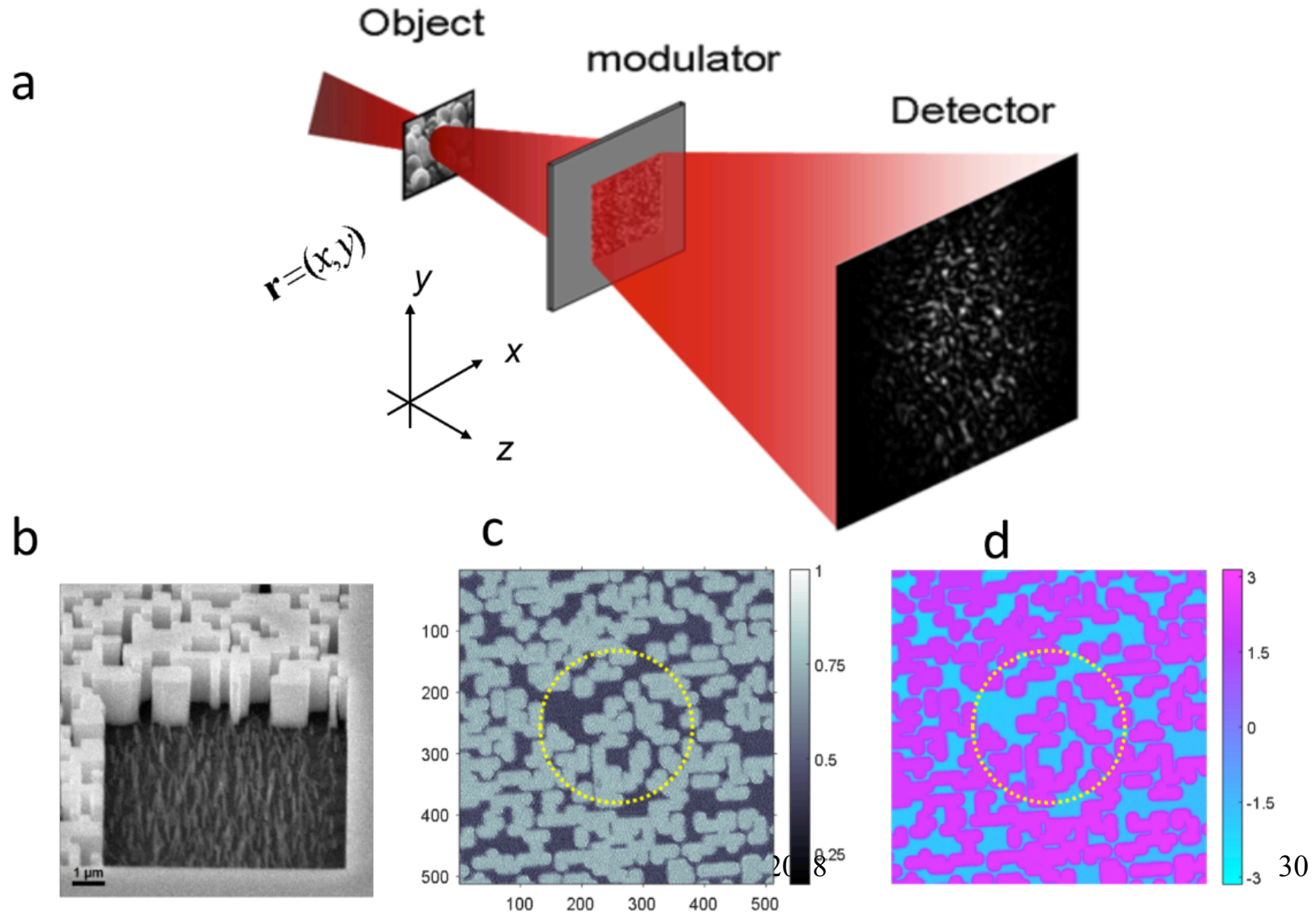
F. Zhang et al., Phys Rev A 75 (2007)

I. Johnson et al., Phys Rev Lett 100 (2008)



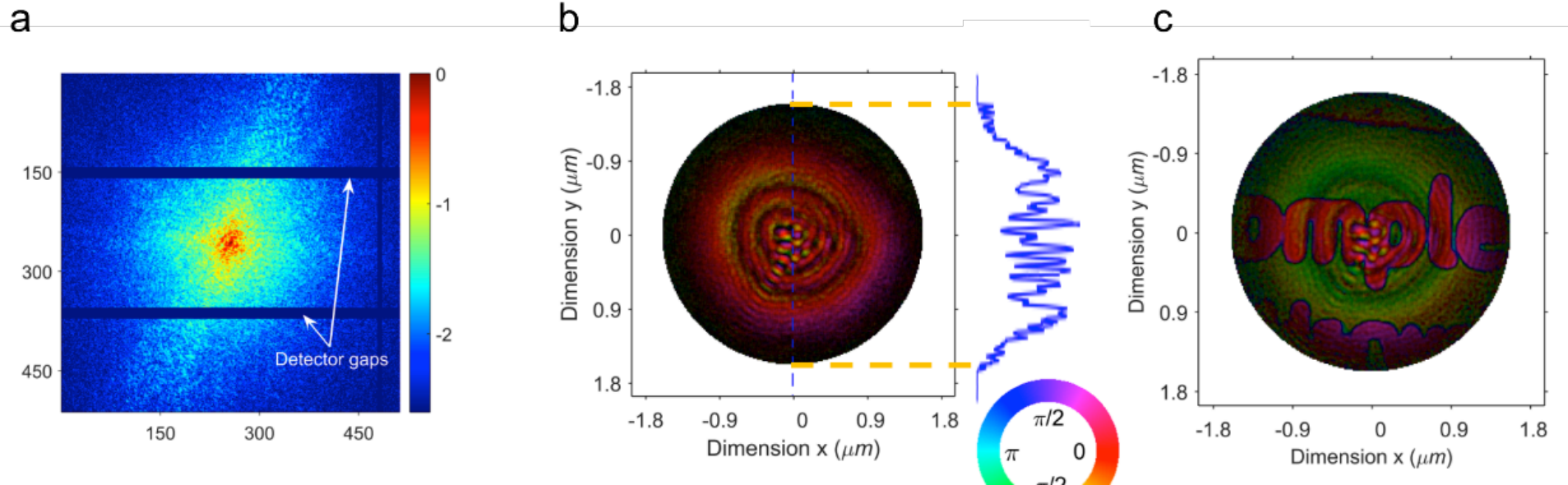
I. K. Robinson, Ghent 2018

X-ray Coherent Modulation Imaging

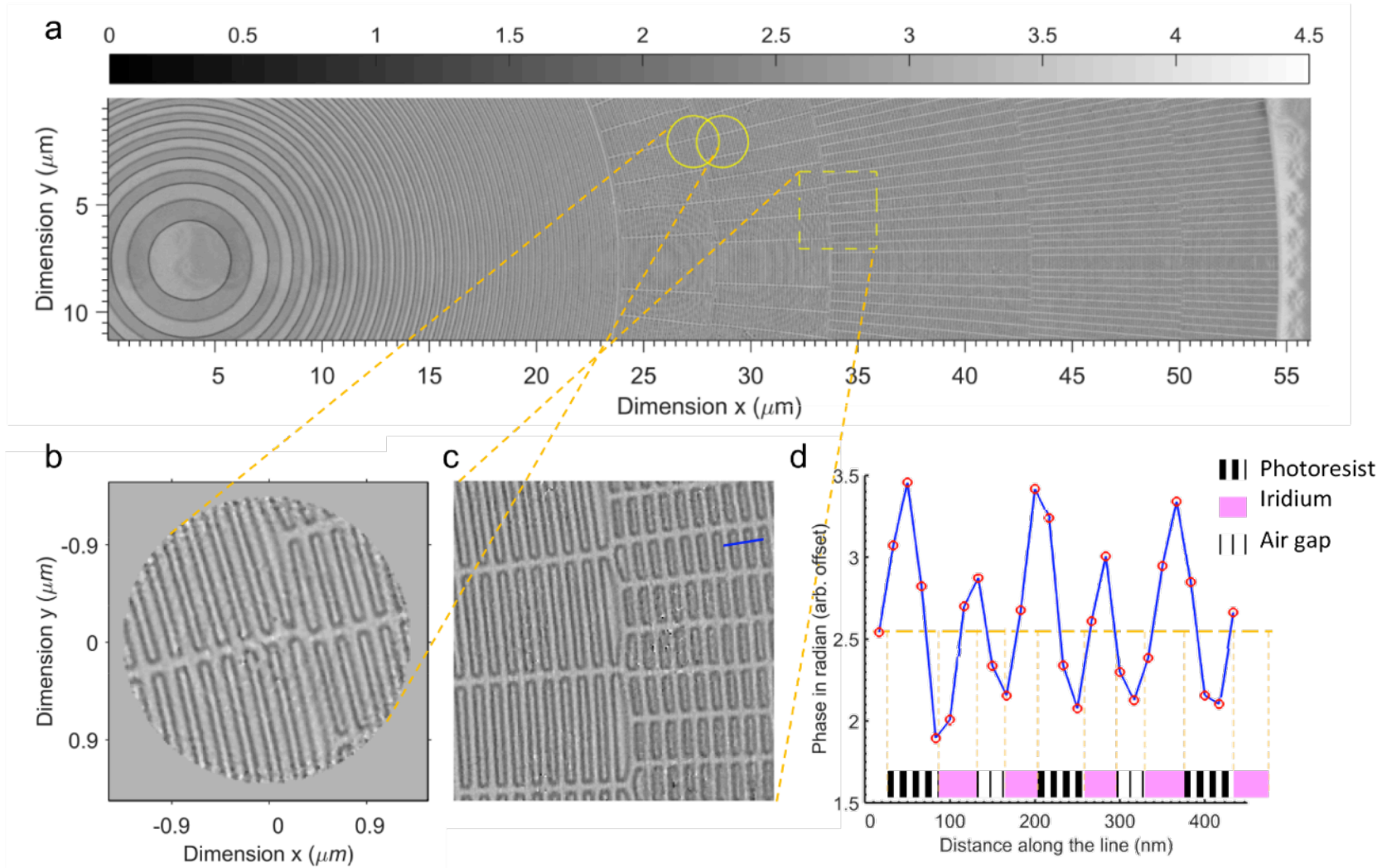


X-ray Coherent Modulation Imaging

Fucaï Zhang, submitted to Nature Photonics

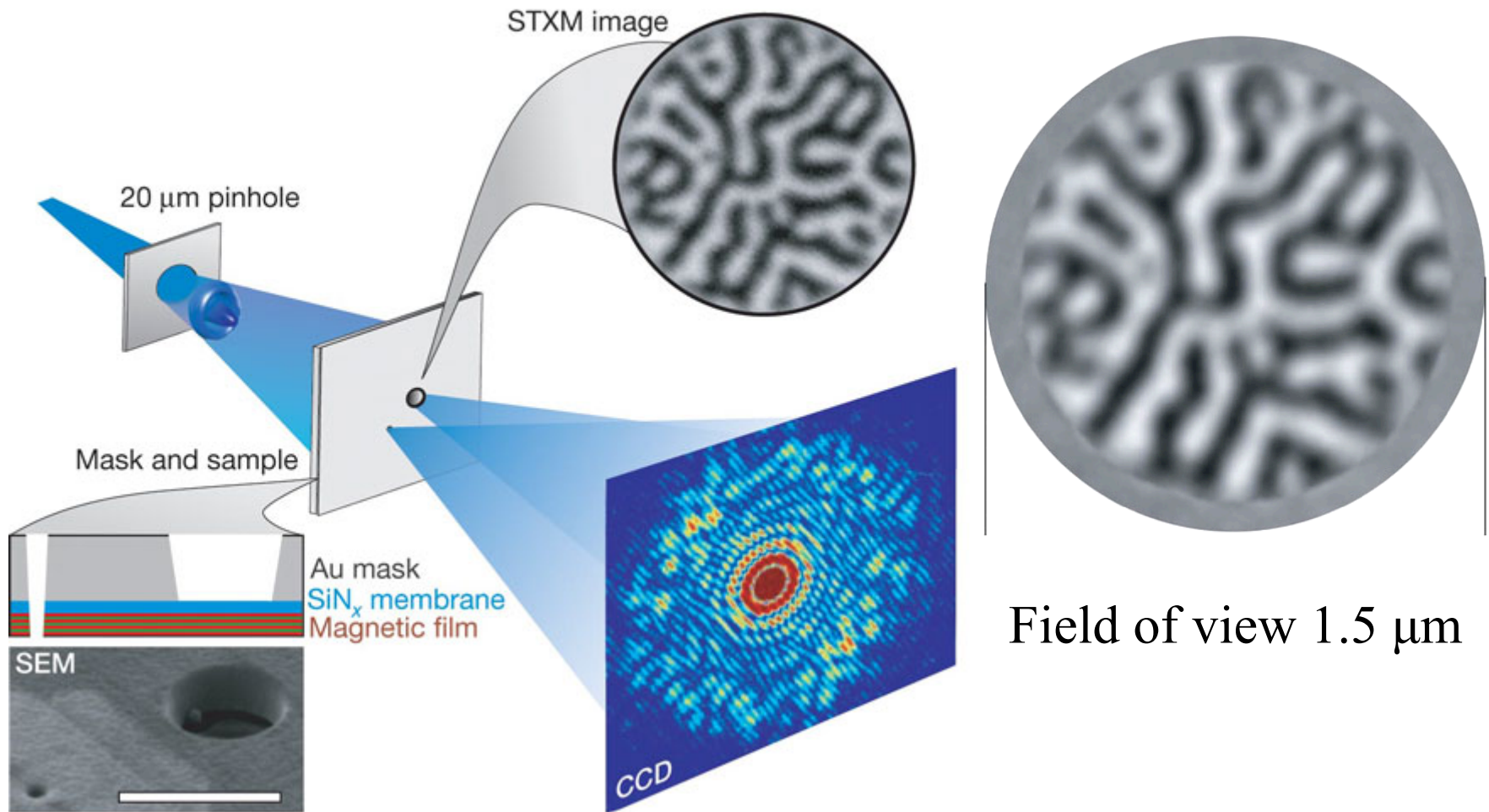


Imaging at Swiss Light Source



X-ray Holography of Pt/CoML Domains

S. Eisebitt et al. Nature 432 885 (2004)

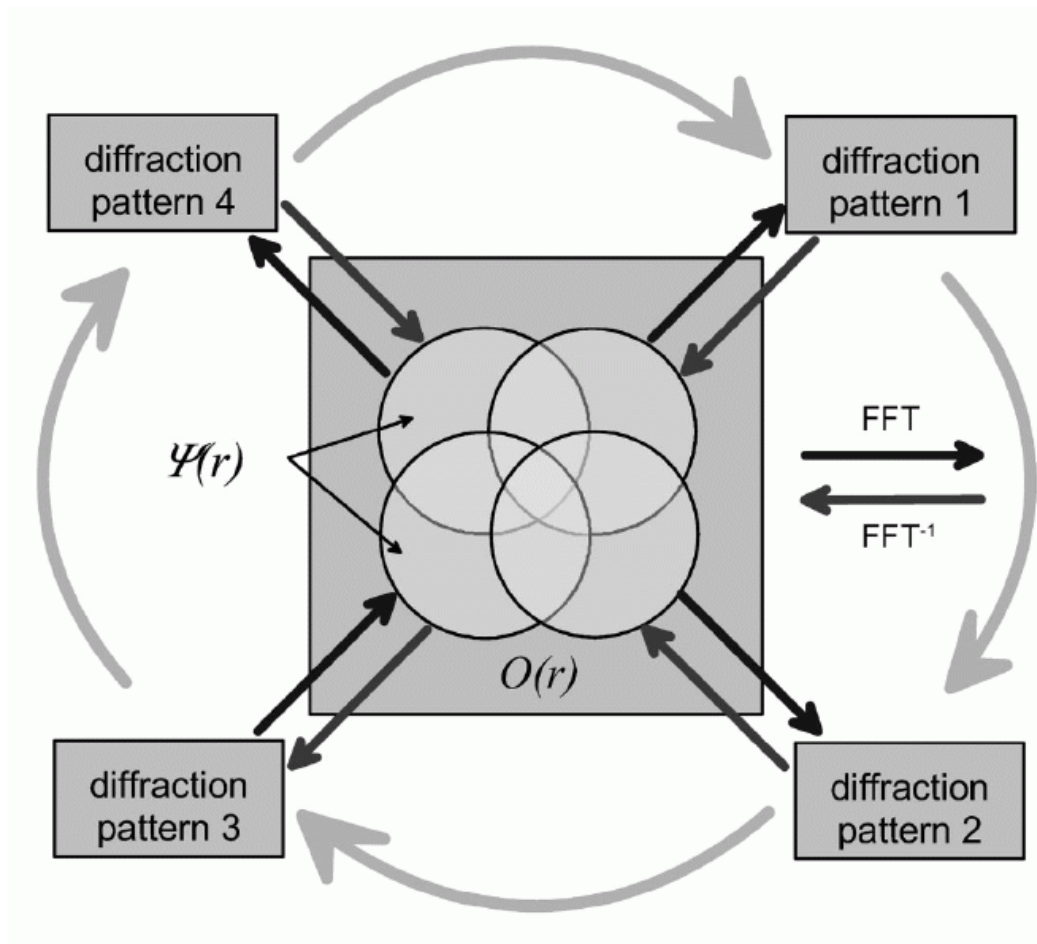


Coherent X-ray Scattering

- I. Coherence
- II. Measuring Coherence
- III. Coherent Imaging Modes
- IV. Ptychography**
- V. Experimental methods

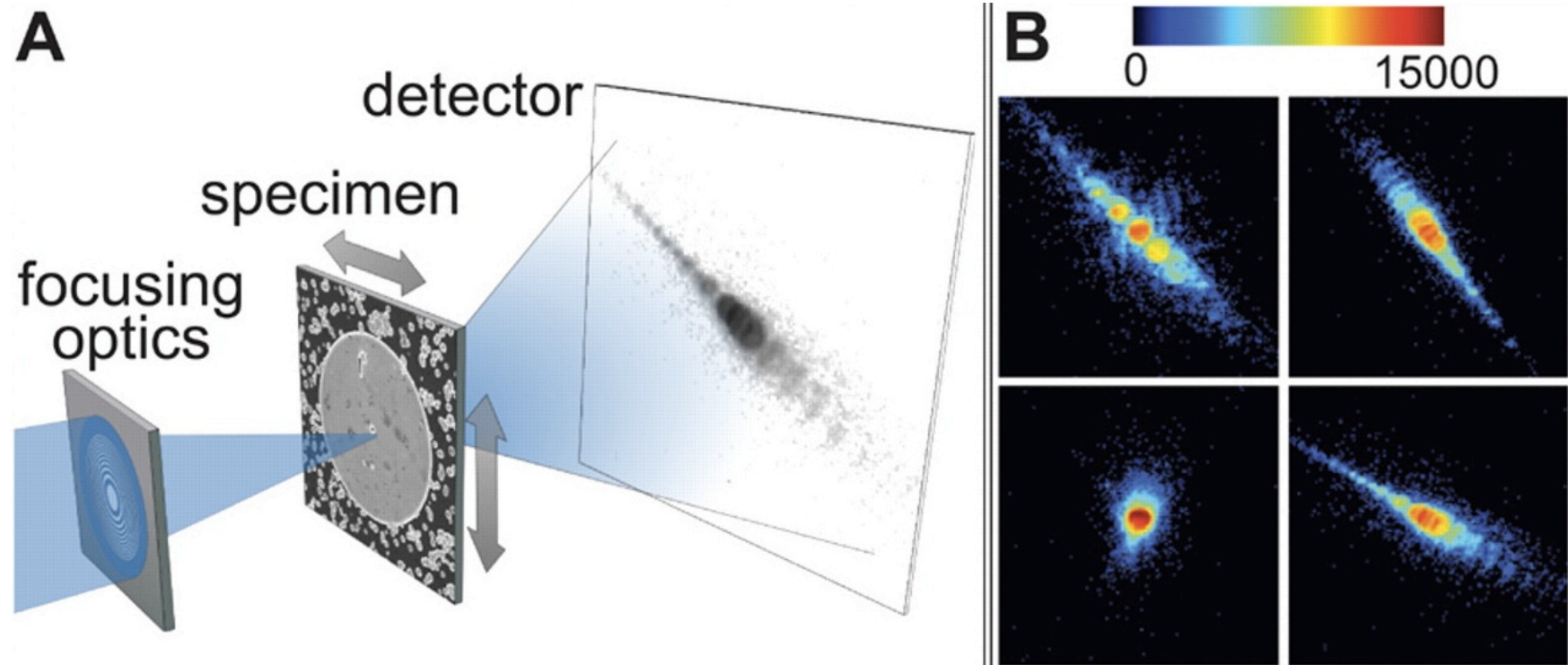
X-ray Ptychography

J. Rodenburg et al, PRL 98, 034801 (2007)



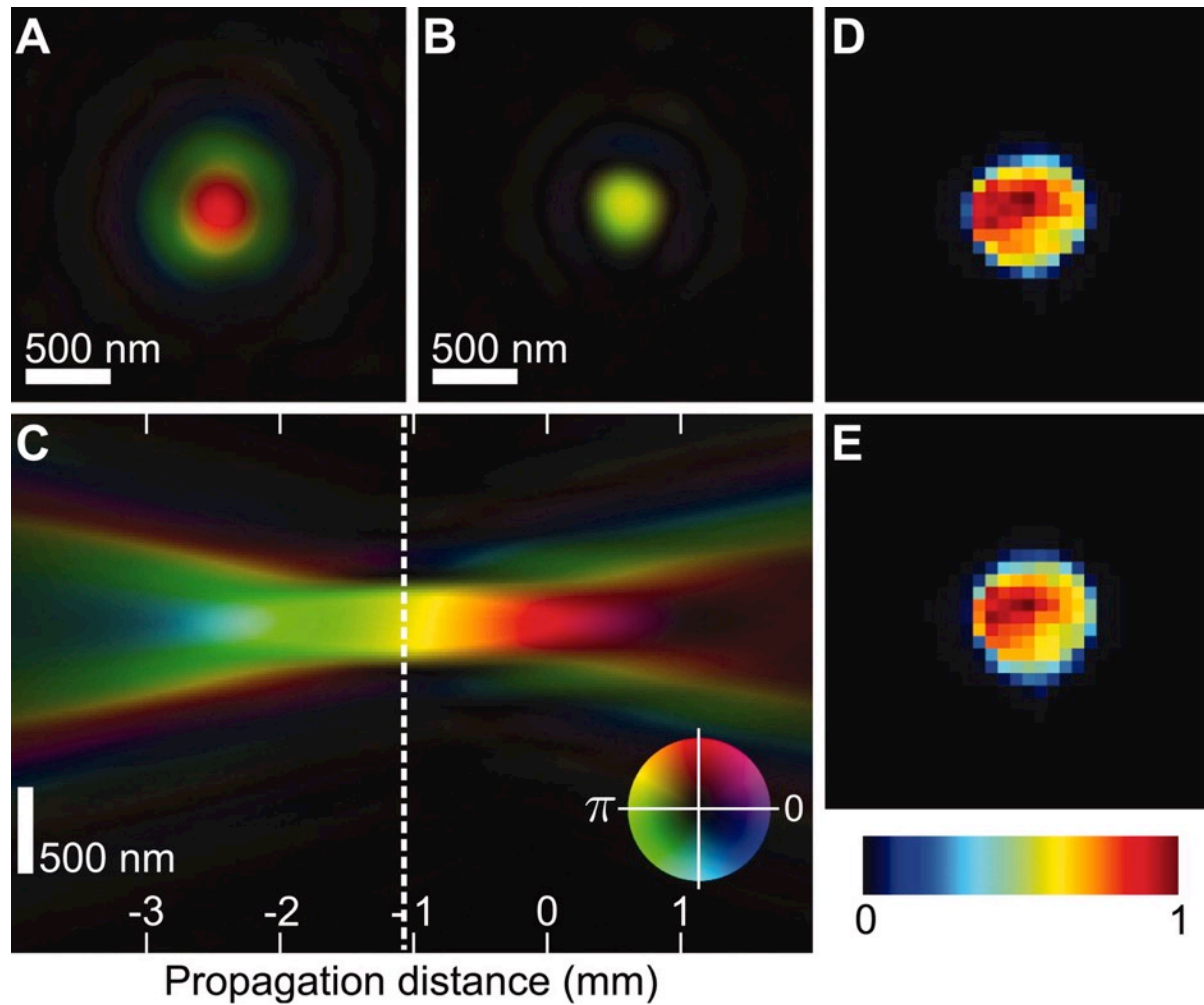
X-ray Ptychography

P. Thibault et al, Science 321 379 (2008)

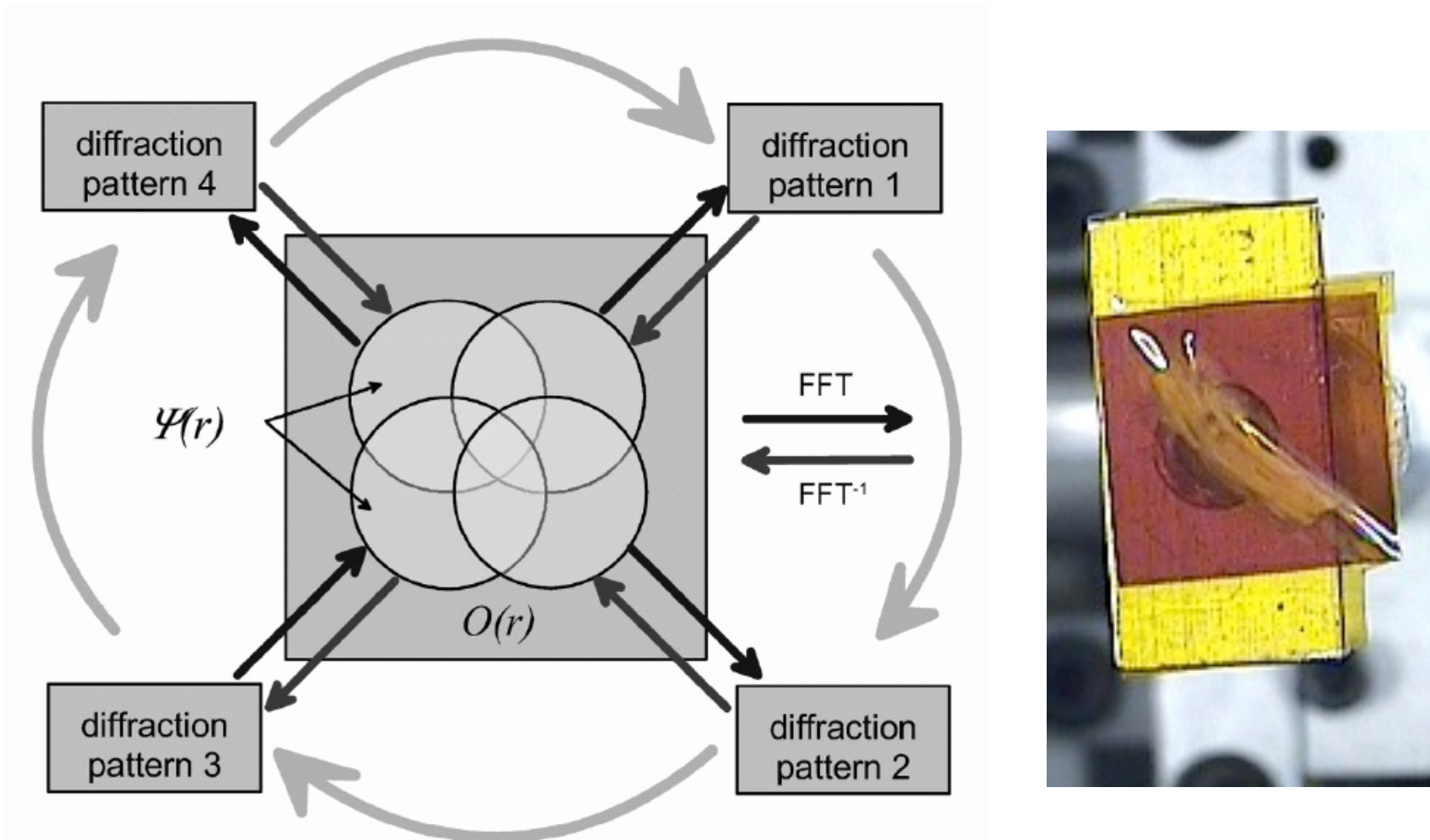


Reconstruction of Probe

P. Thibault et al, Science 321 379 (2008)



Collagen Ptychography

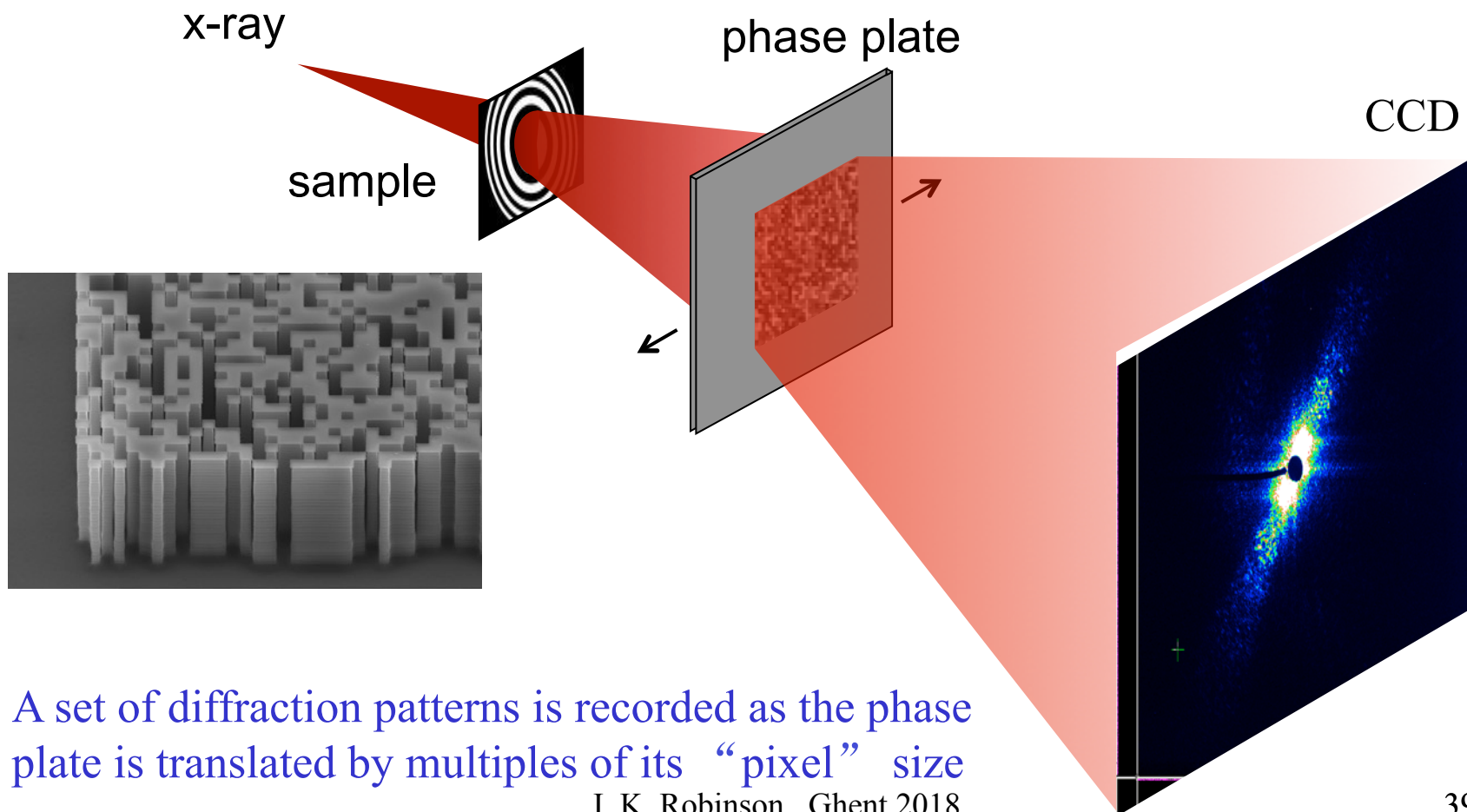


J. M. Rodenburg et al, Phys. Rev. Lett. 98 034801 (2007)

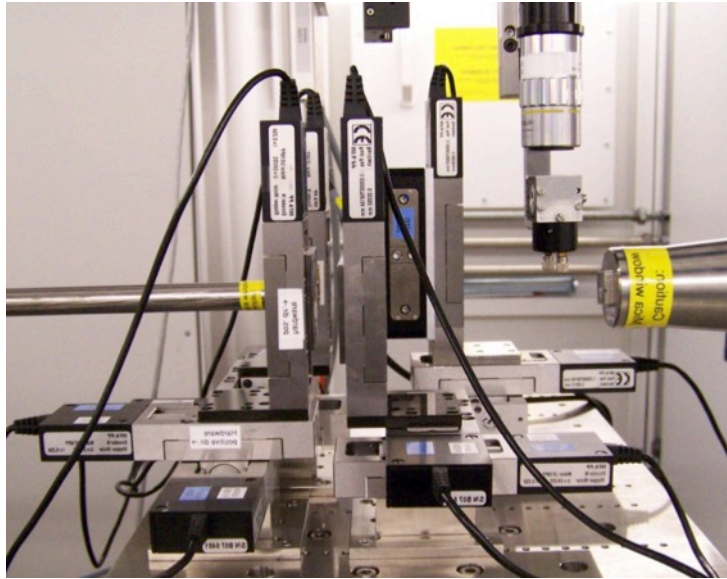
I. K. Robinson, Ghent 2018

Imaging by wavefront modification

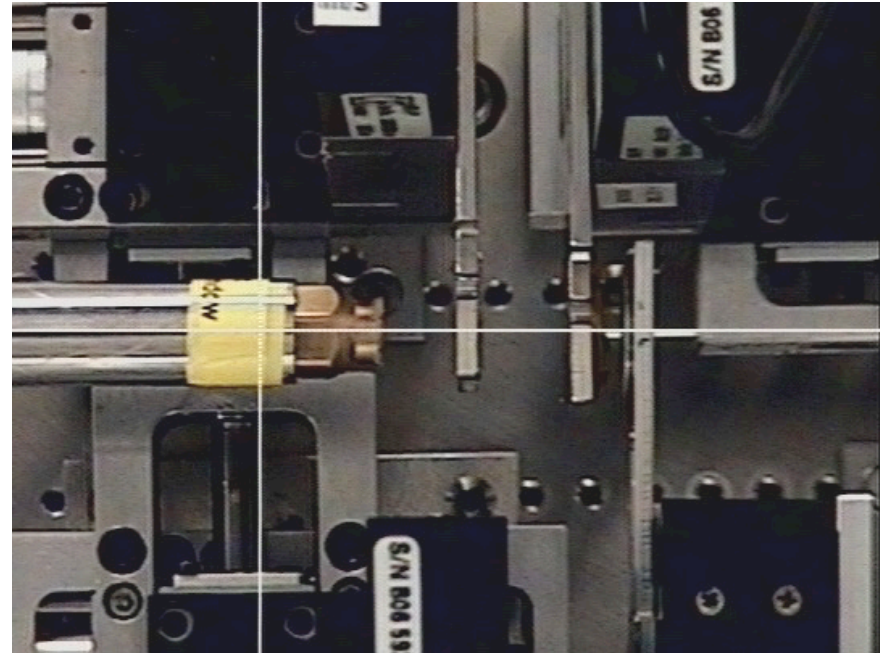
F. Zhang *et al.*, Phys Rev A 75 (2007)
I. Johnson *et al.*, Phys Rev Lett 100 (2008)



Experimental setup cSAXS (SLS)



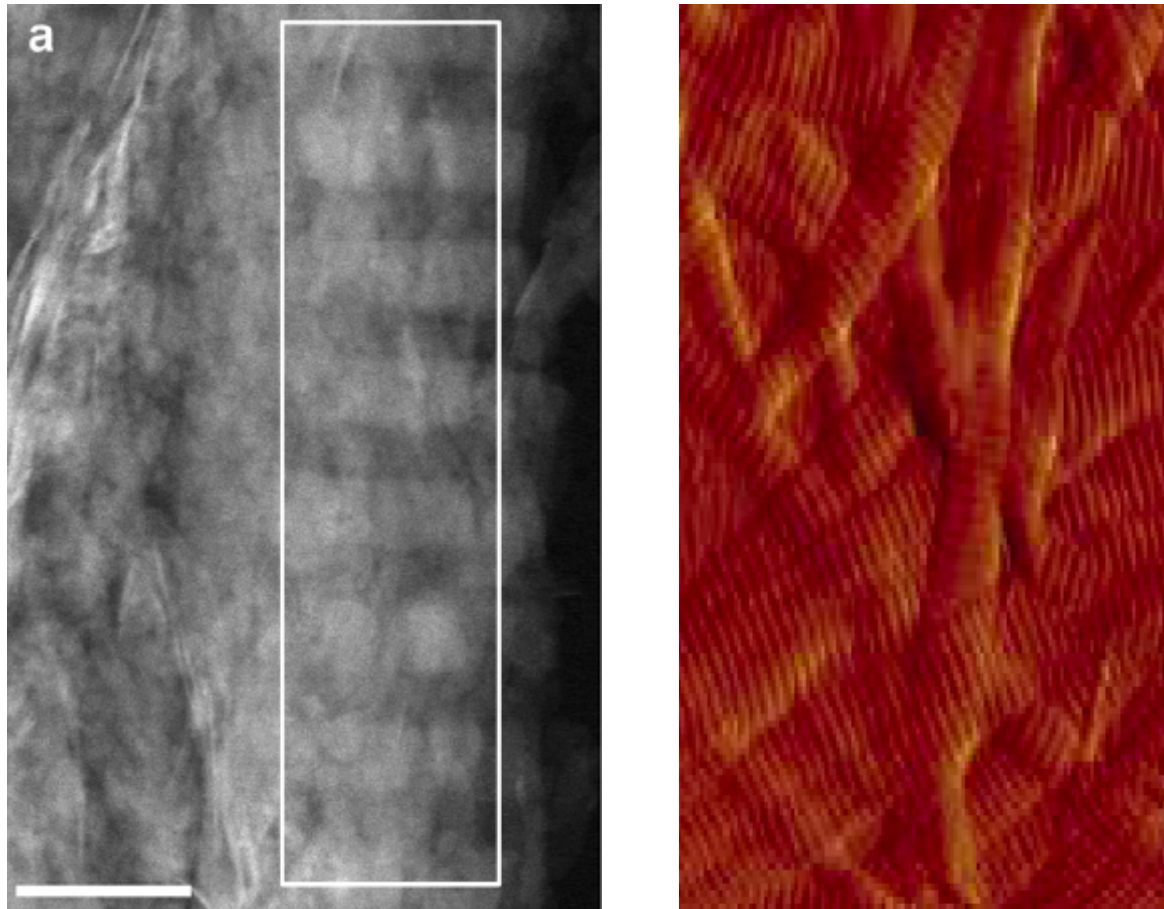
Side view



Top view (zoomed in)

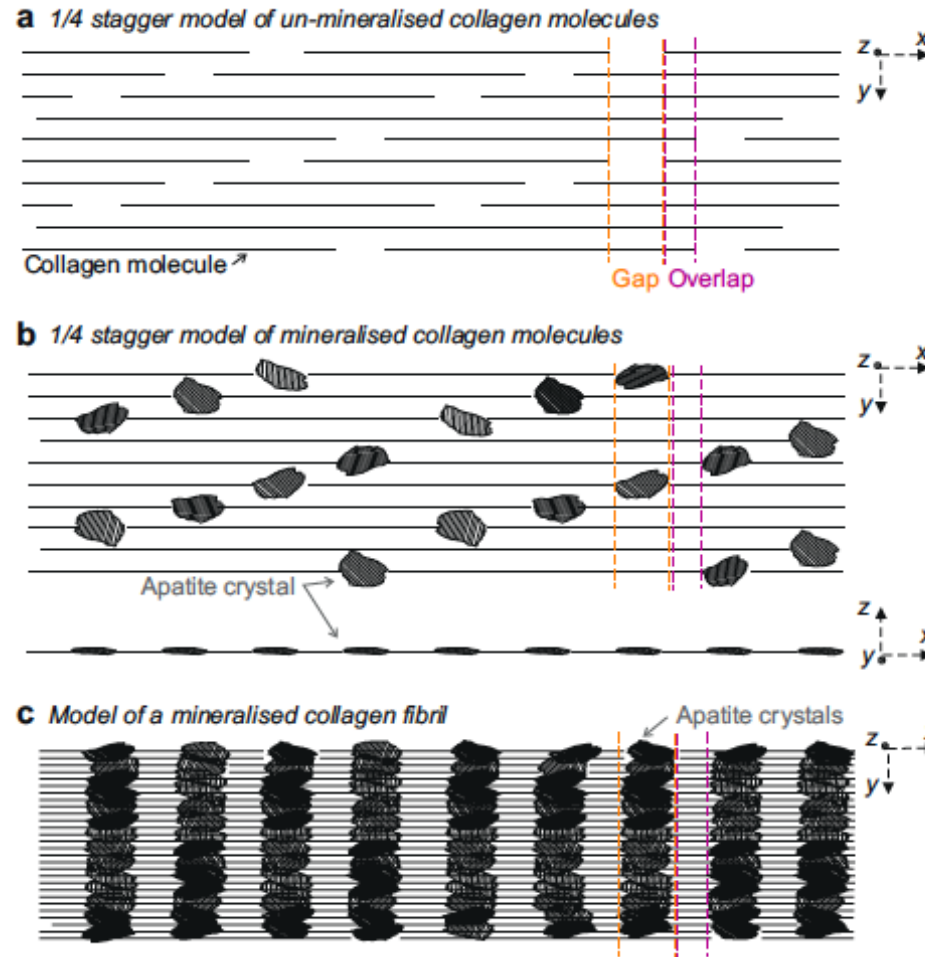
STEM biom mineralisation, AFM

Mike Horton and Laurent Bozec

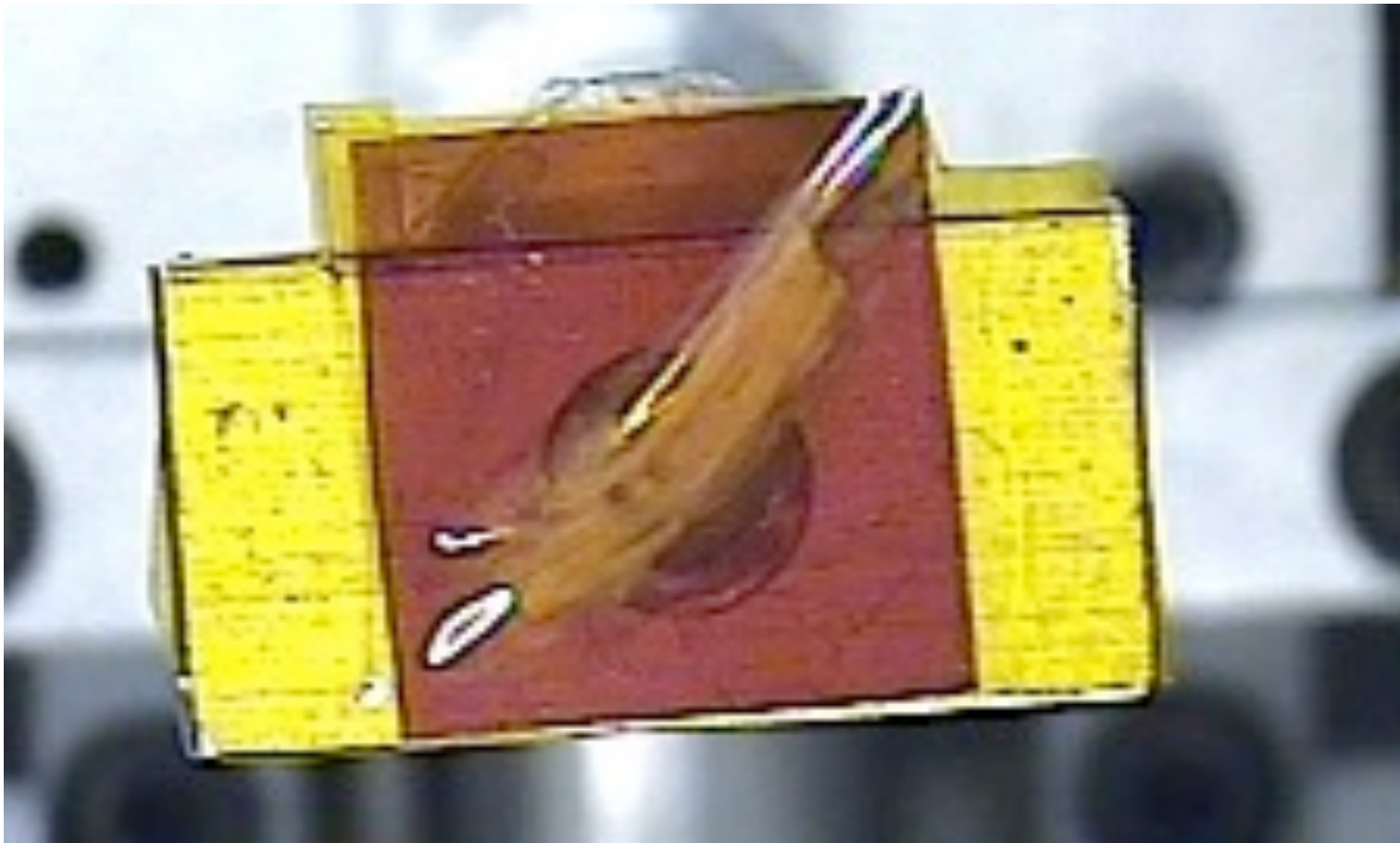


Biom mineralisation Model

Jantou-Morris, V, Horton, MA, McComb, DW
Biomaterials 31 5275 (2010)

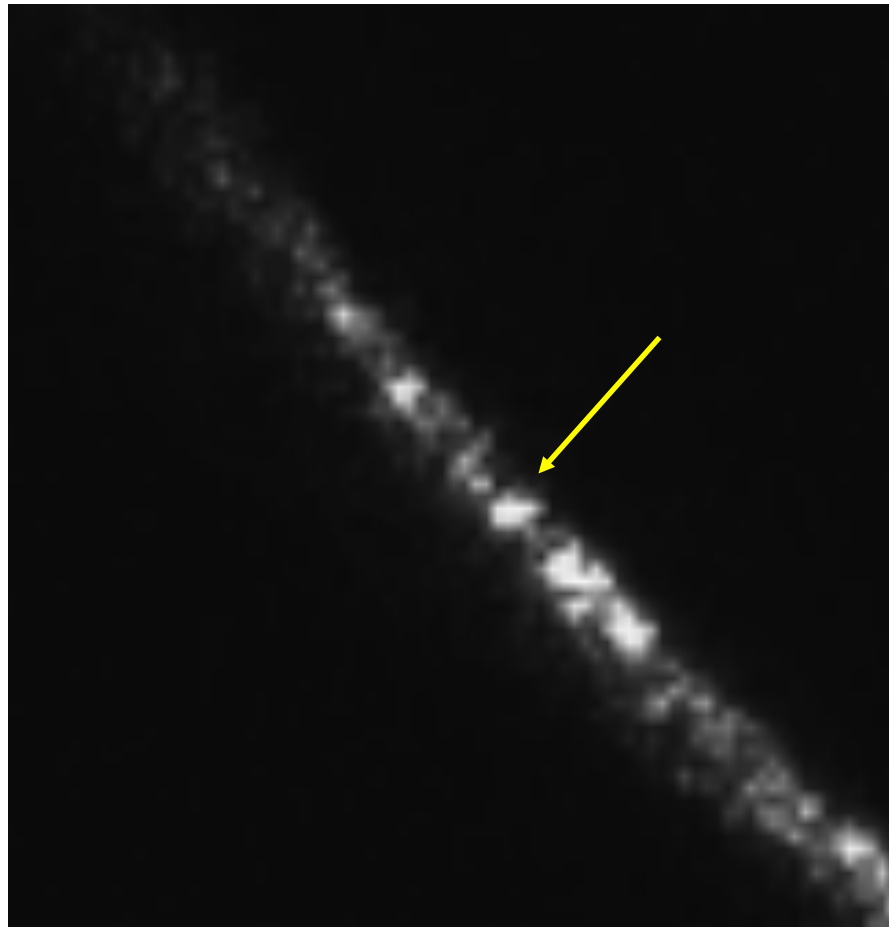


First Collagen Sample Preparation

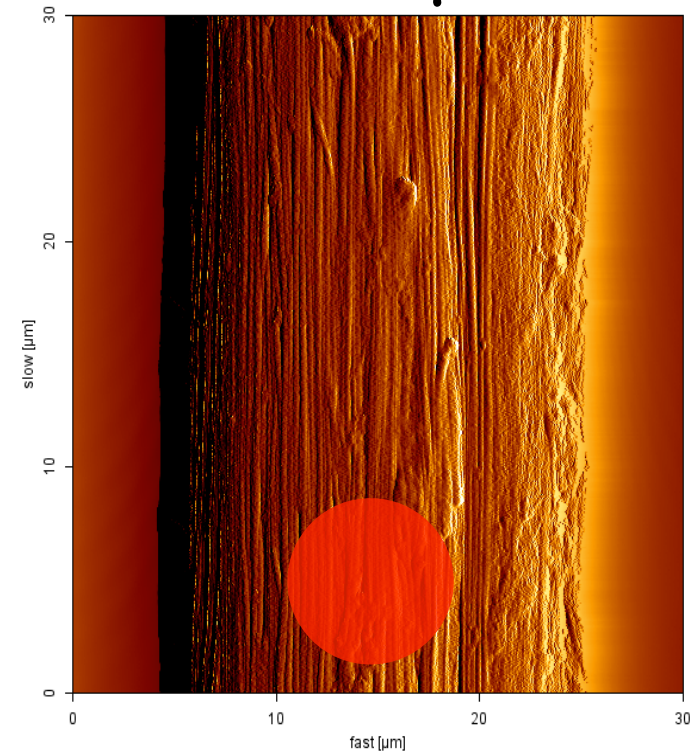


Collagen X-ray Ptychography

67nm meridional reflection



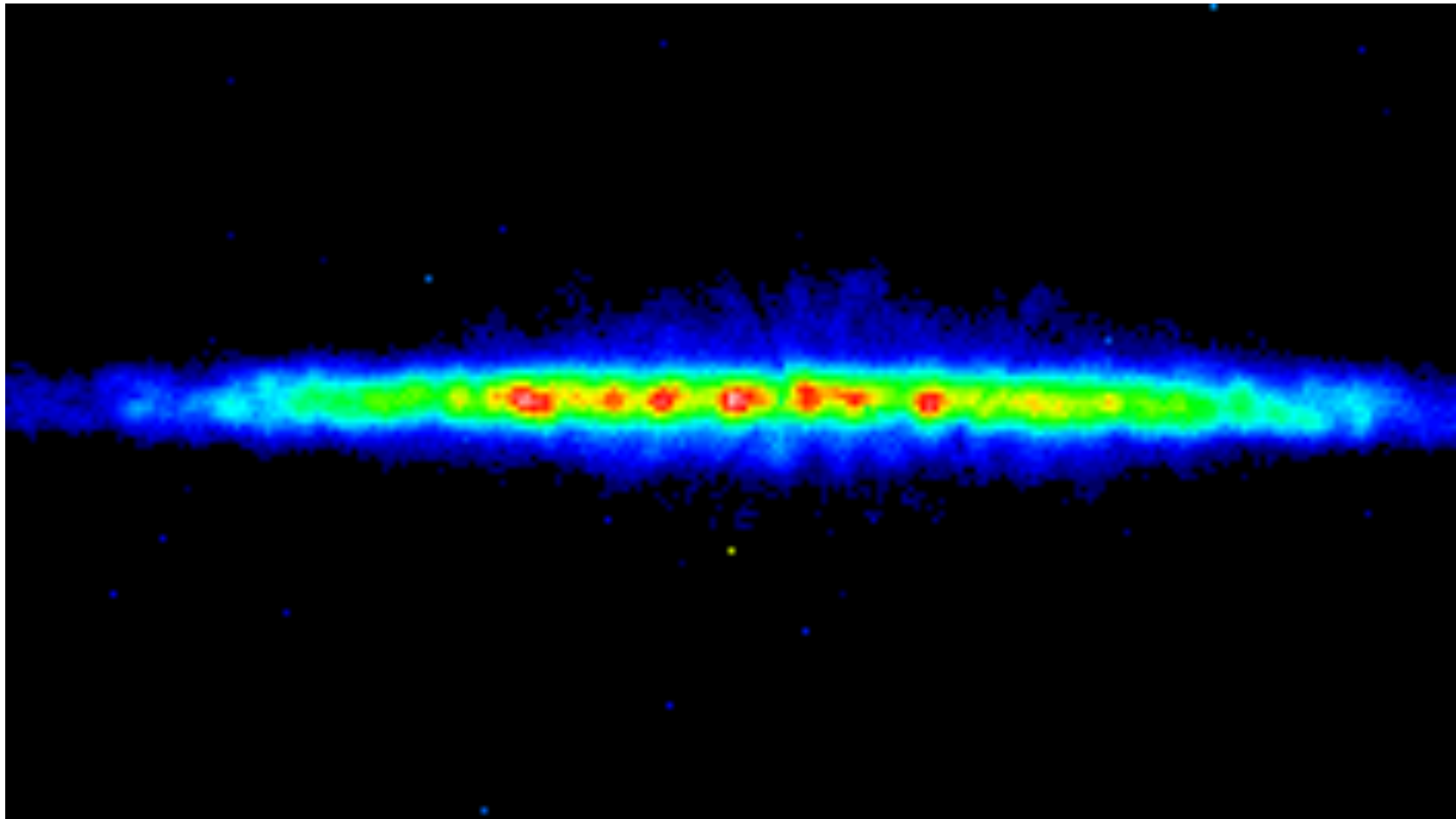
10 μm beam



Dark field imaging:
collagen distribution in different
tissues

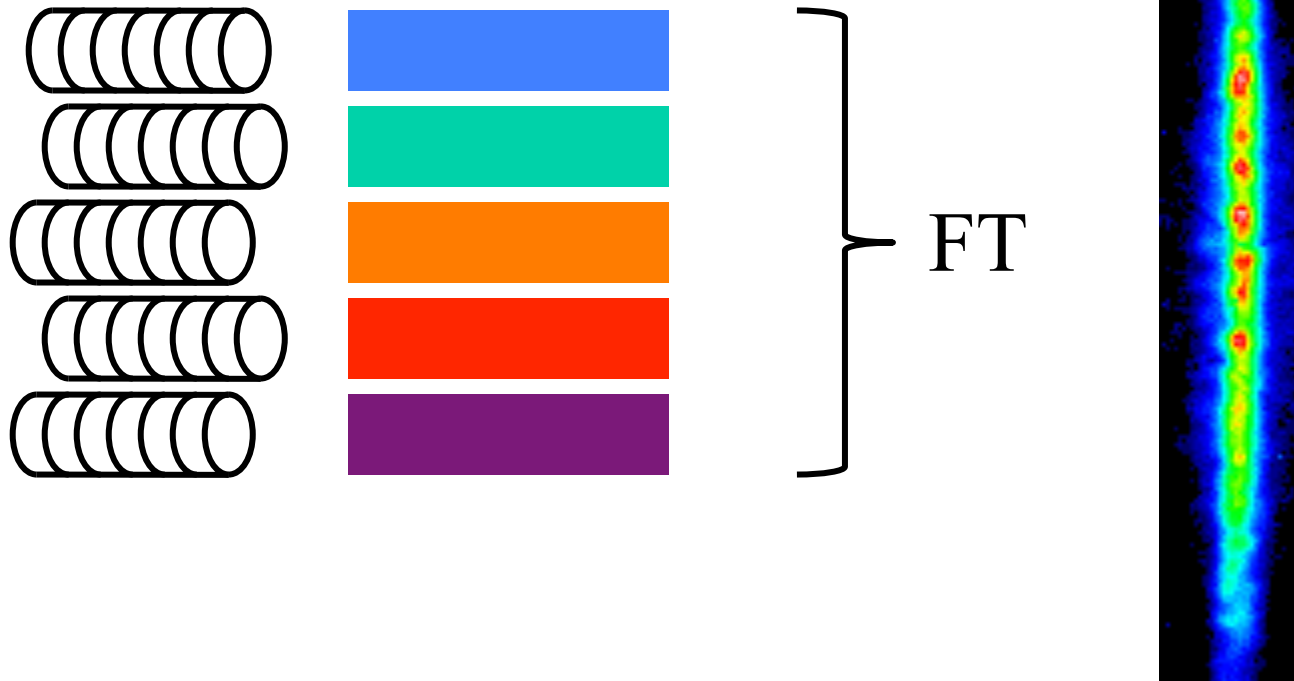
Improved collagen sample prep

Diamond I-22, Nov 2008



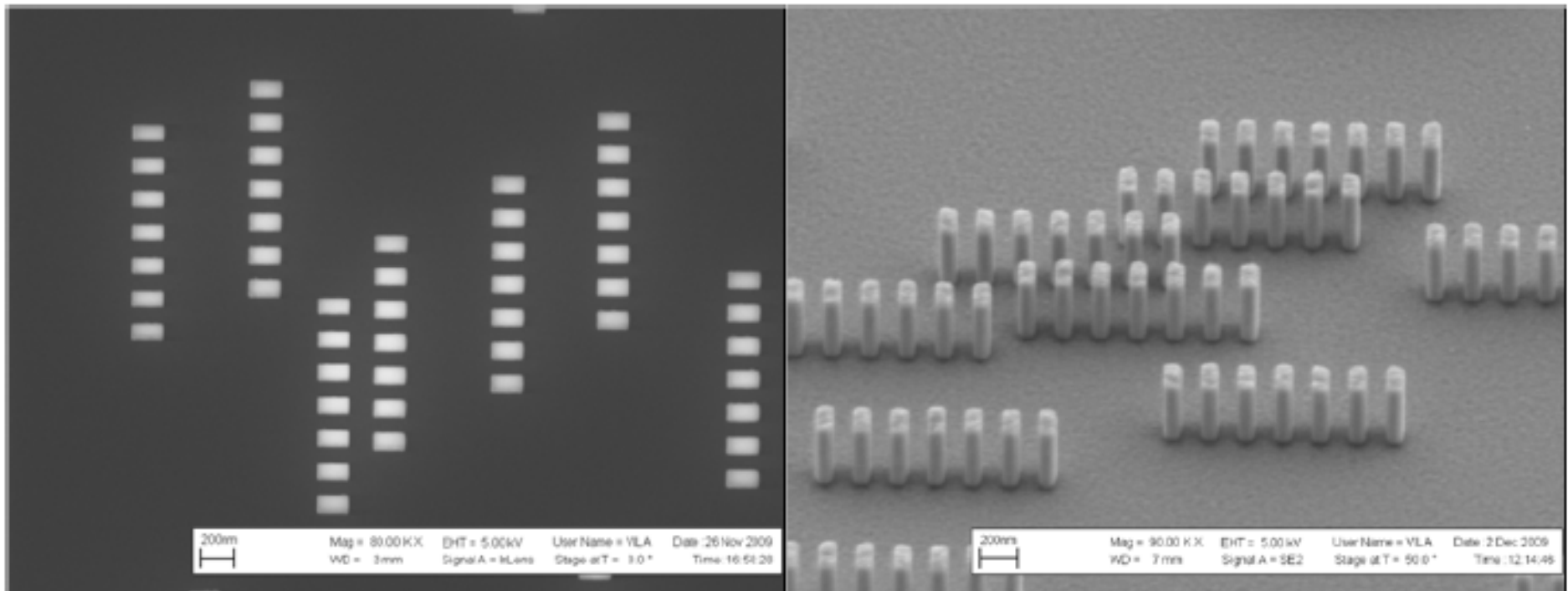
Collagen imaged at 67nm Bragg peak

1 μm fibrils cut by 20 μm beam

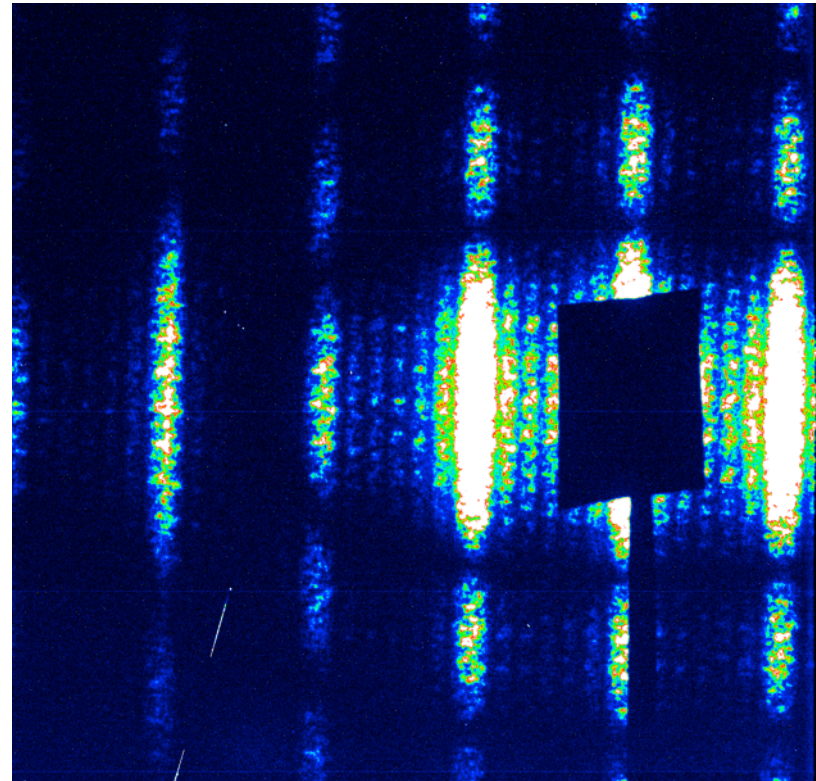
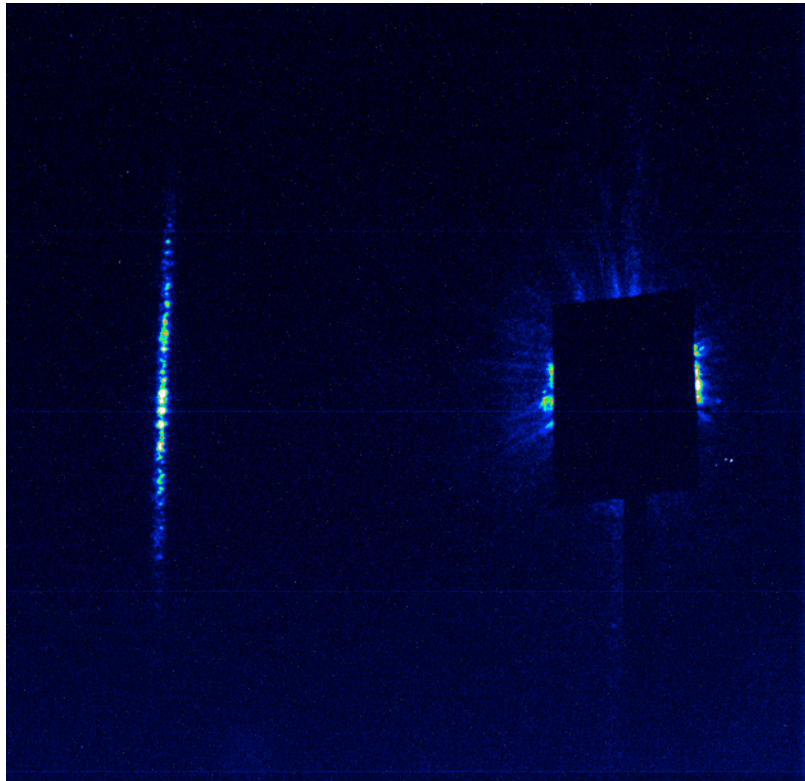


Collagen test object: ladder array

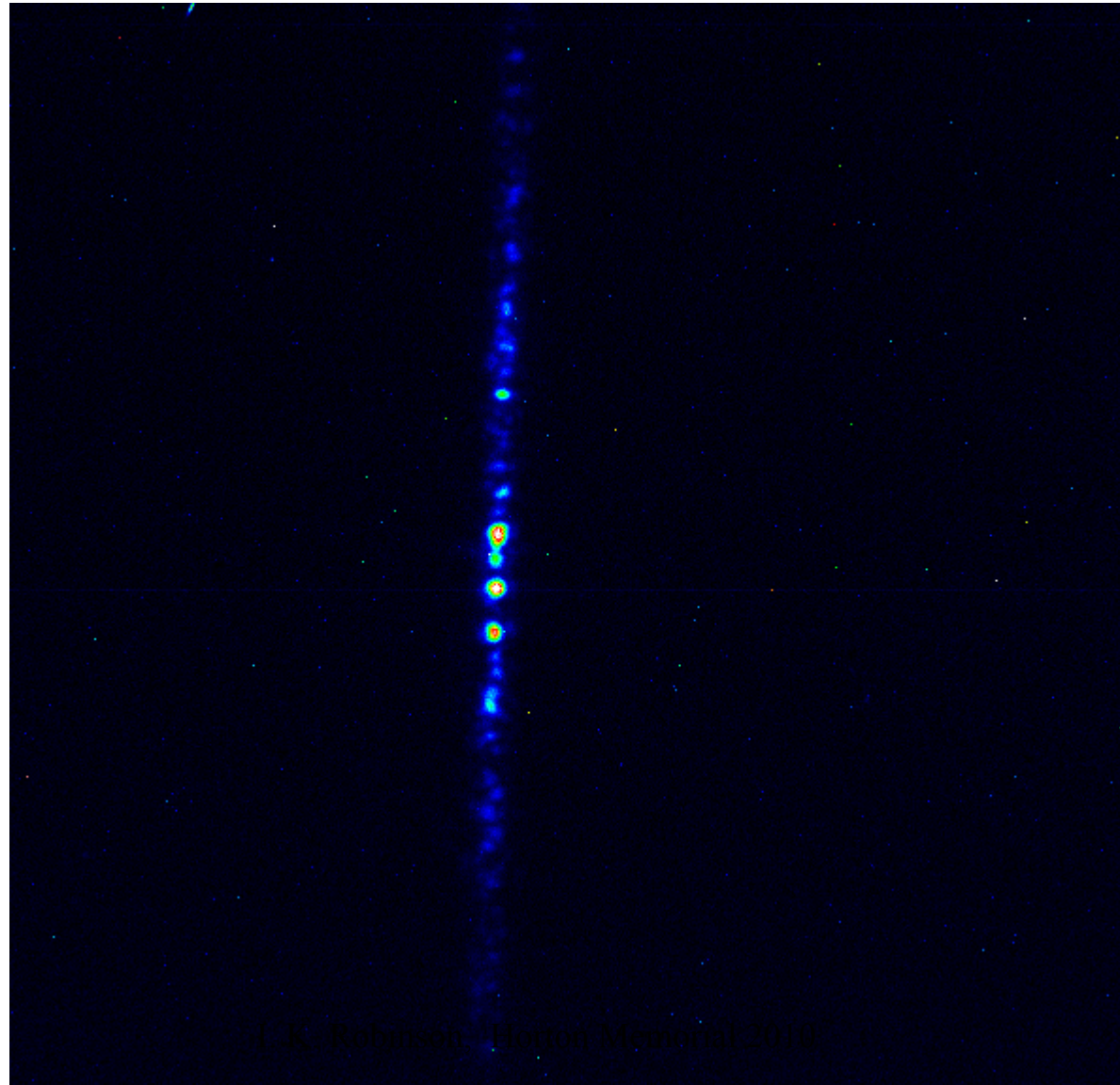
R. Bean and J. Vila-Comamala, PSI



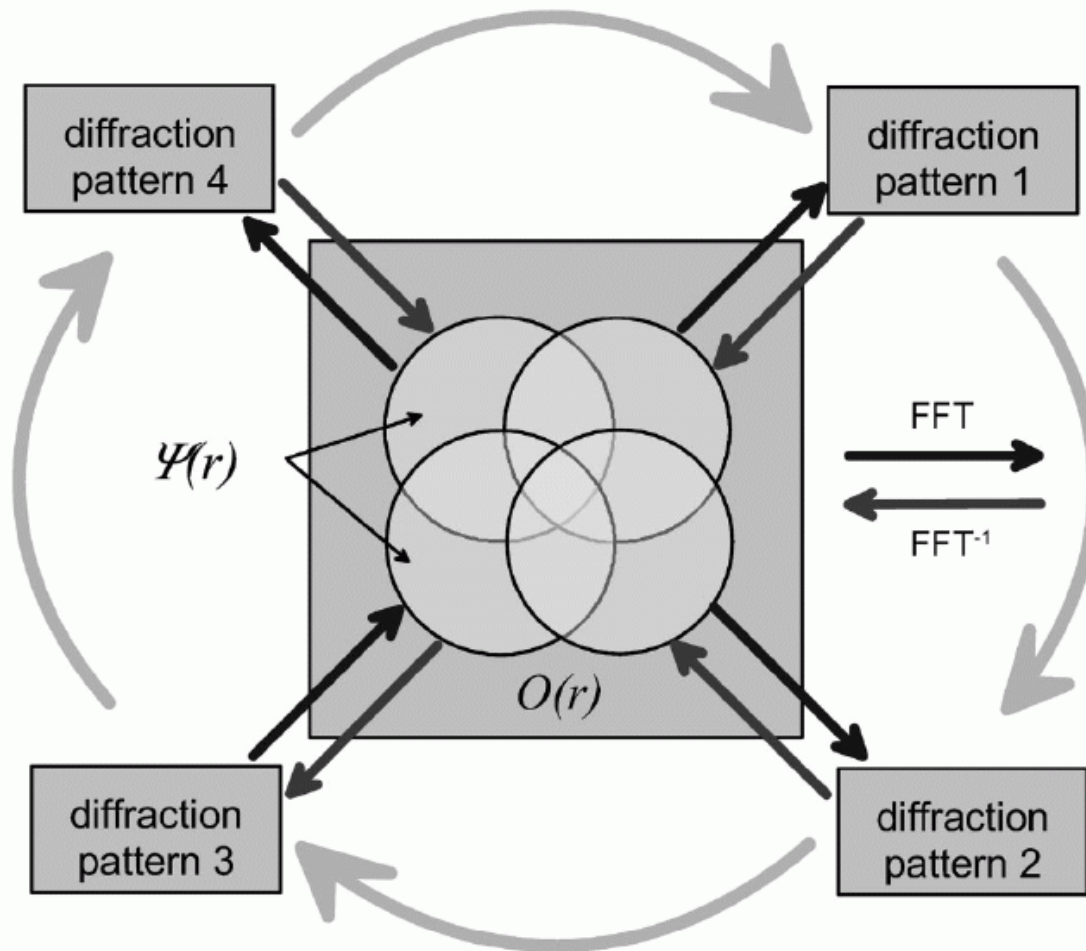
Collagen in liquid cell +/- phase plate



Sample+phase plate interference



Collagen Ptychography

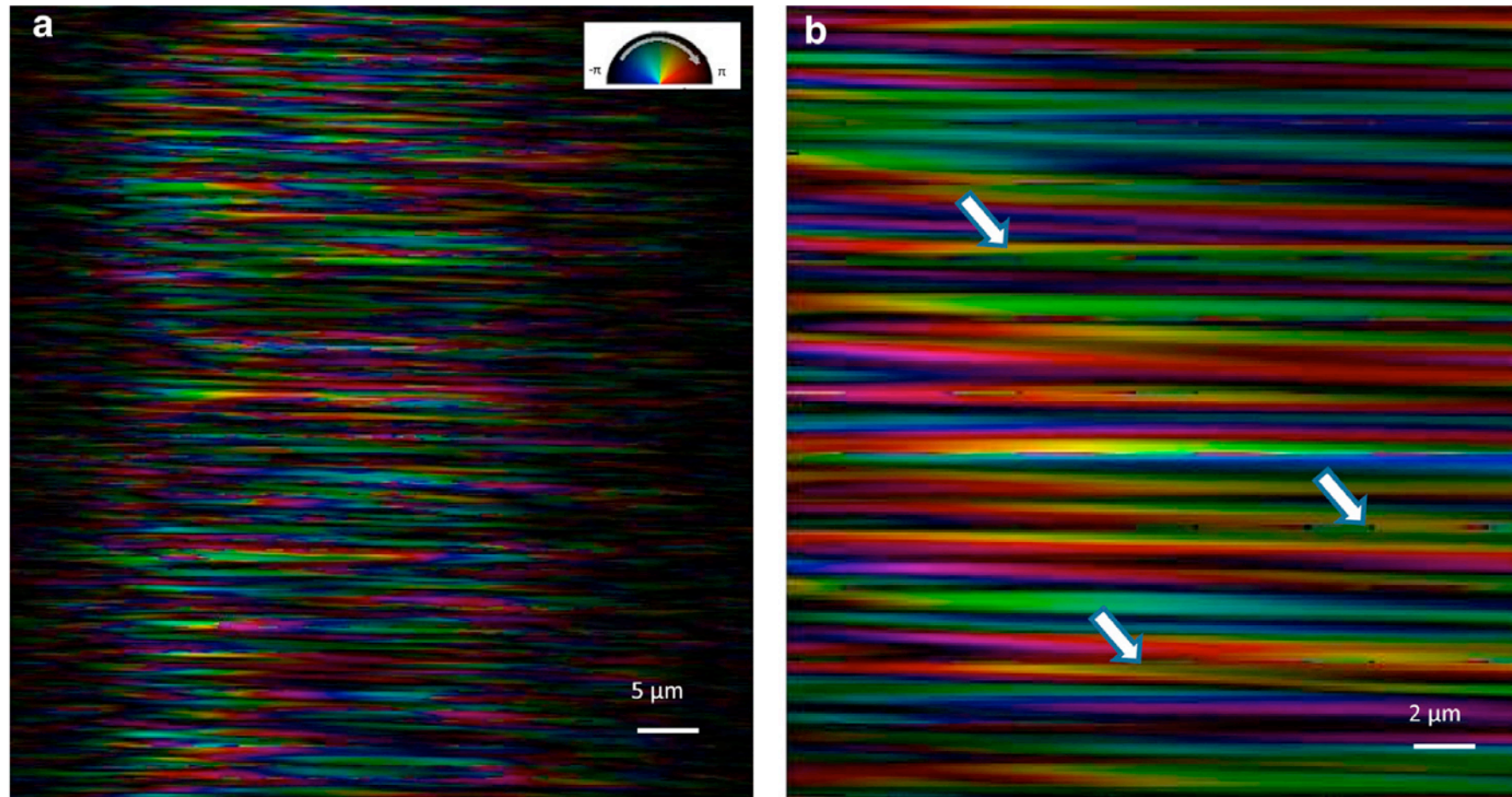


J. M. Rodenburg et al, Phys. Rev. Lett. 98 034801 (2007)

I. K. Robinson, Ghent 2018

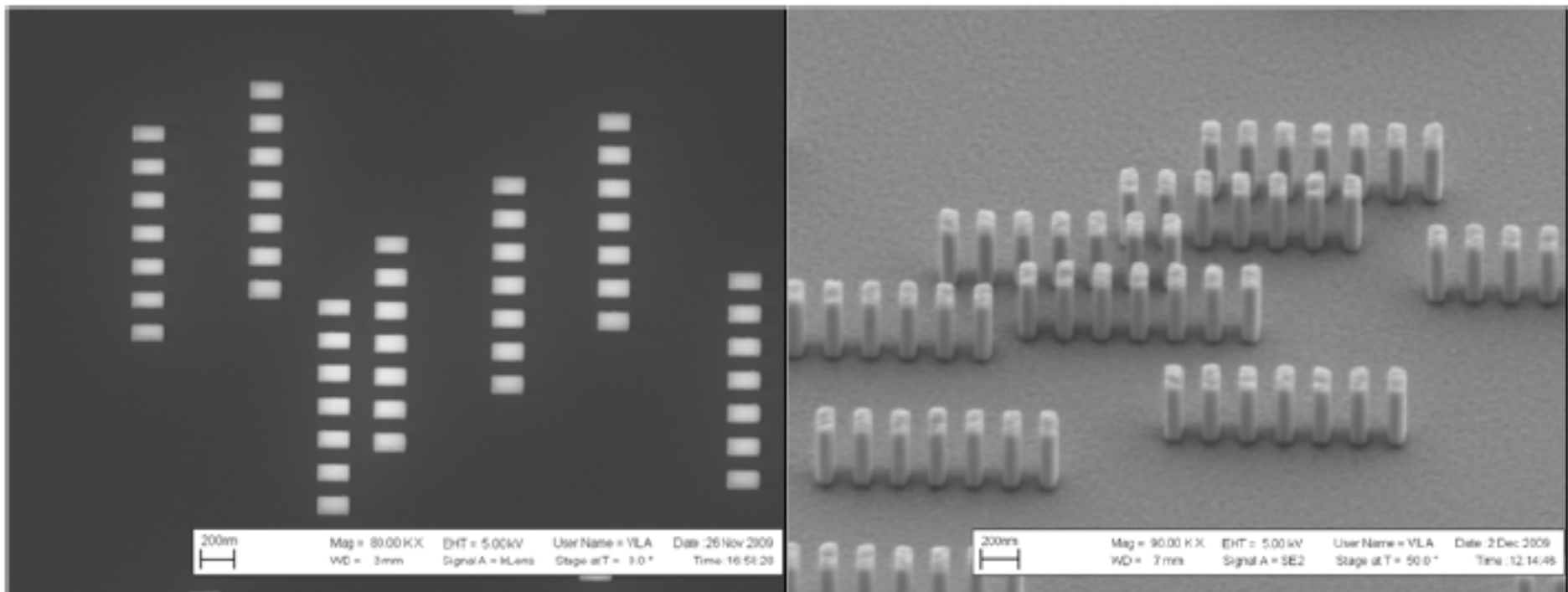
Collagen imaged with Bragg peak

Felisa Berenguer et al, Biophys. J. **106** 459 (2014)



New phase plate design: ladder array

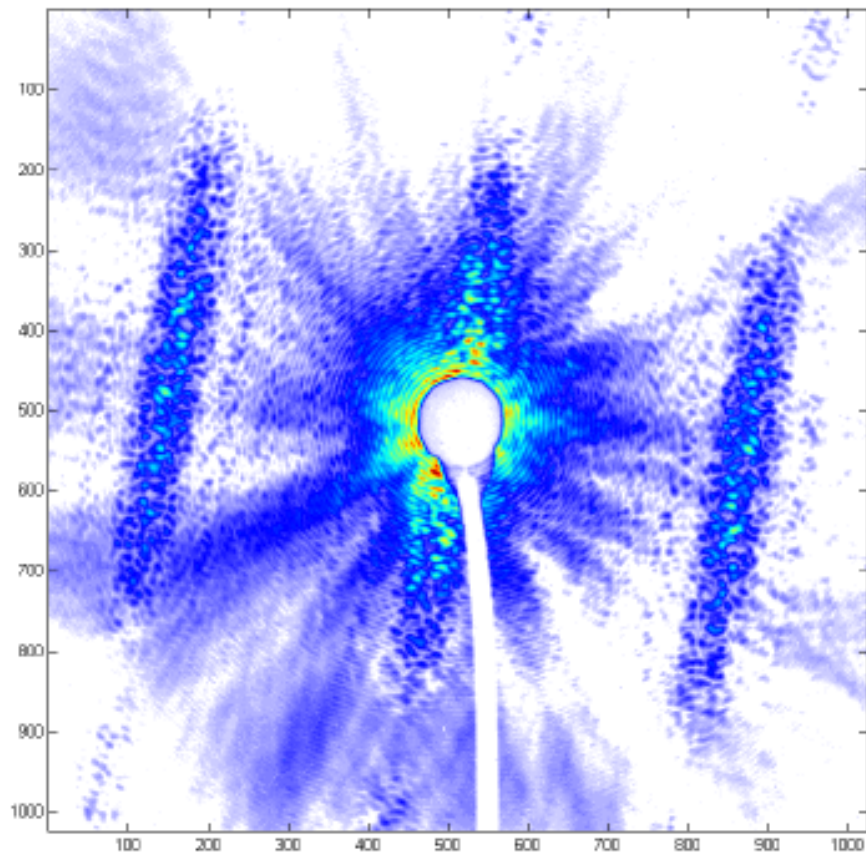
R. Bean and J. Vila-Comamala, PSI



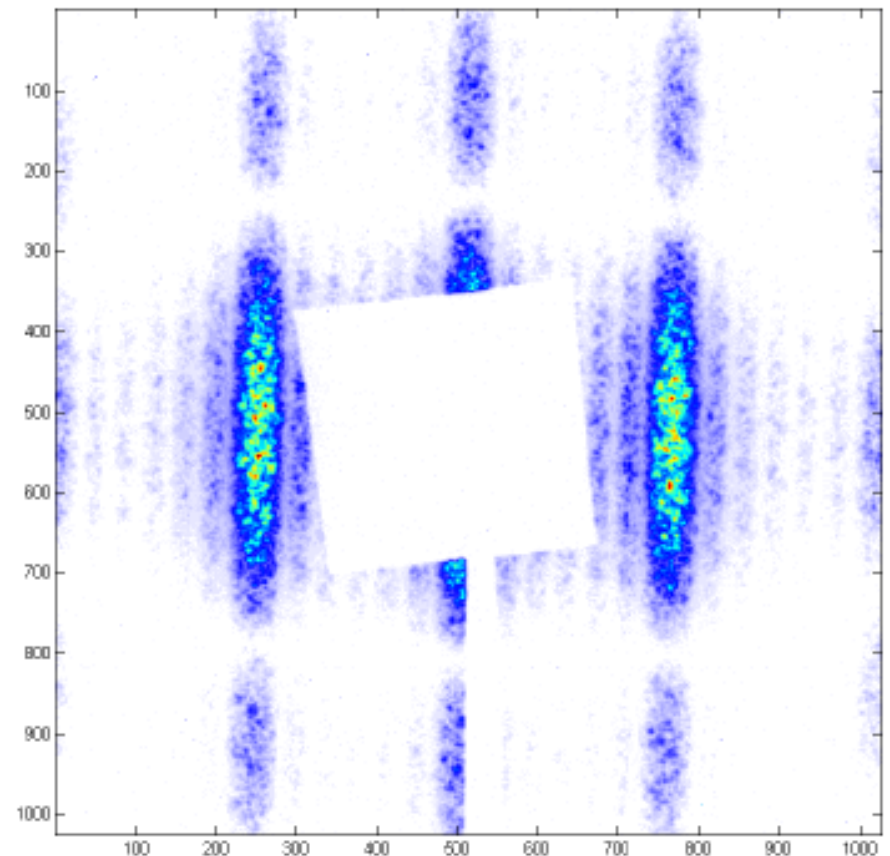
Bragg Ptychography: First Order Peak

Richard Bean, PhD Thesis 2012

Effect of clean-up pinhole



(a)

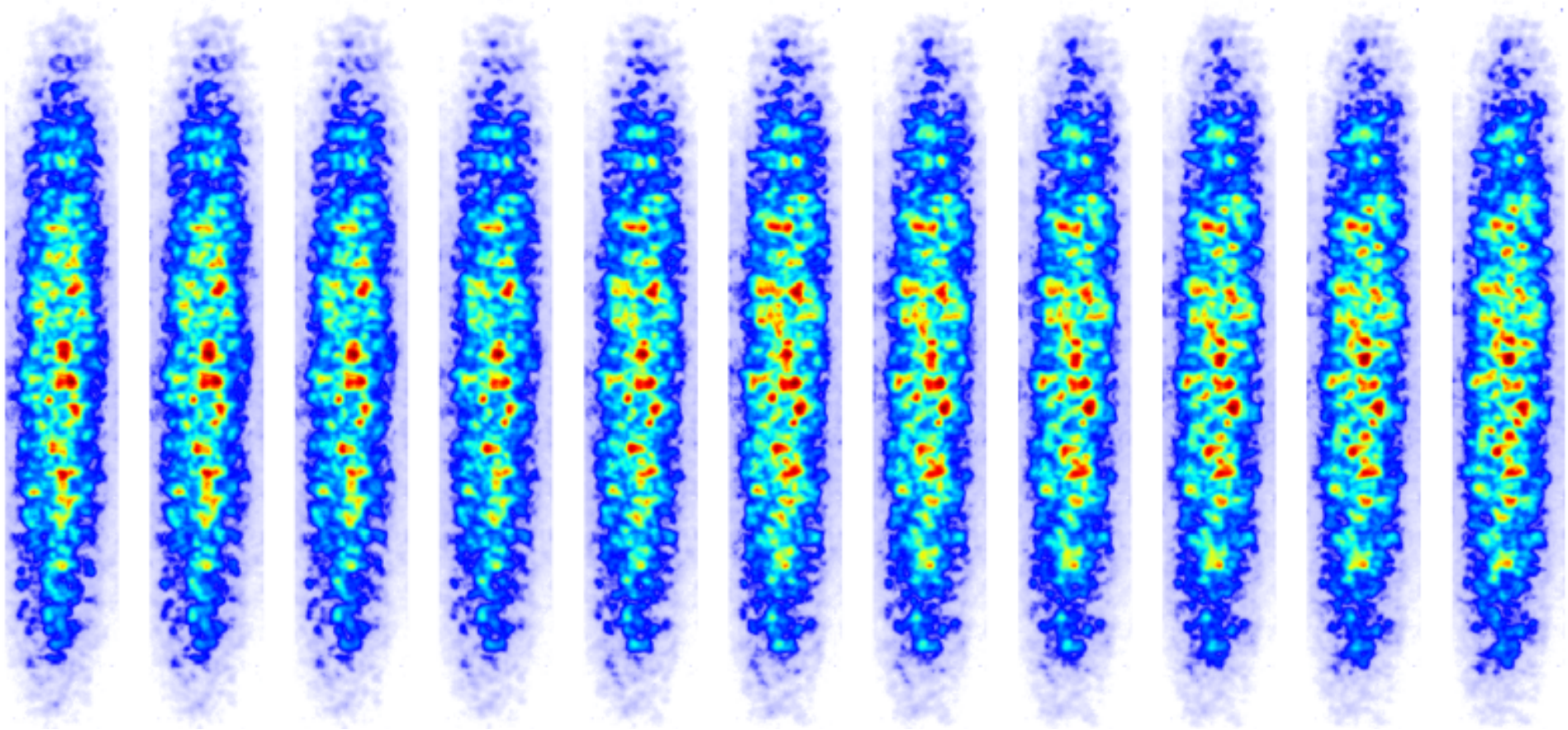


(b)

Bragg Ptychography: First Order Peak

Richard Bean, PhD Thesis 2012

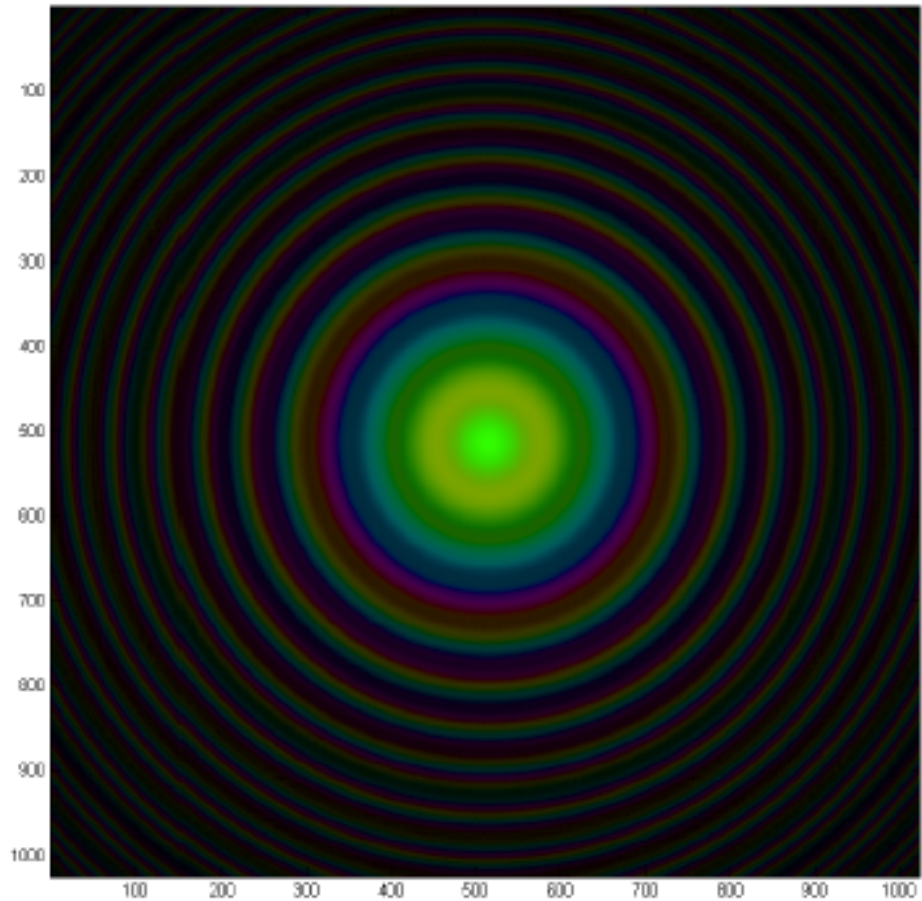
Measured ptychographic series



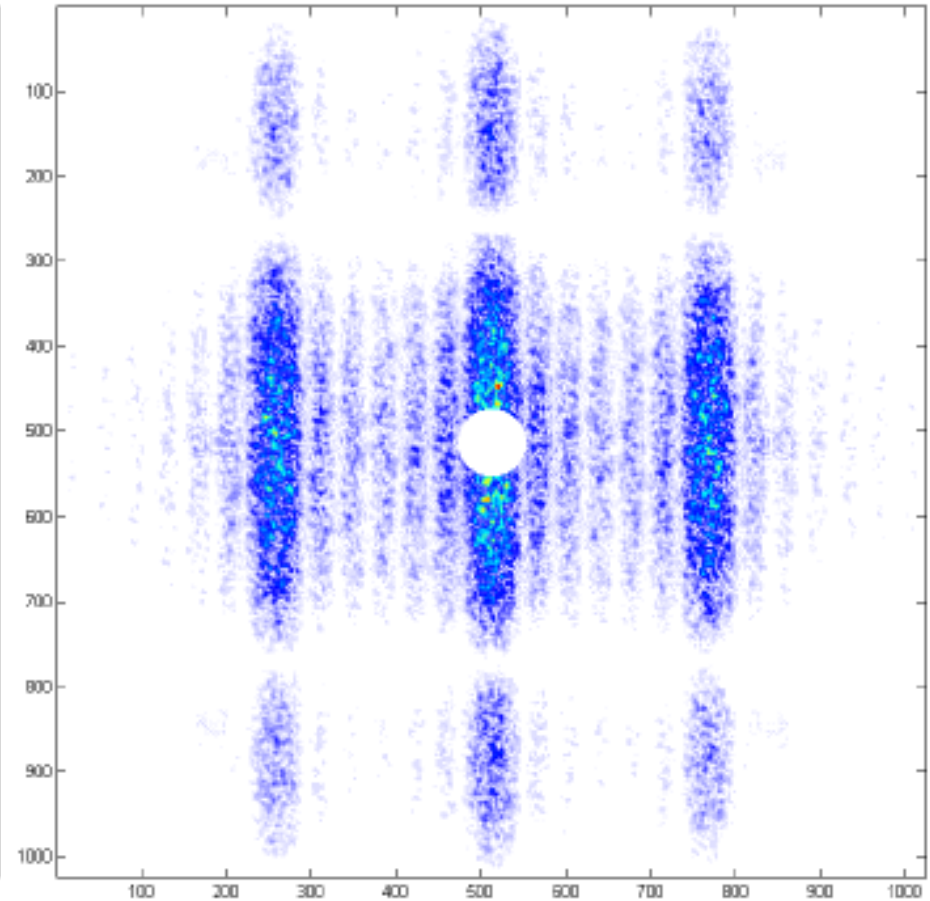
Bragg Ptychography: First Order Peak

Richard Bean, PhD Thesis 2012

Simulated probe and diffraction pattern



(a)



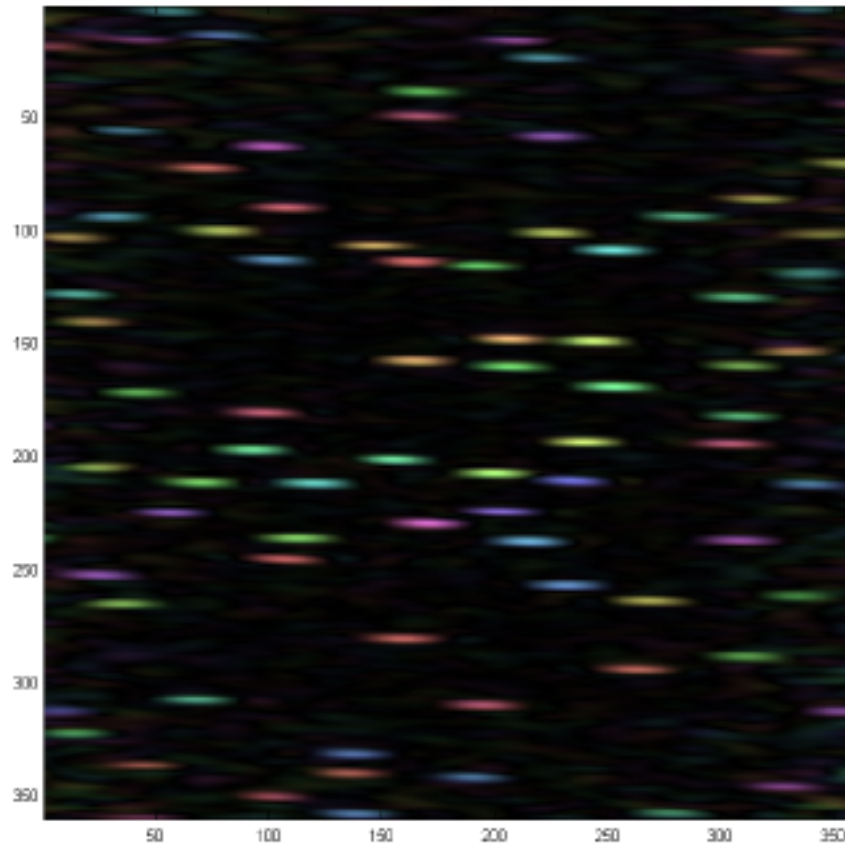
(b)

Bragg Ptychography: First Order Peak

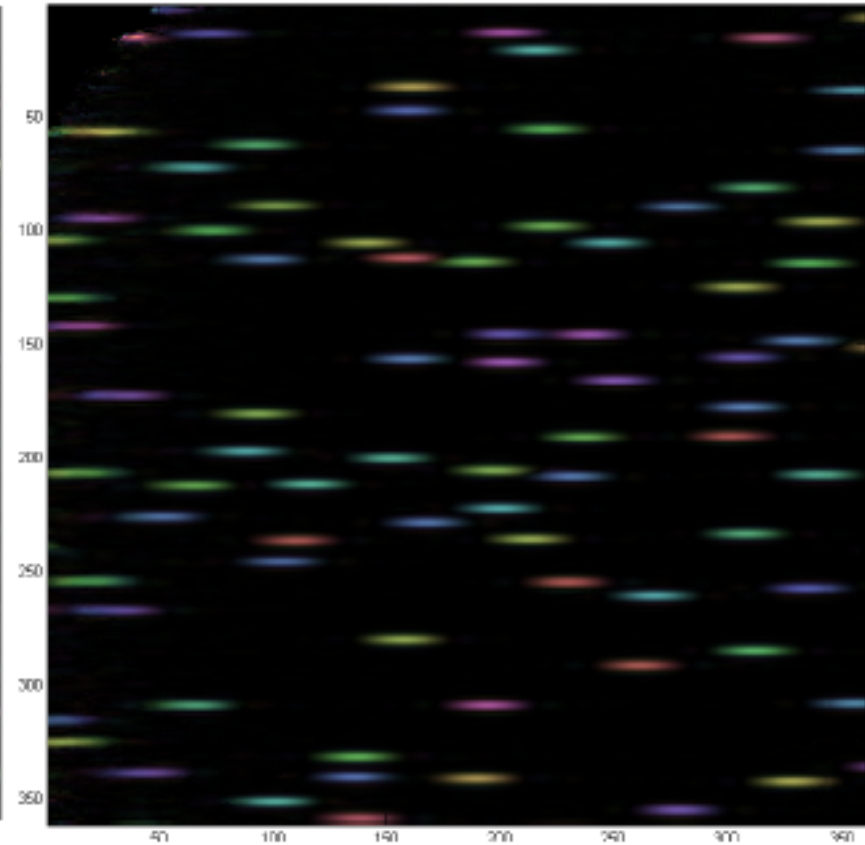
Richard Bean, PhD Thesis 2012

Measured Object

Simulated Object



(a)



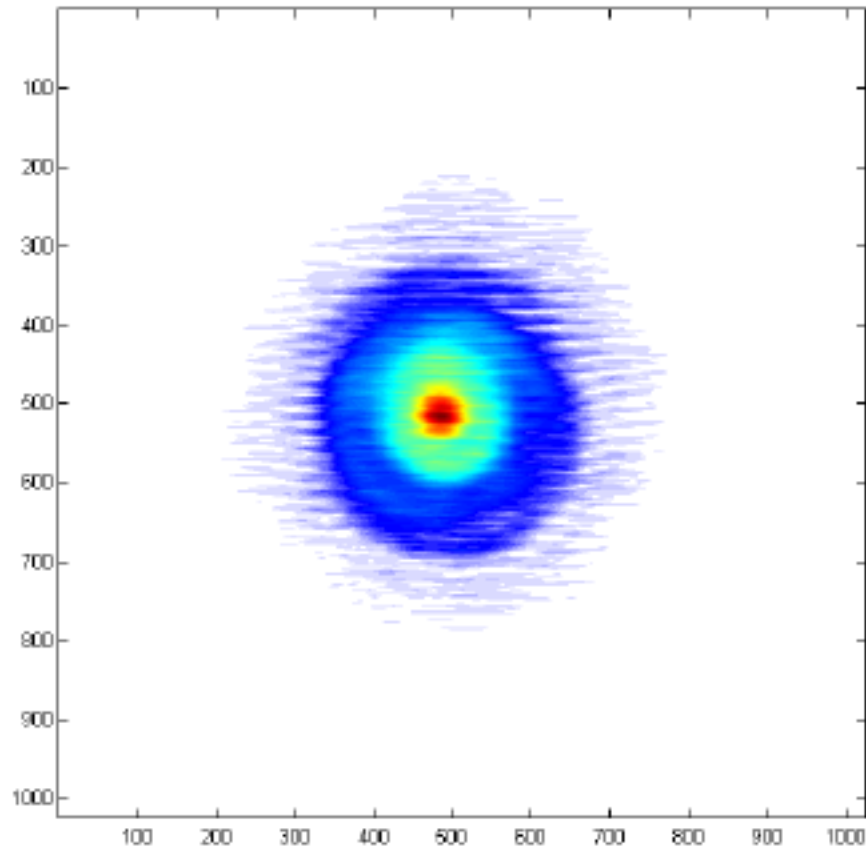
(b)

Bragg Ptychography: First Order Peak

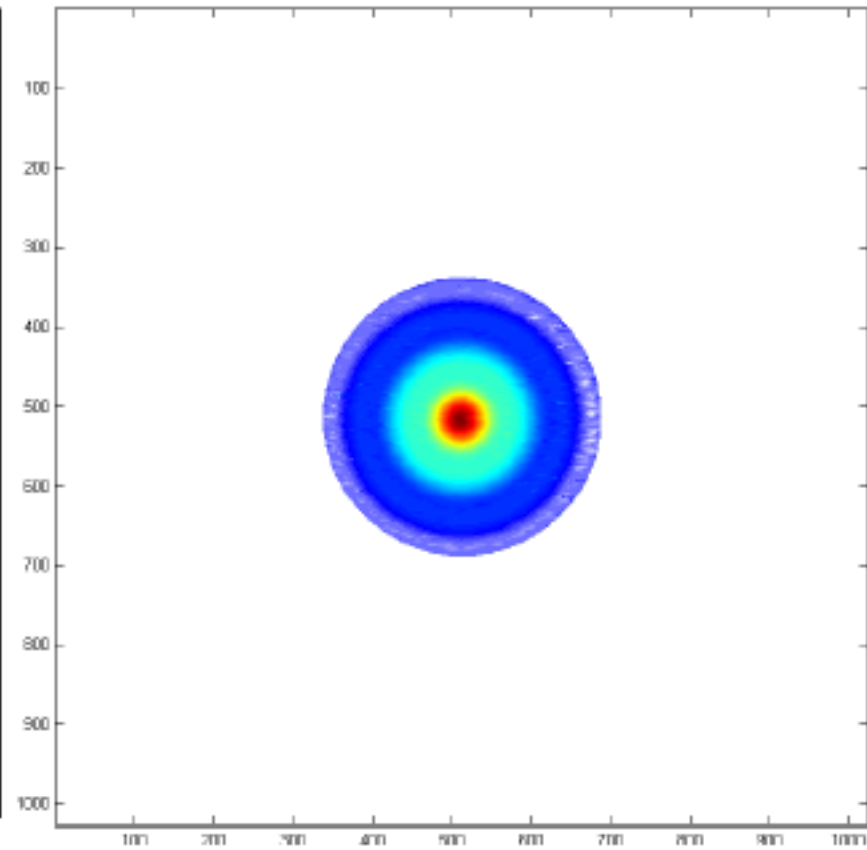
Richard Bean, PhD Thesis 2012

Measured Probe

Simulated Probe

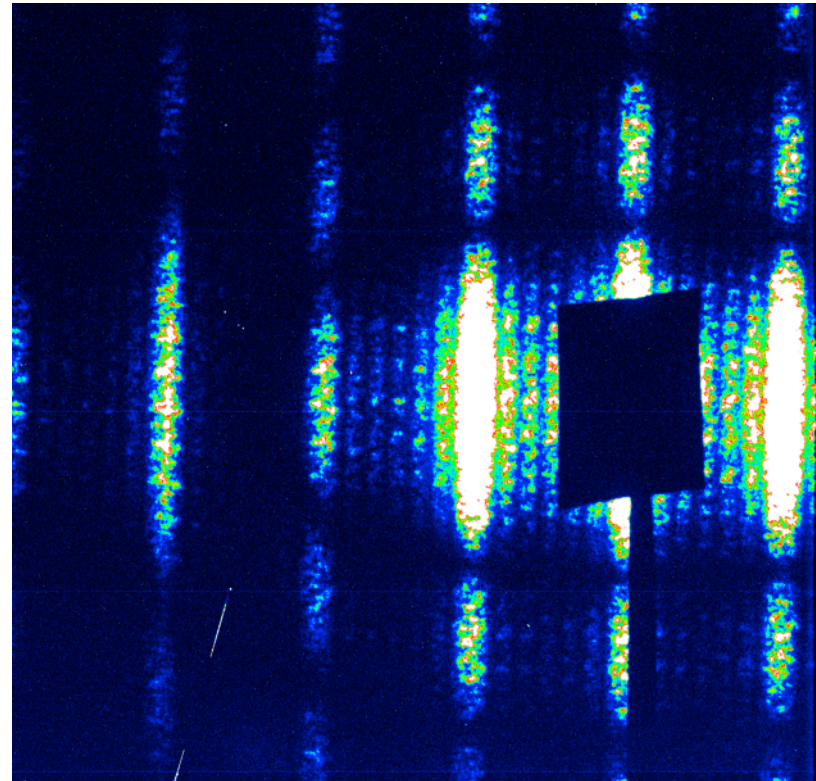
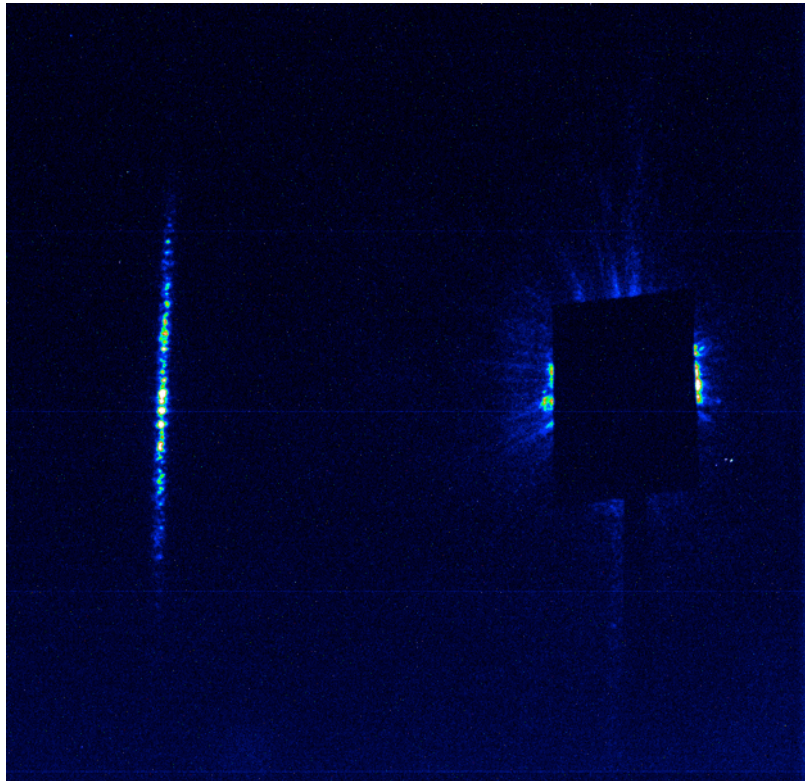


(a)

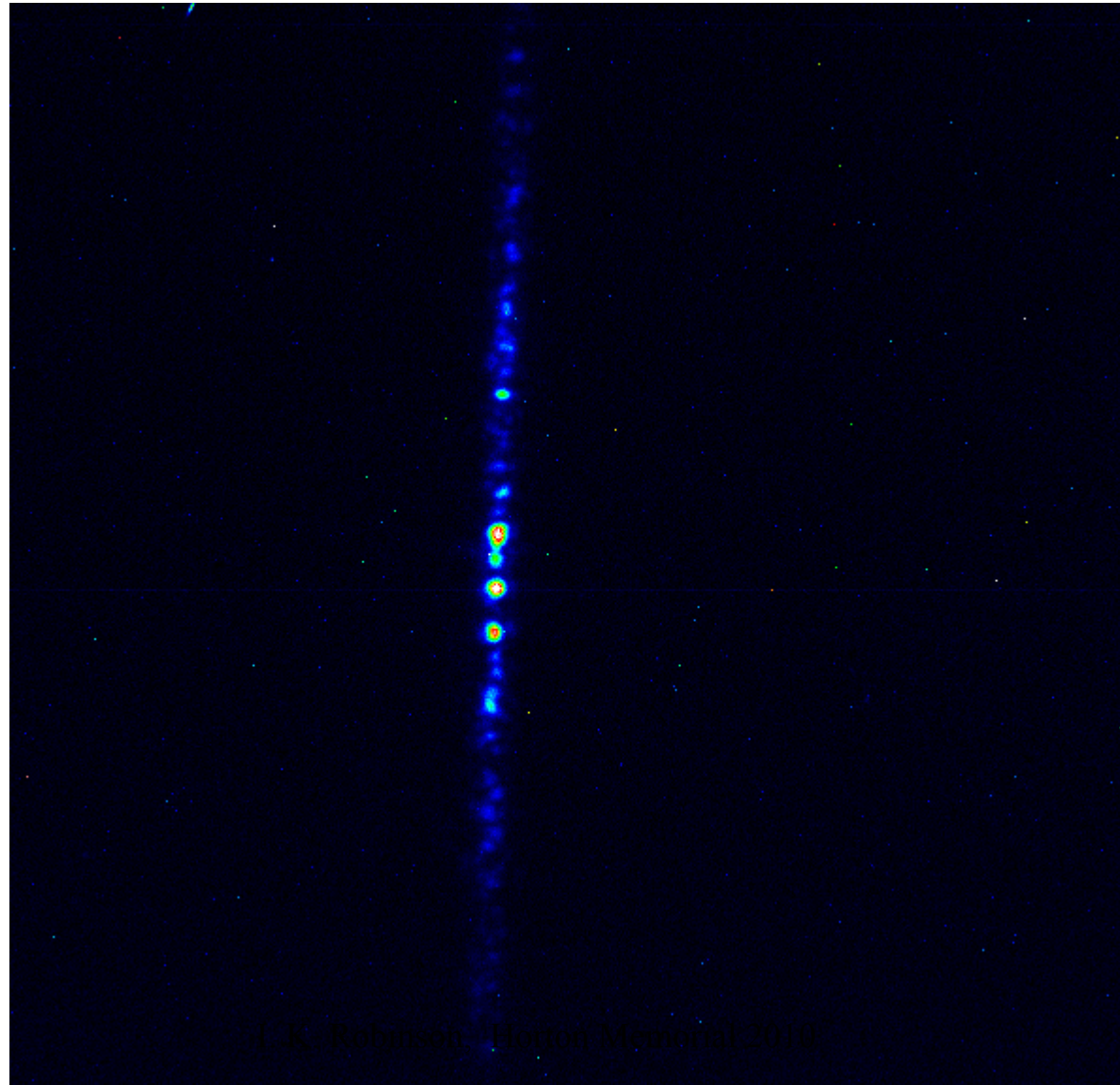


(b)

Collagen in liquid cell +/- phase plate



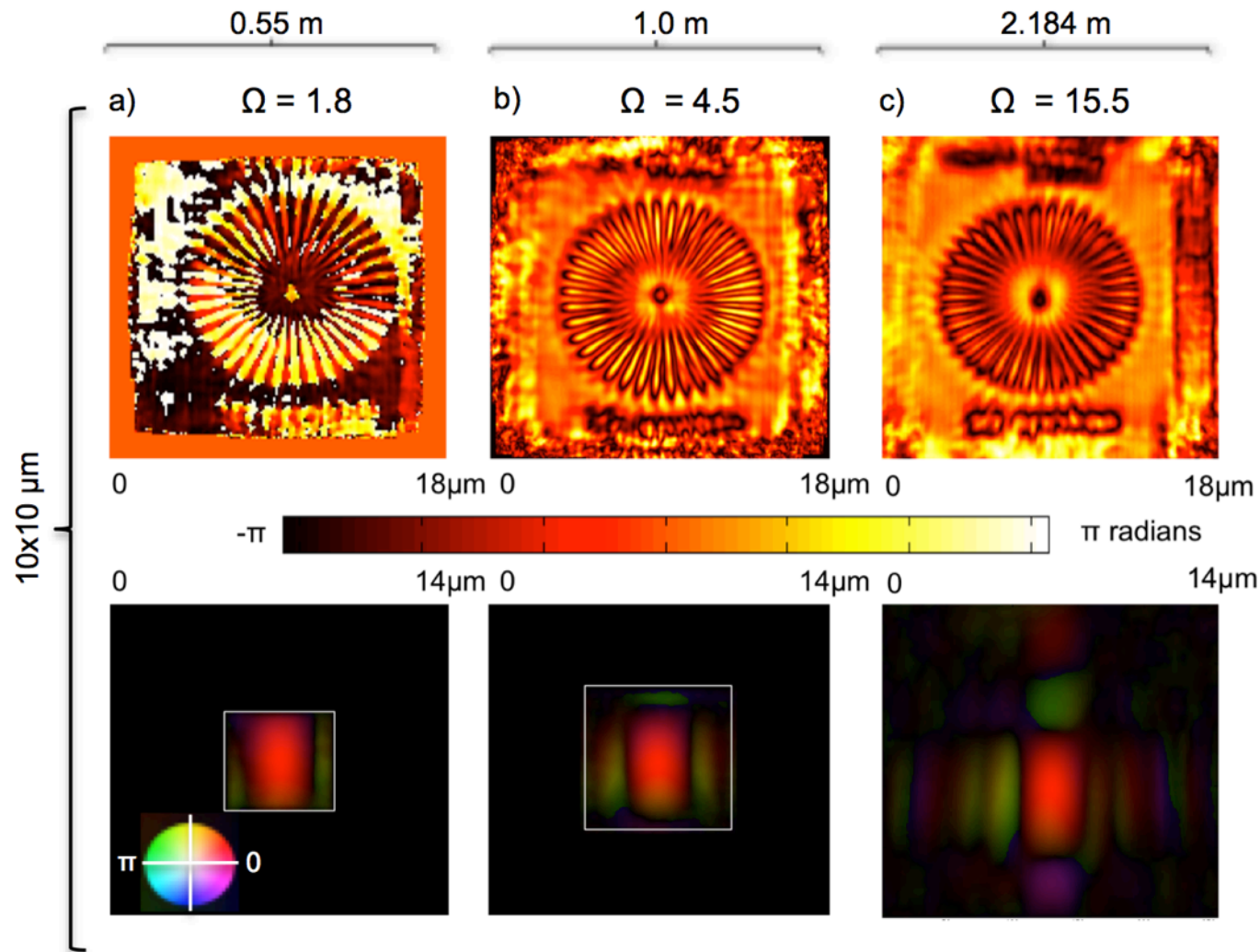
Sample+phase plate interference



J. K. Robinson, Hottel Memorial 2010

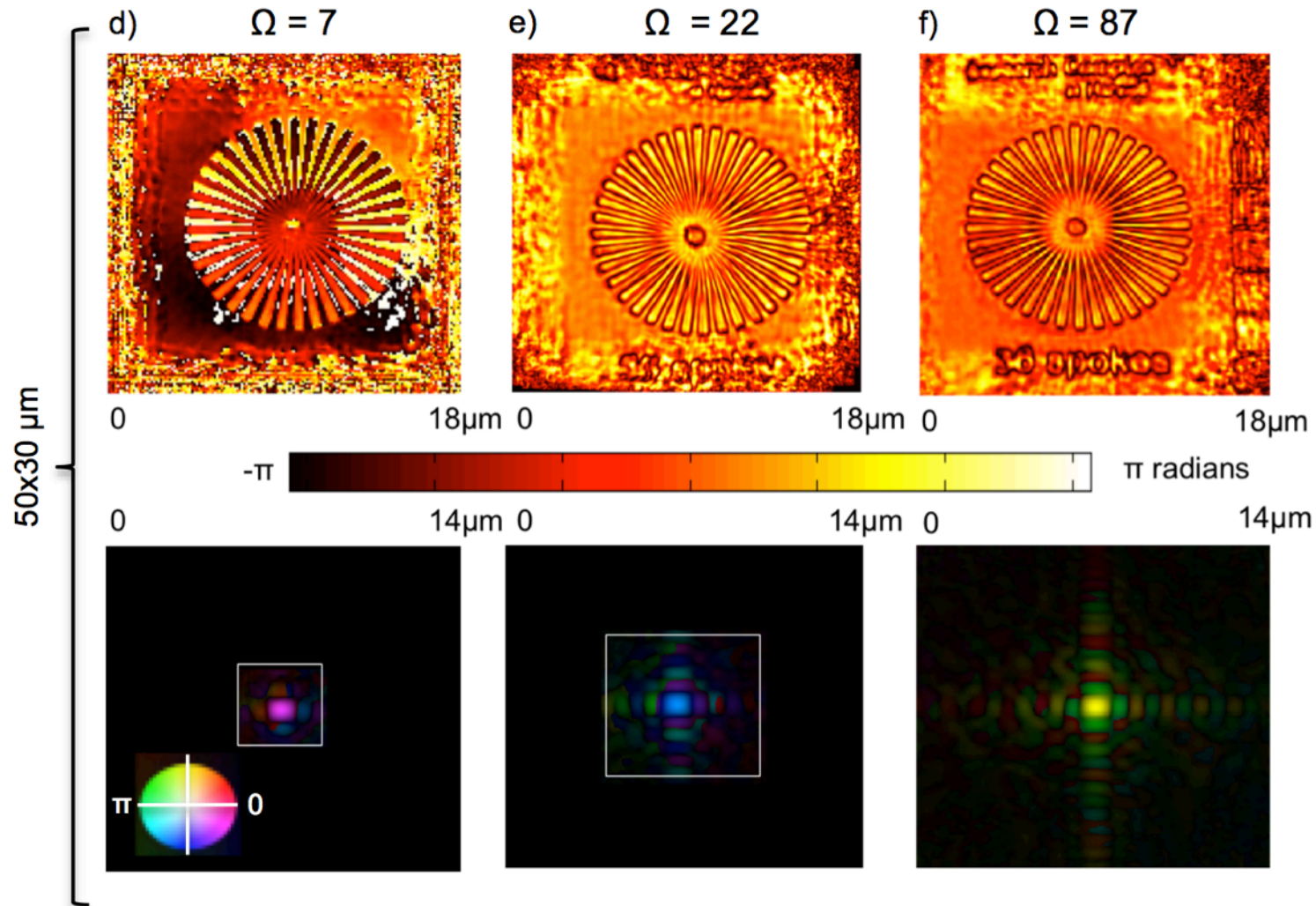
Diversity in Ptychography

Nicolas Burdet et al, Optics Express 22 10294 (2014)



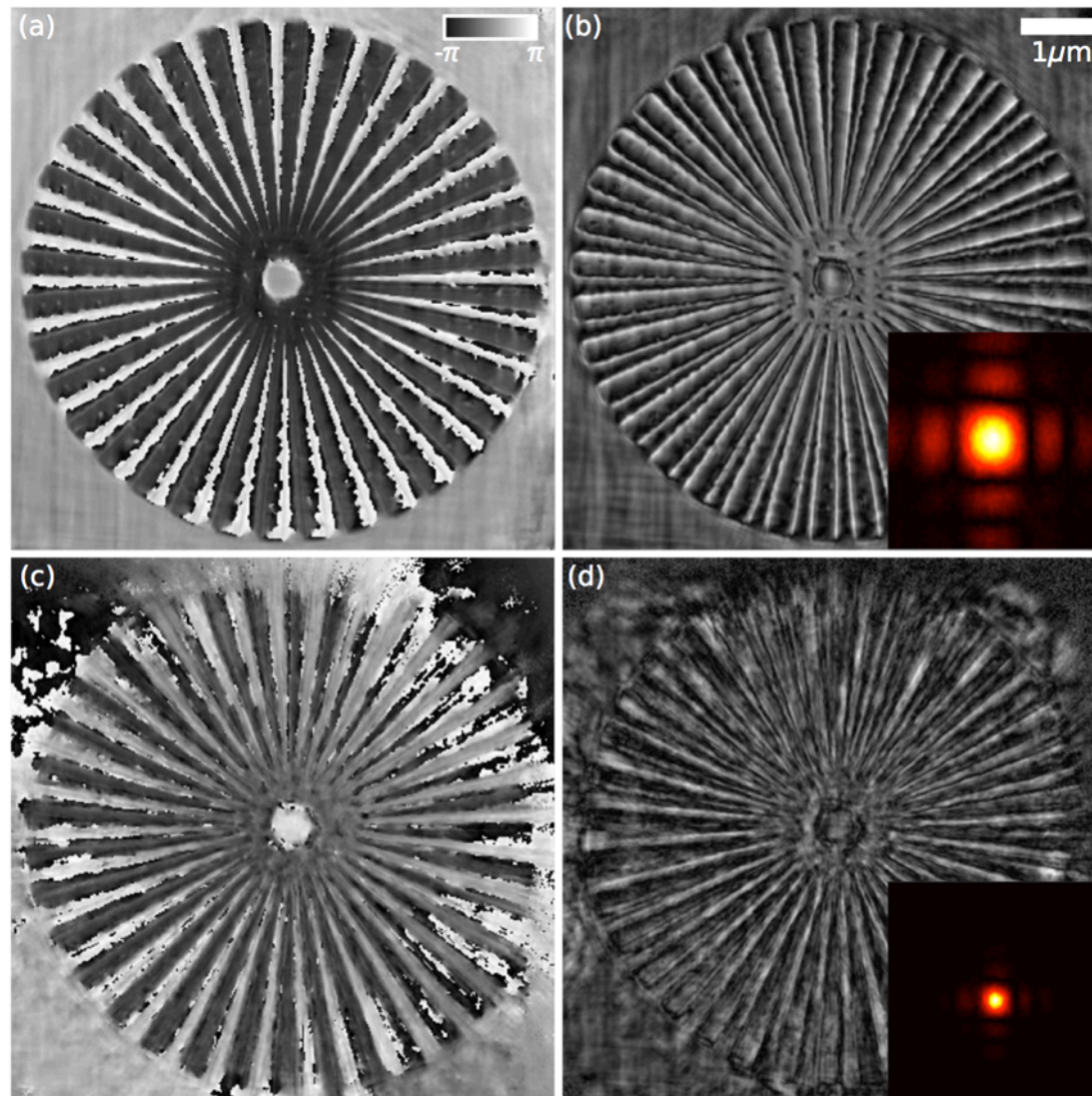
Diversity in Ptychography

Nicolas Burdet et al, Optics Express 22 10294 (2014)



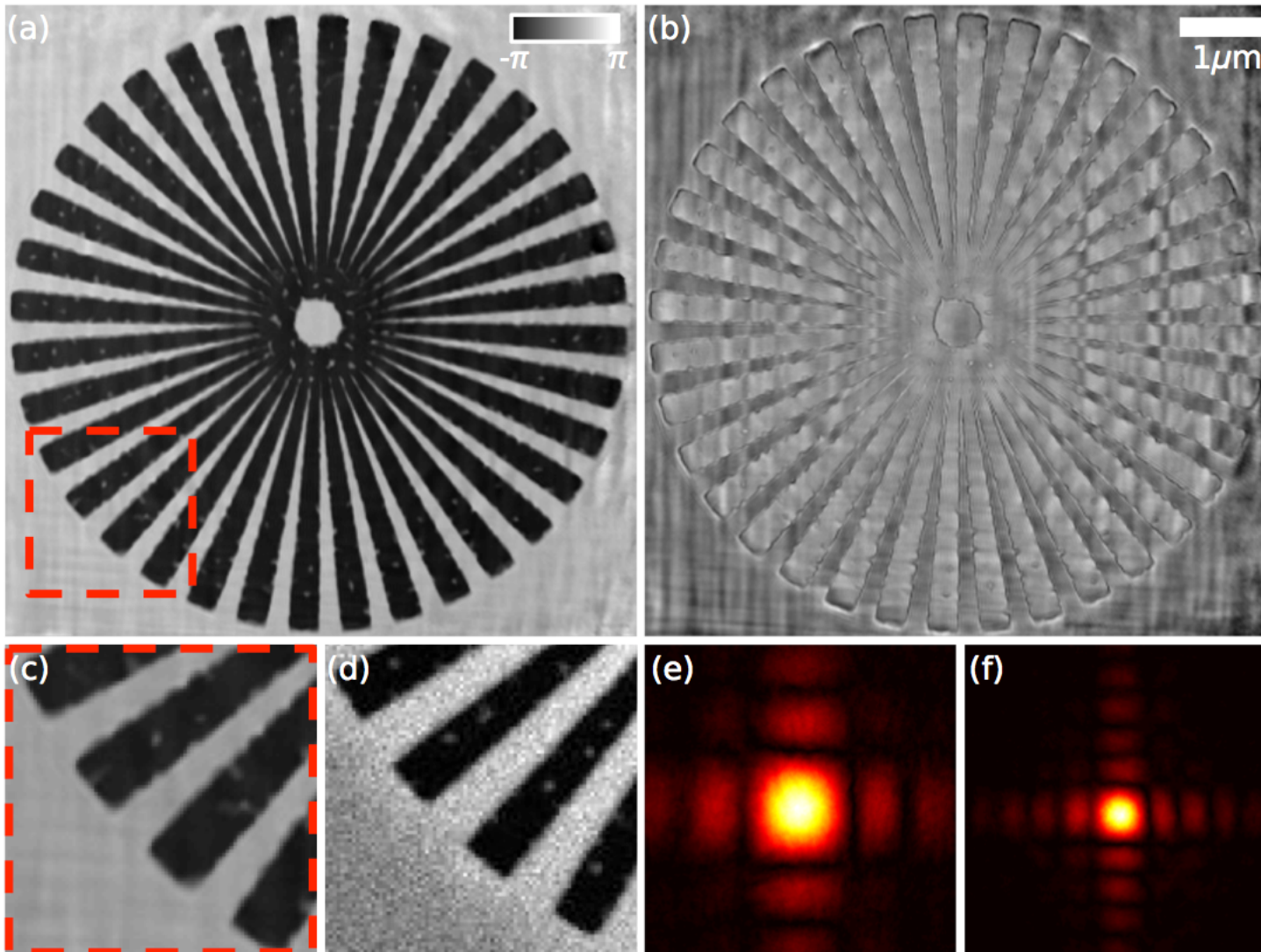
Probe-diverse Ptychography

I. Peterson, et al submitted to Optics Express



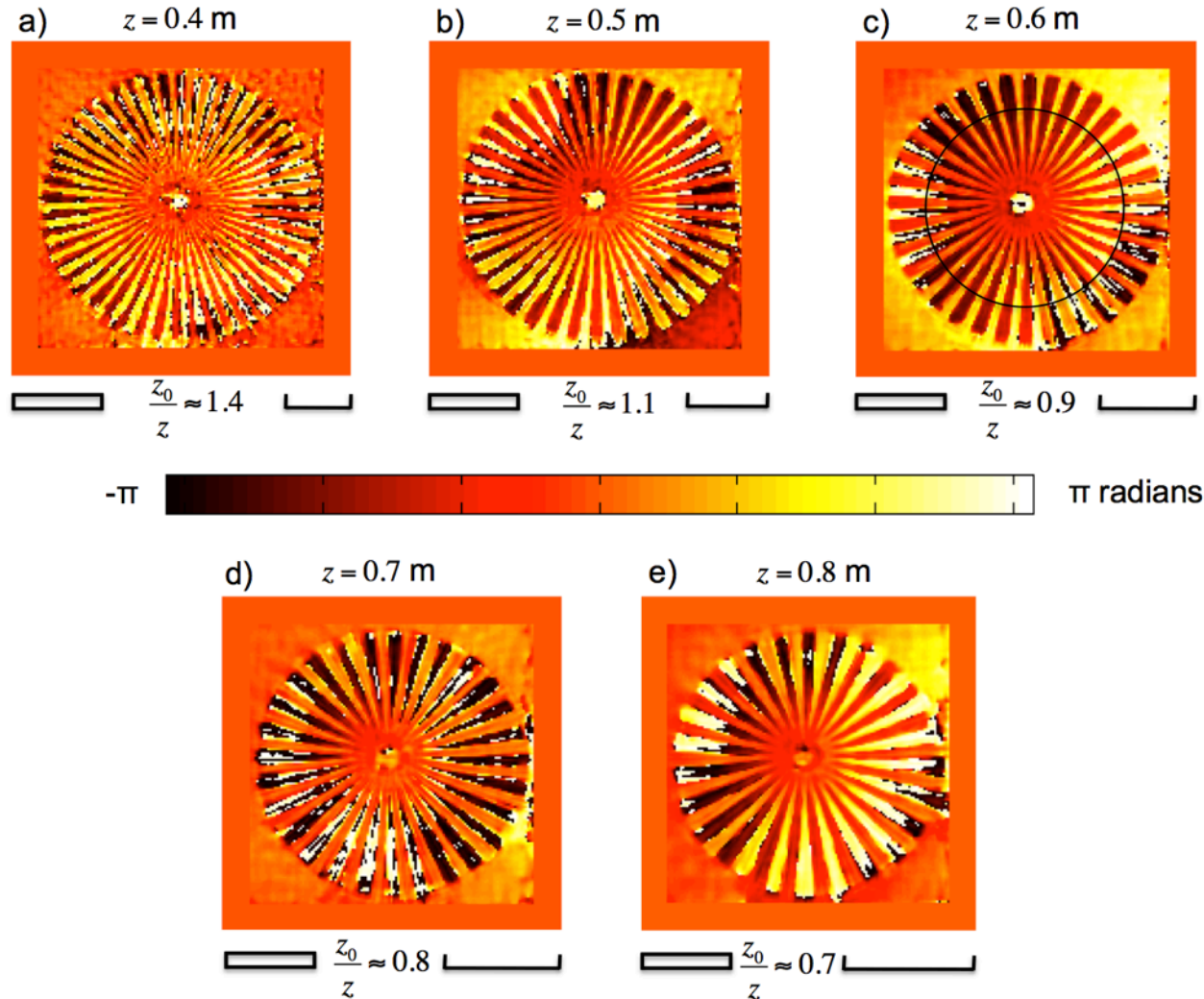
Probe-diverse Ptychography

Isaac Peterson, et al submitted to Optics Express



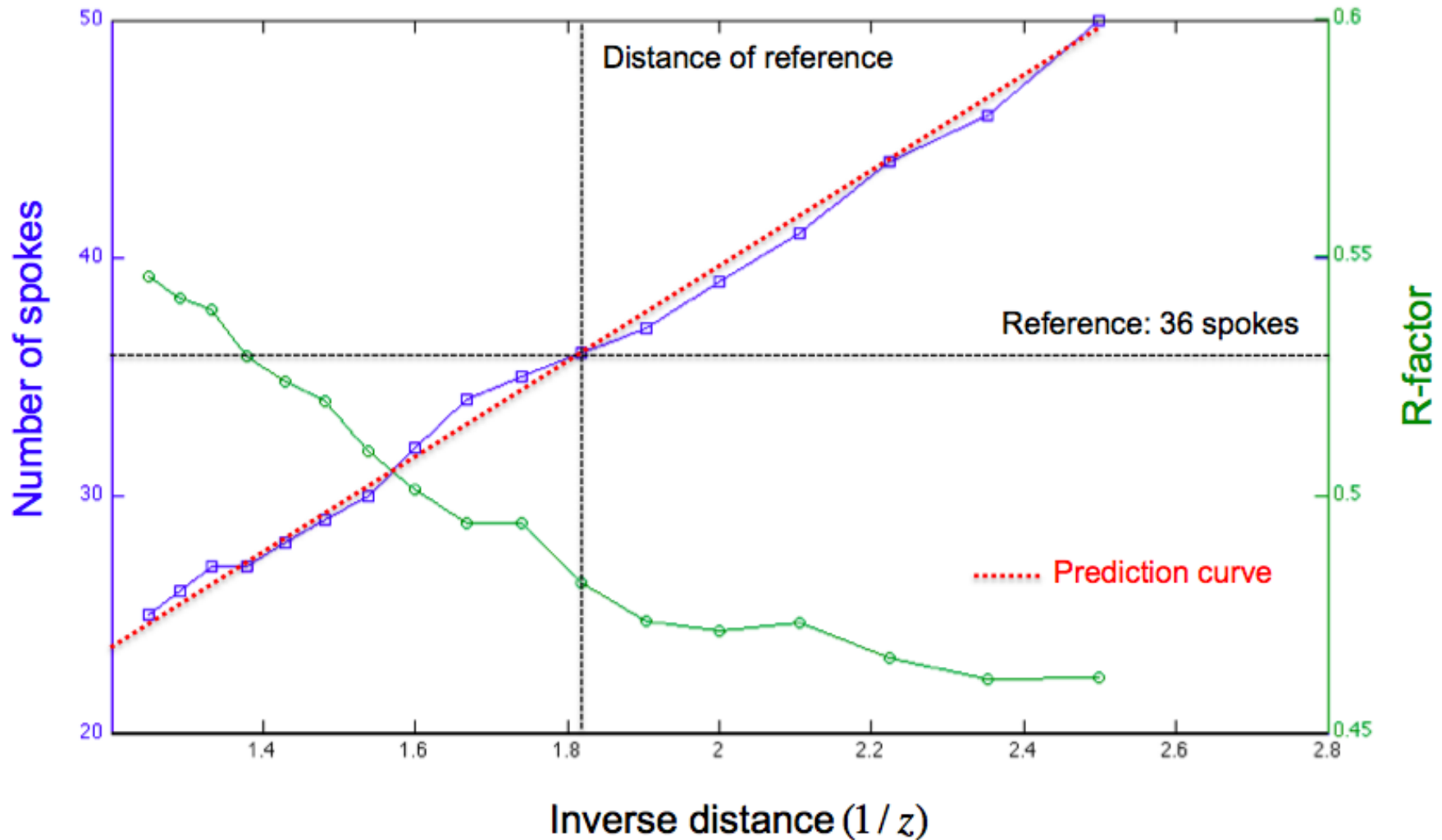
Ptychography Artefacts?

Nicolas Burdet et al, Optics Express 22 10294 (2014)



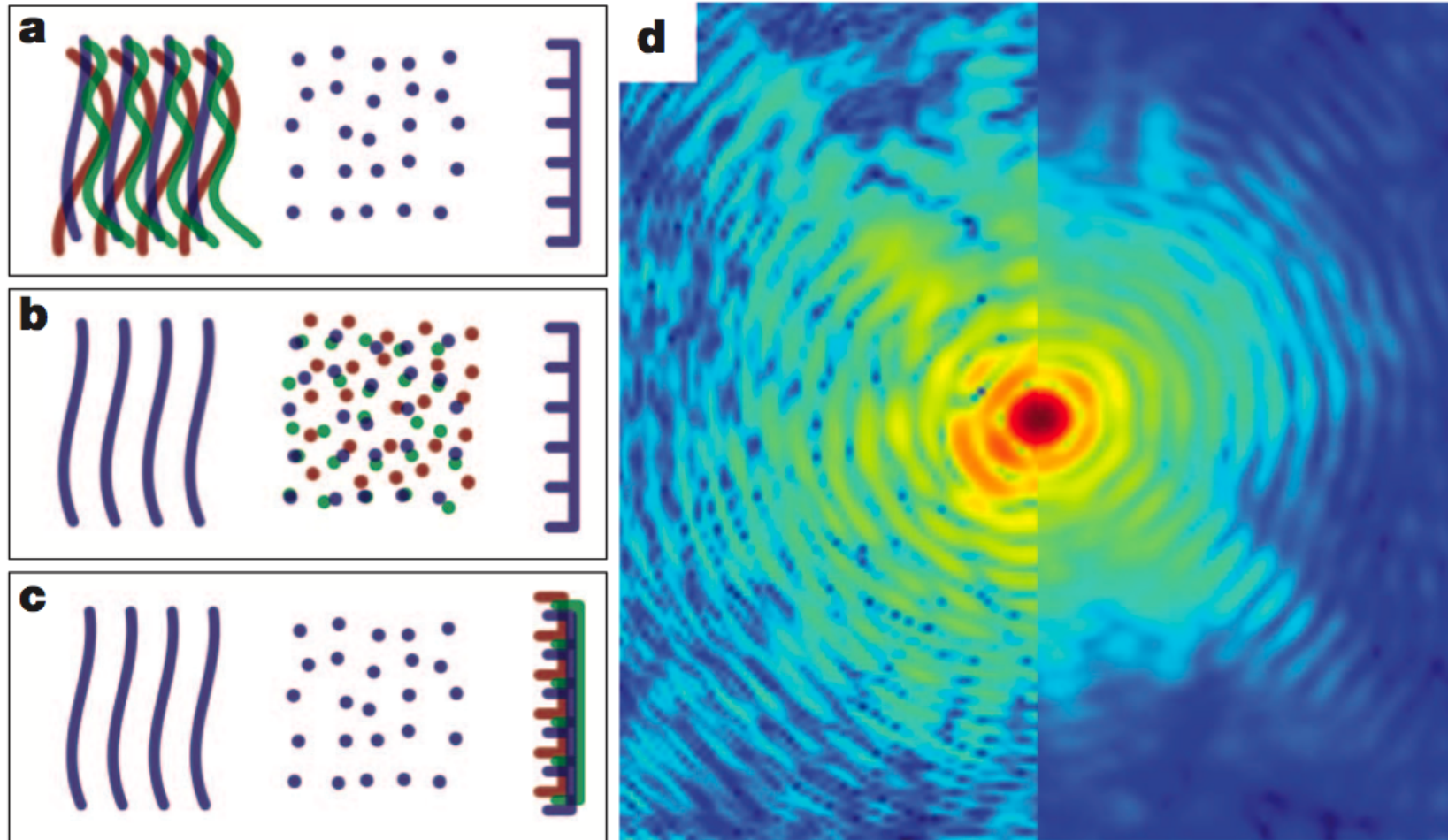
Artefacts in X-ray ptychography

Nicolas Burdet et al, Optics Express 22 10294 (2014)



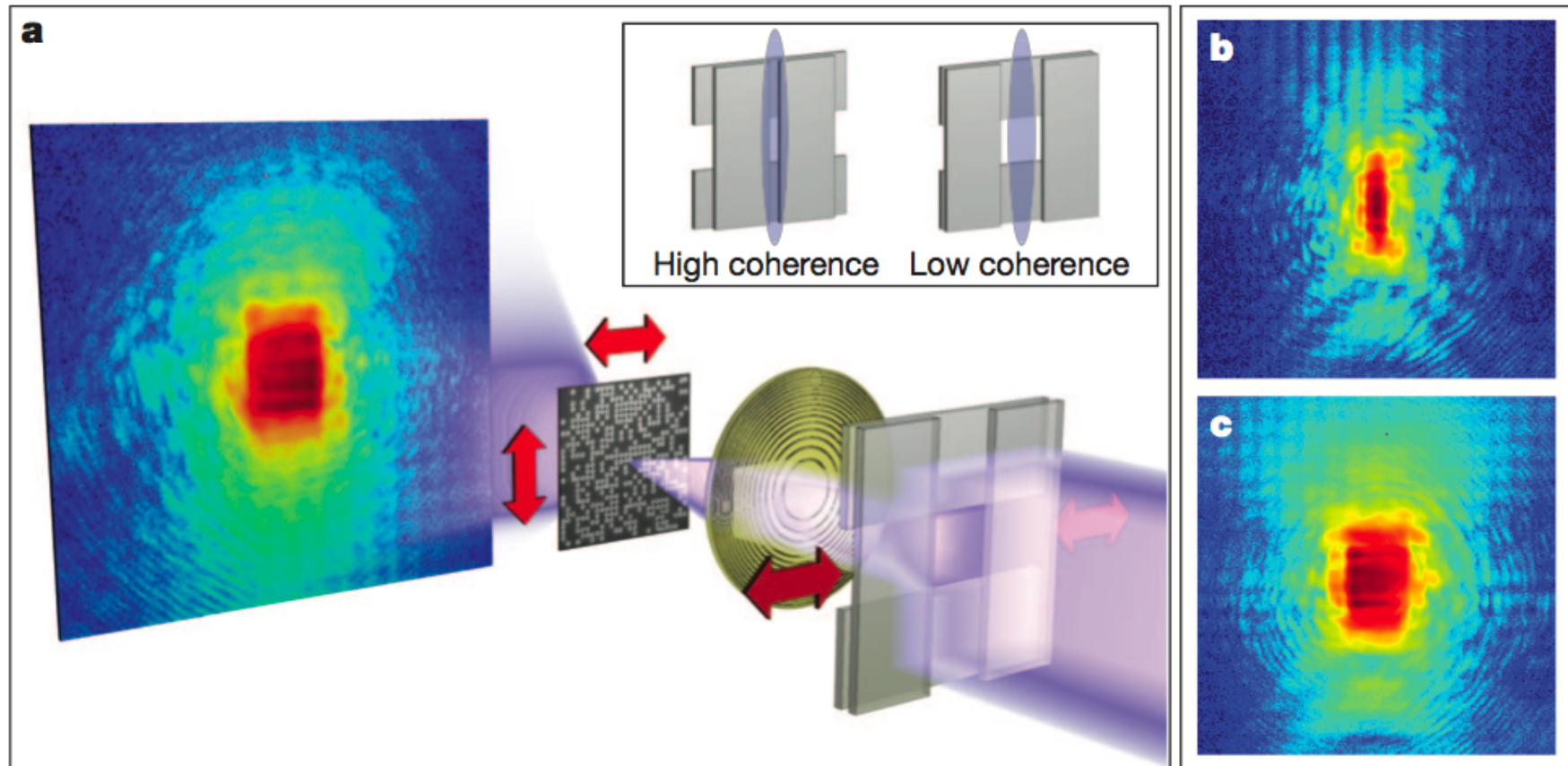
Modal Decomposition in Ptychography

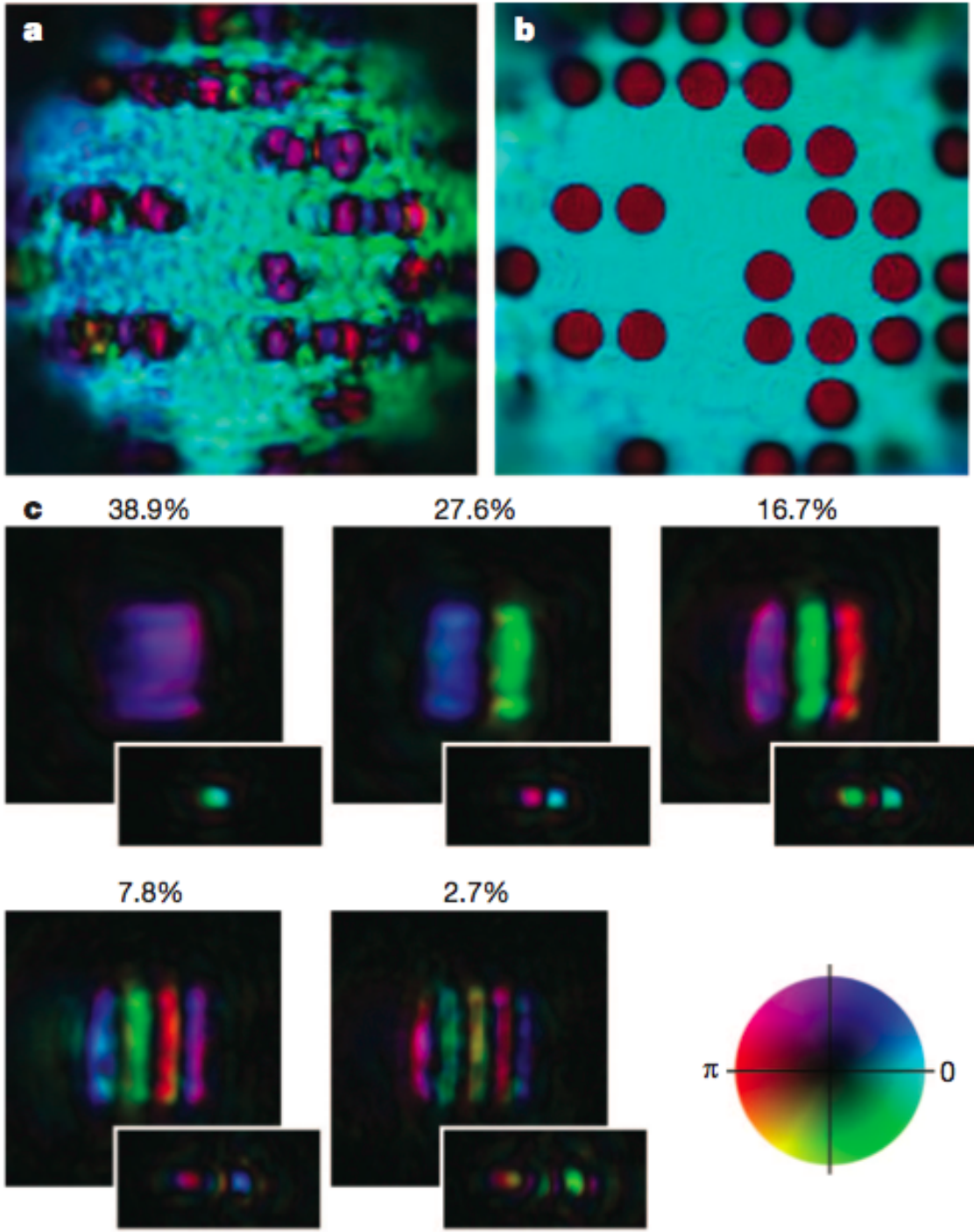
Pierre Thibault & Andreas Menzel, Nature 494 68 (2013)



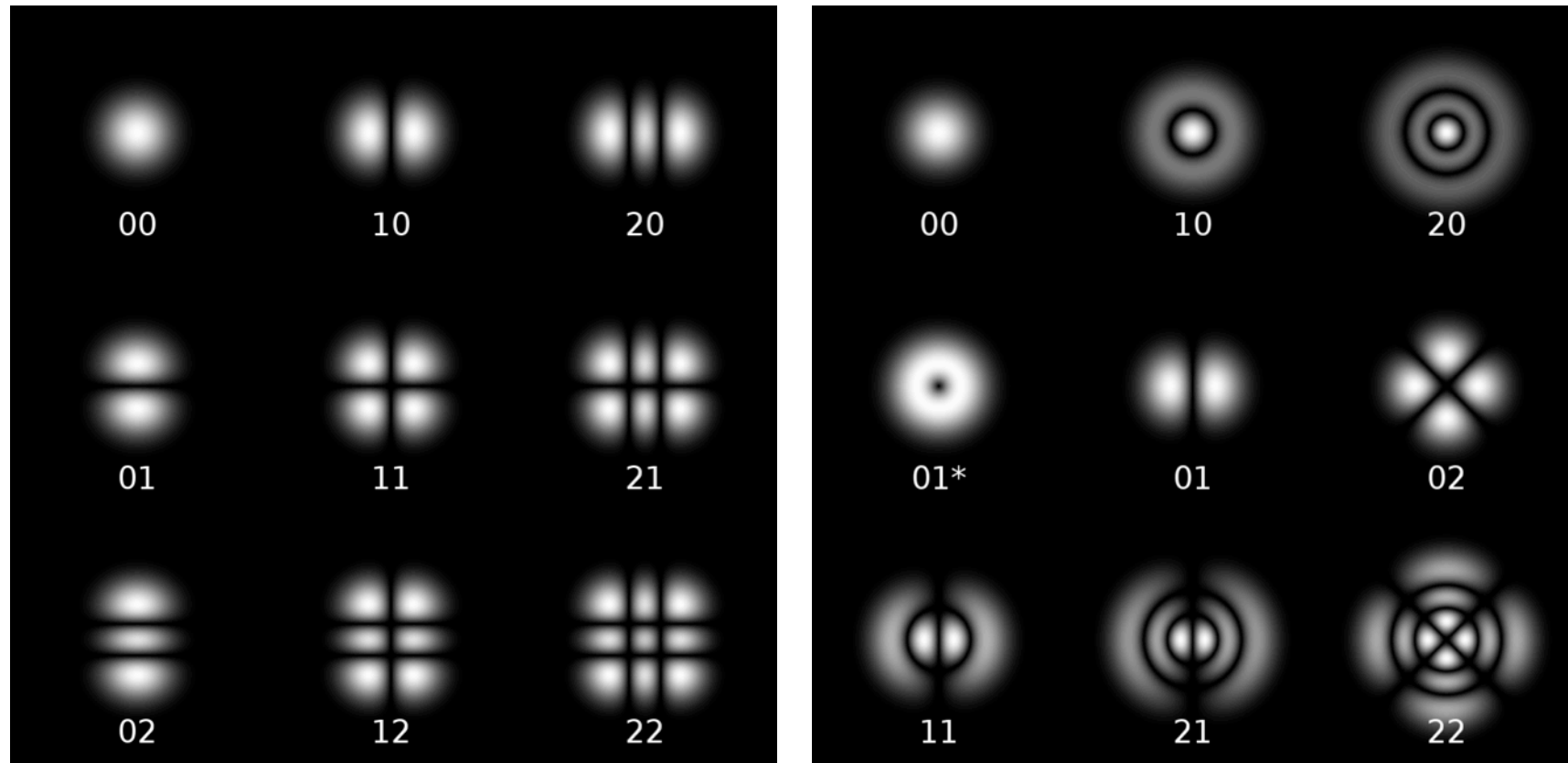
Modal Decomposition in Ptychography

Pierre Thibault & Andreas Menzel, Nature 494 68 (2013)



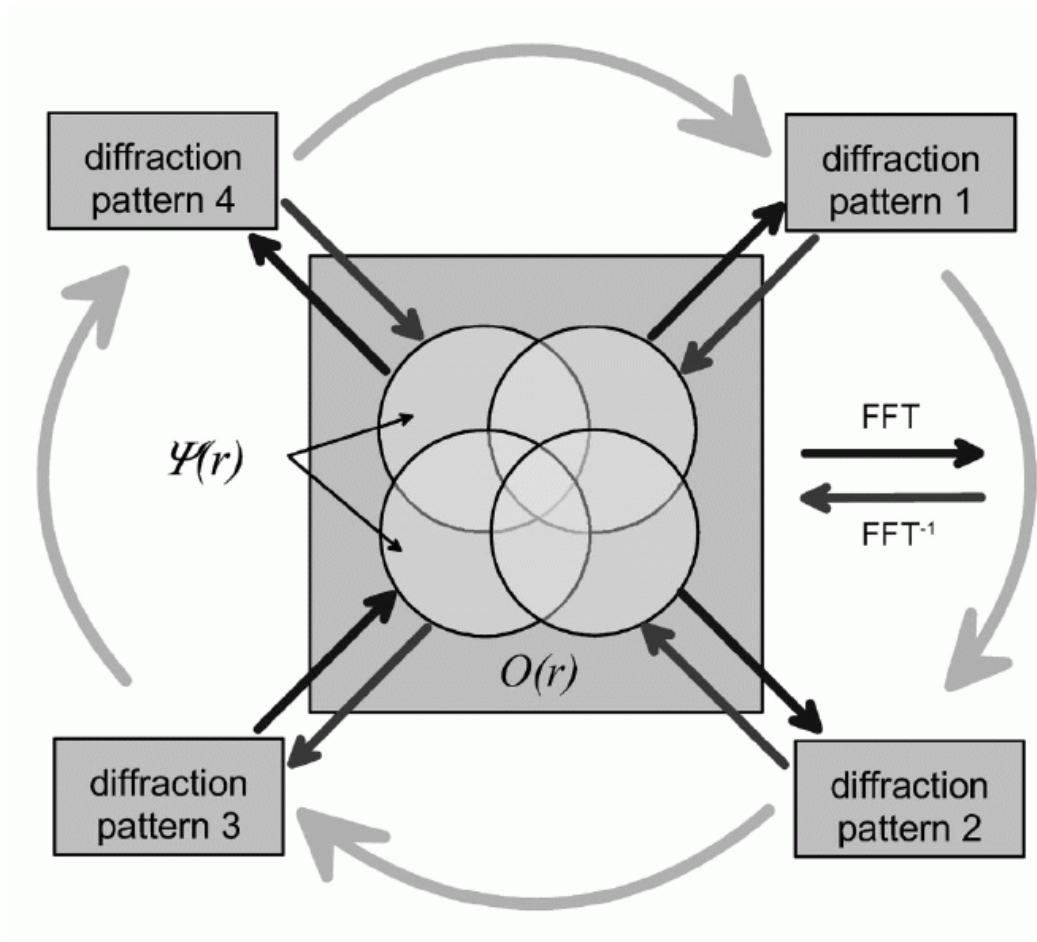


TEM modes: Laguerre-Gaussian



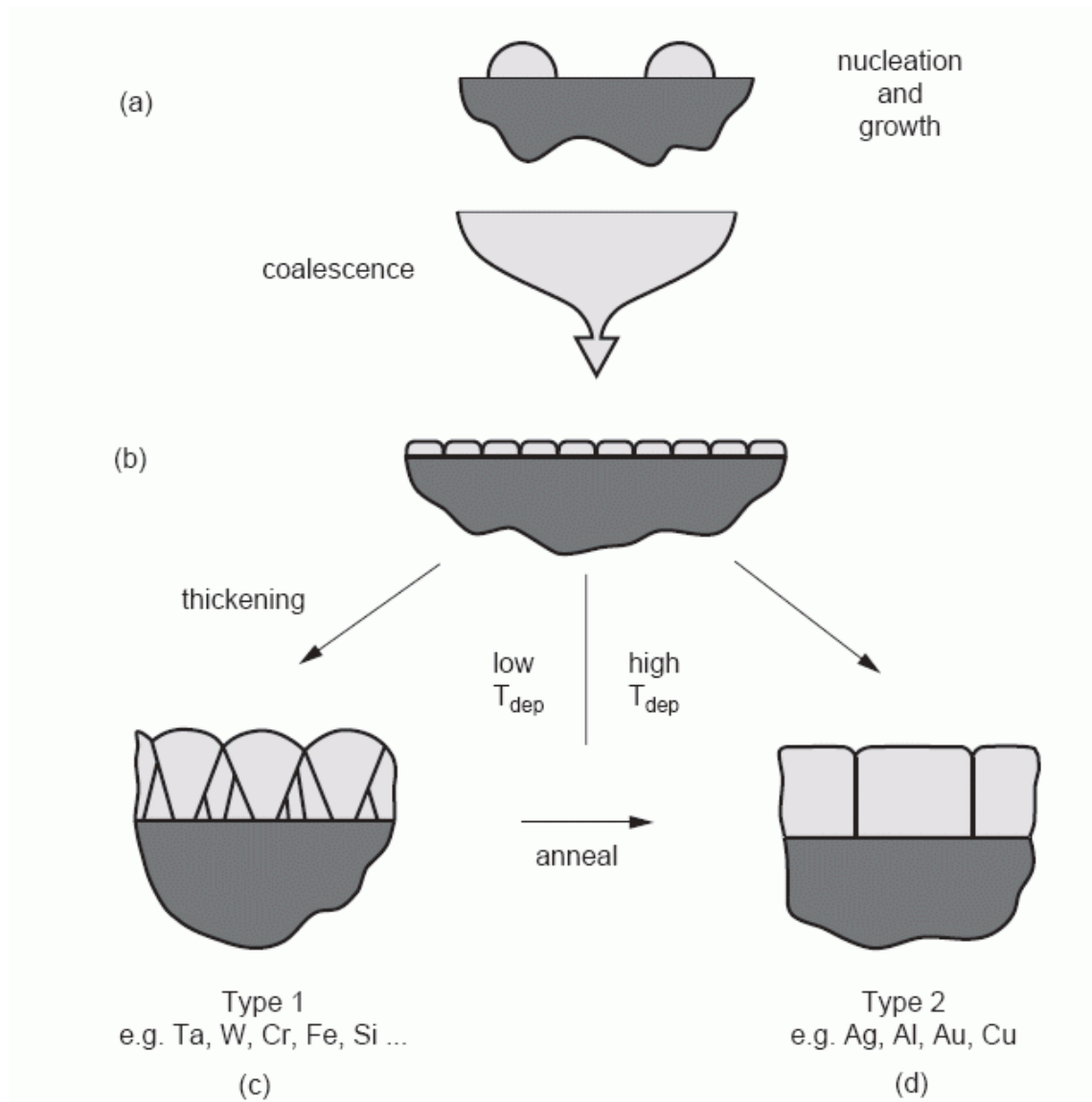
X-ray Ptychography

J. Rodenburg et al, PRL 98, 034801 (2007)

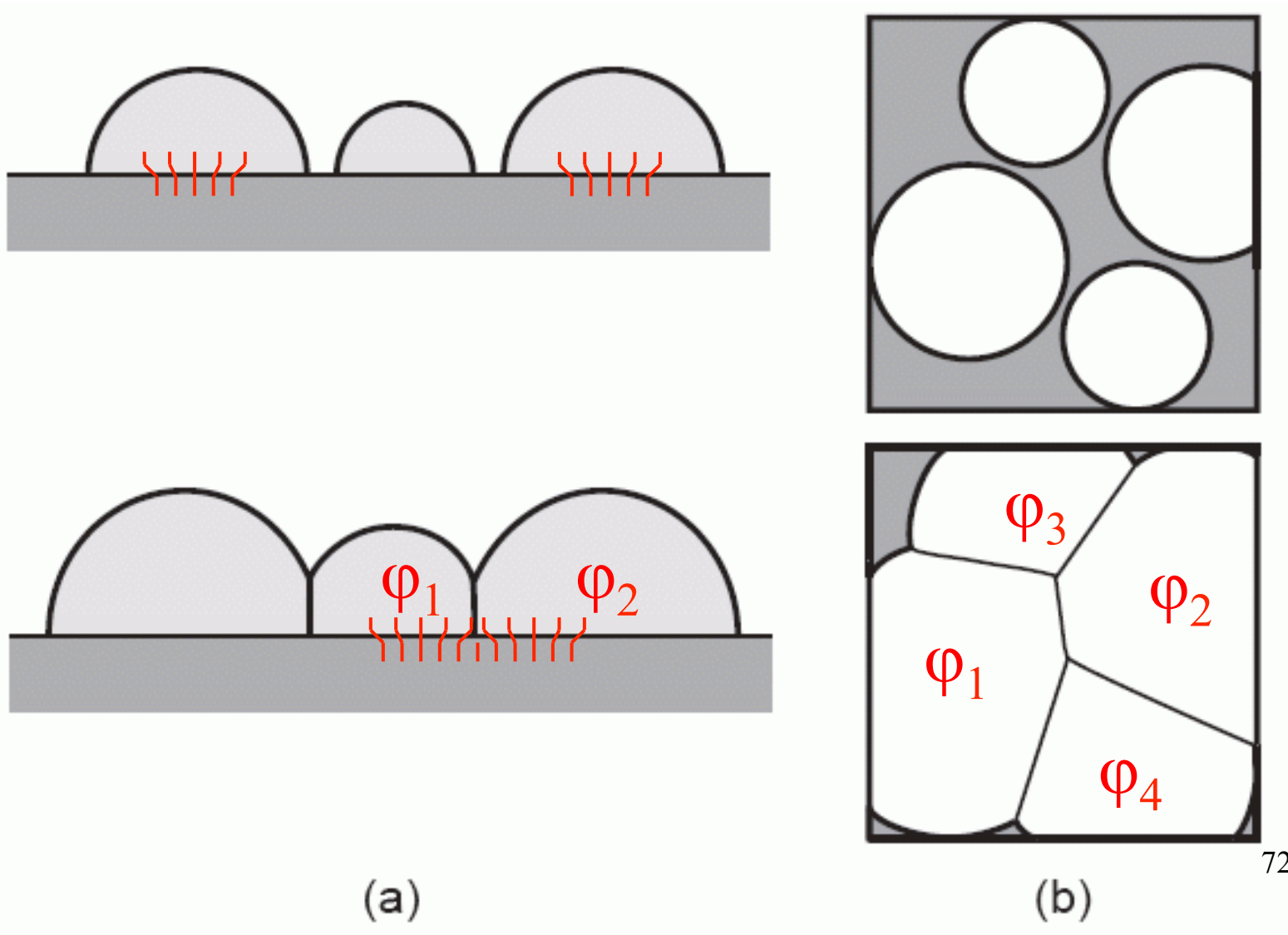


Thin film growth after deposition

C. V. Thompson, Annu. Rev. Mater. Sci. 2000. 30:159–90



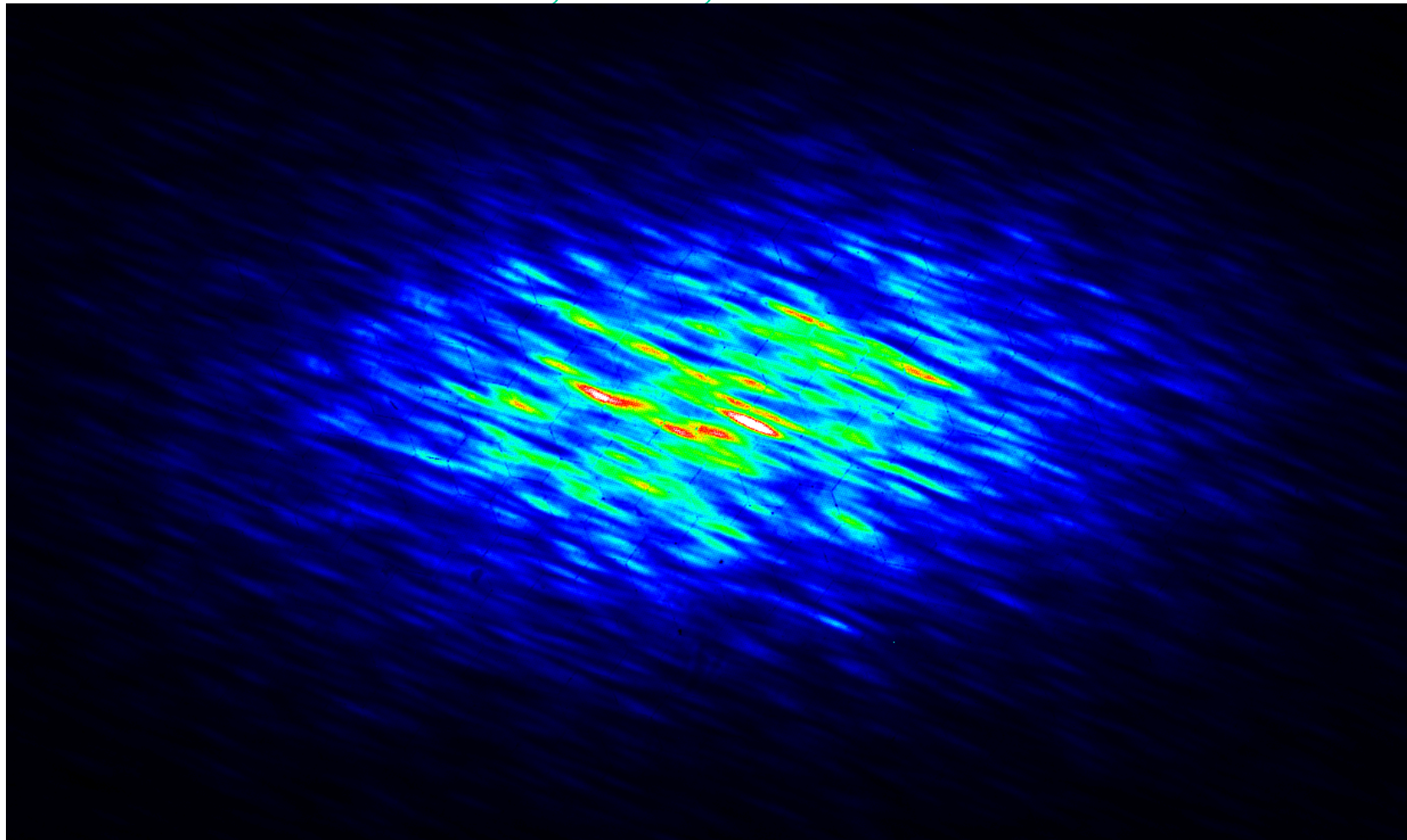
Epitaxial growth effects



Niobium (110) Thin Film Grains

1 μm steps across 3 μm beam of KB mirror focus

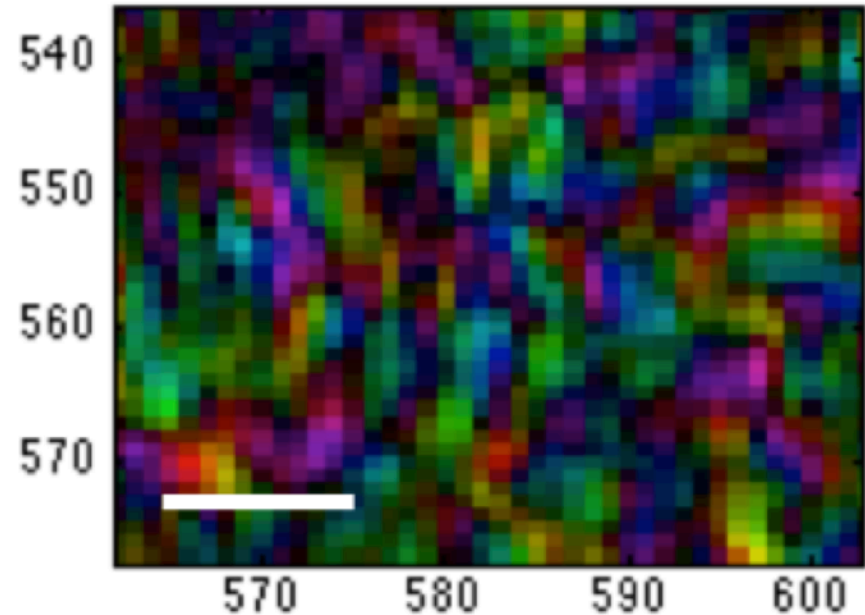
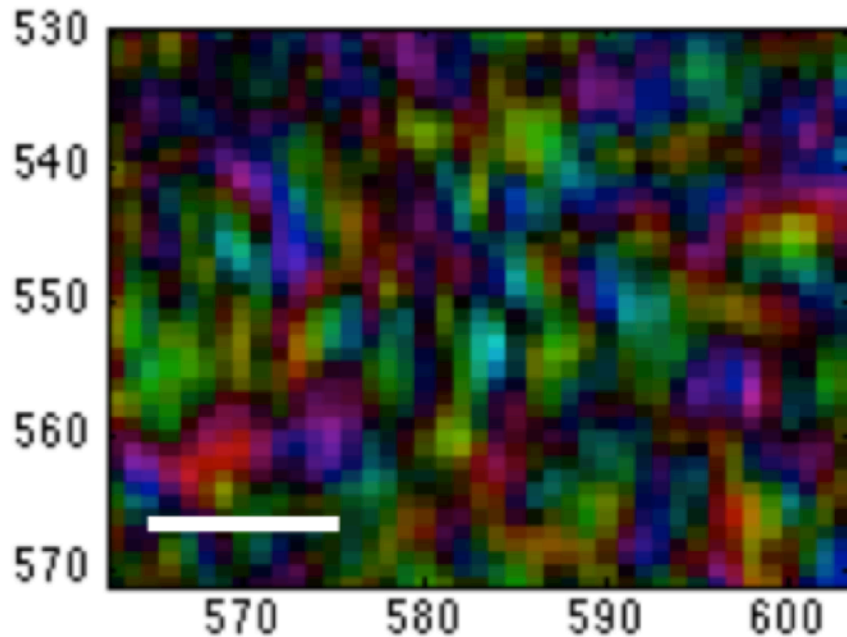
Richard Bean, I-16, Nb110-35 Jan 2009



Reconstruction of Nb domains

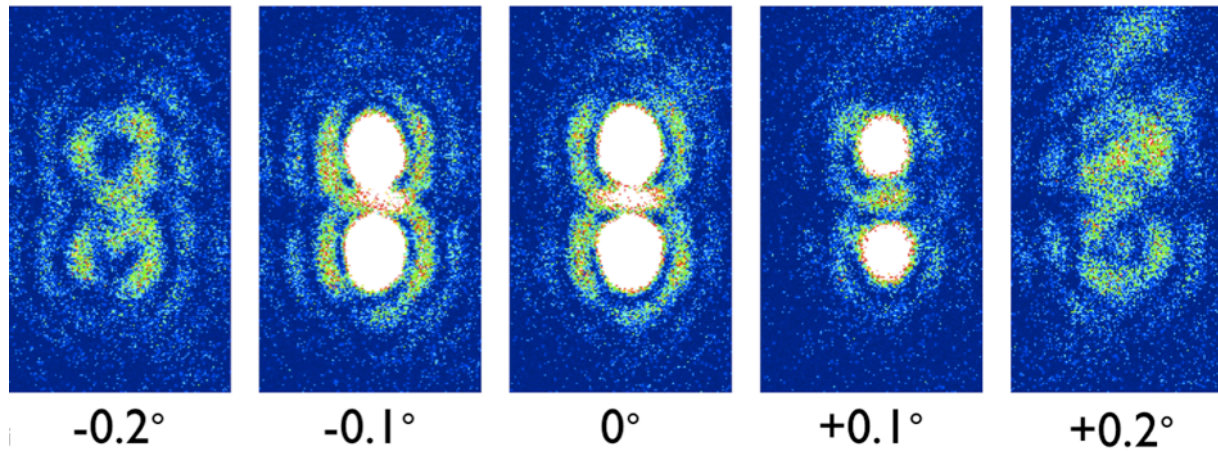
Nicolas Burdet, PhD Thesis (2015)

Scale bar = 150nm; multiple illumination modes

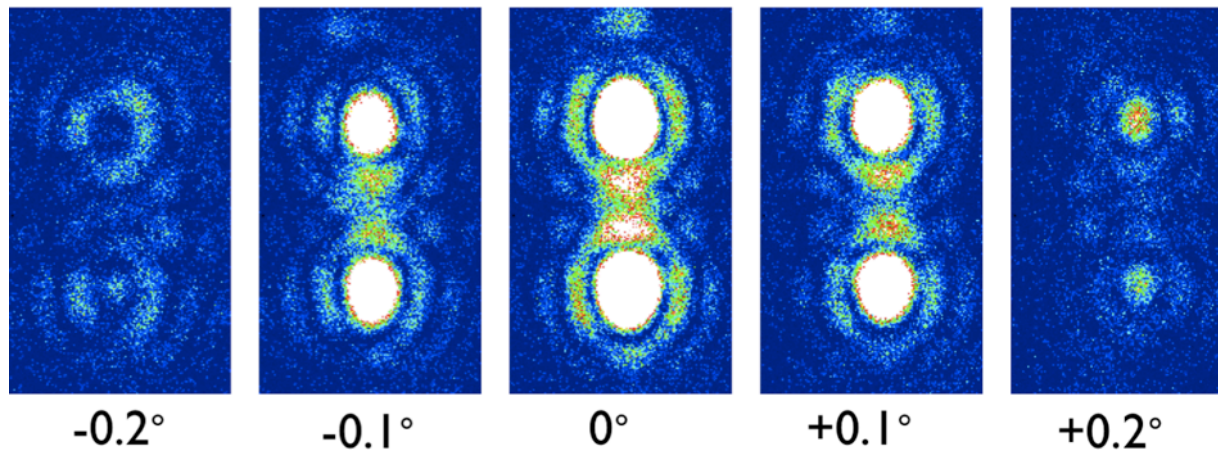


Au nanocrystal, doubled CXD

Au606-49, $\alpha_i = 0.1^\circ$

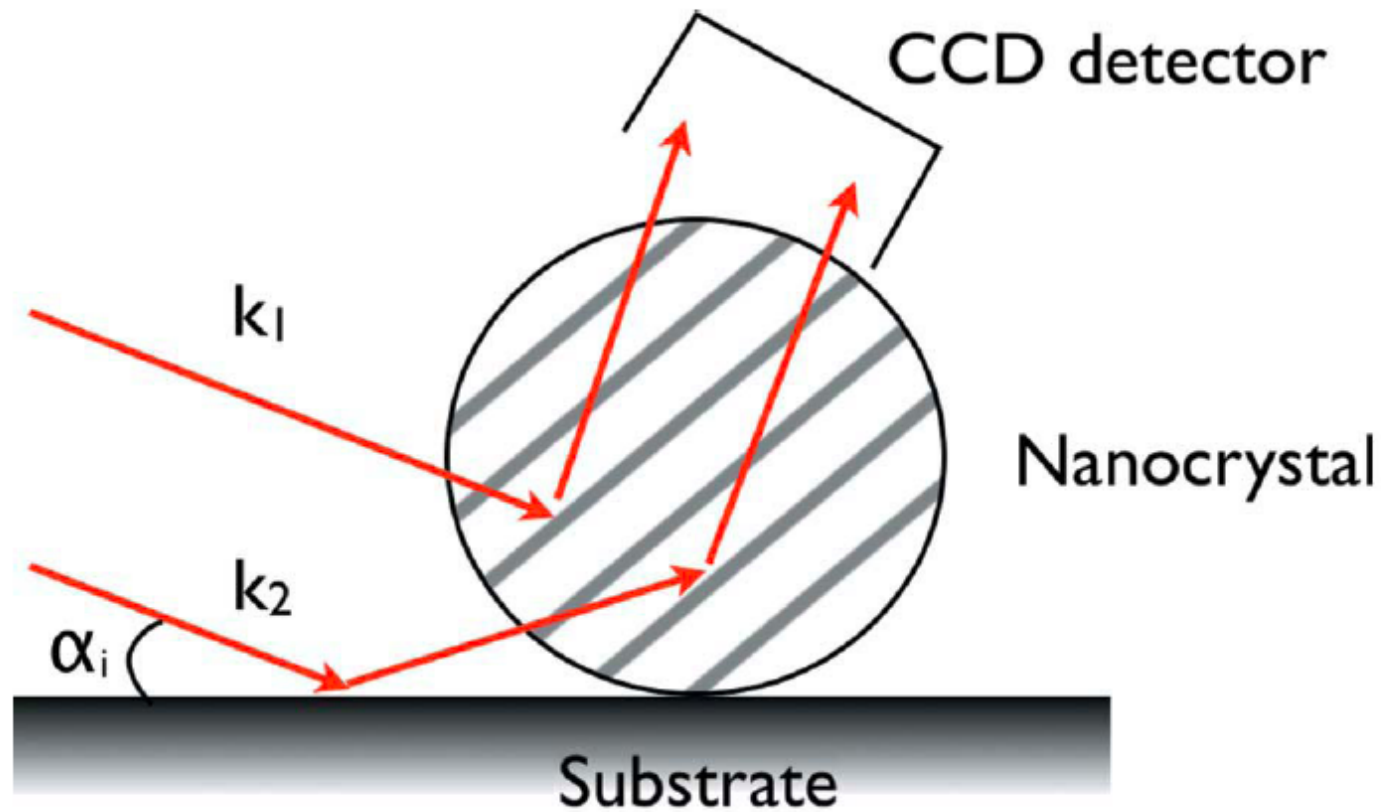


Au606-51, $\alpha_i = 0.15^\circ$



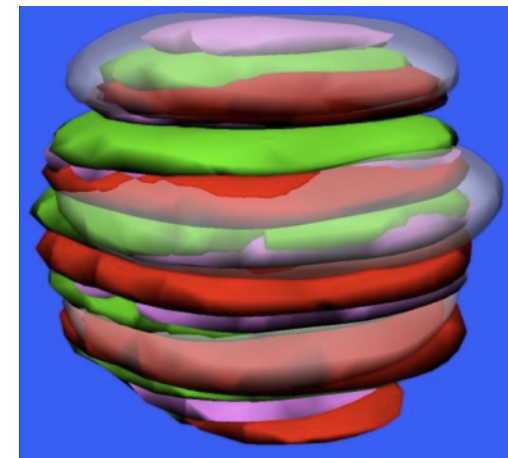
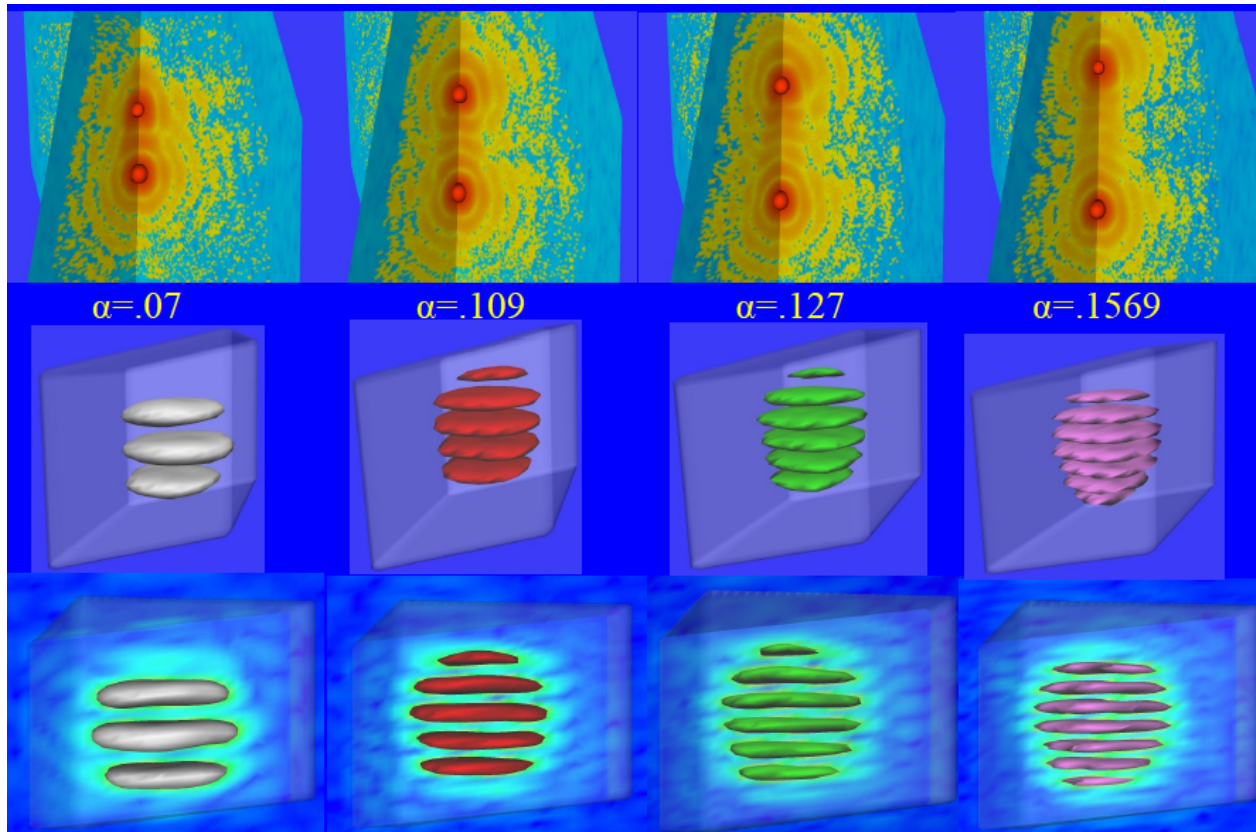
Standing Wave Illumination

Piotr Gryko et al, JSR 14 471-476 (2007)



Reconstructed Au images

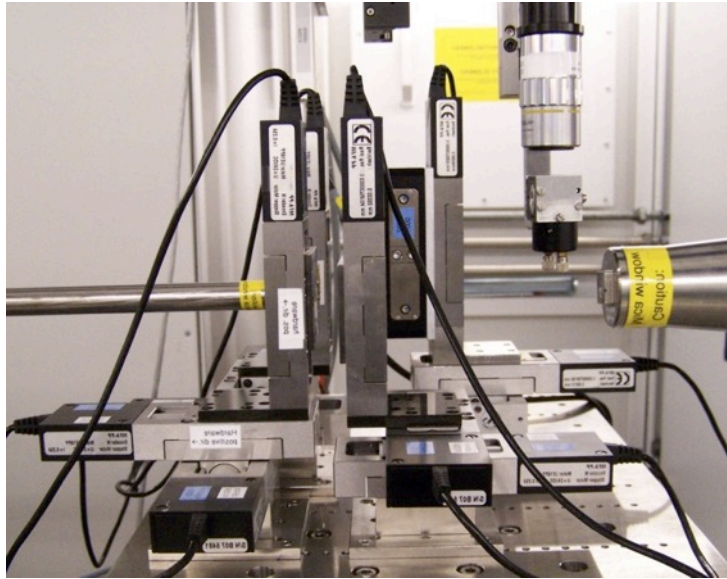
$$\alpha_i = 0.07, 0.11, 0.13, 0.16$$



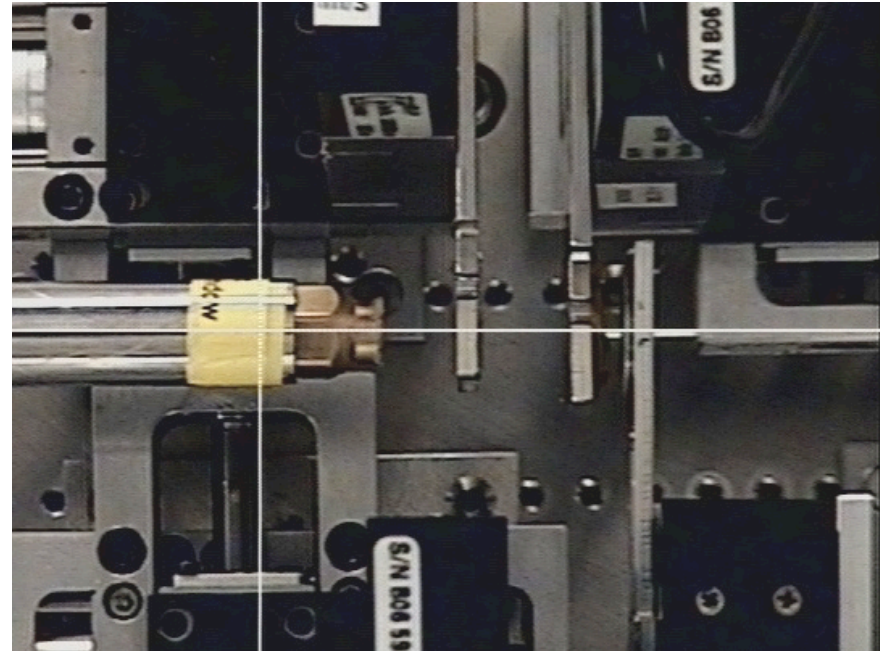
Coherent X-ray Scattering

- I. Coherence
- II. Measuring Coherence
- III. Coherent Imaging Modes
- IV. Ptychography
- V. Experimental methods**

Experimental setup cSAXS (SLS)



Side view



Top view (zoomed in)

XPP working environment

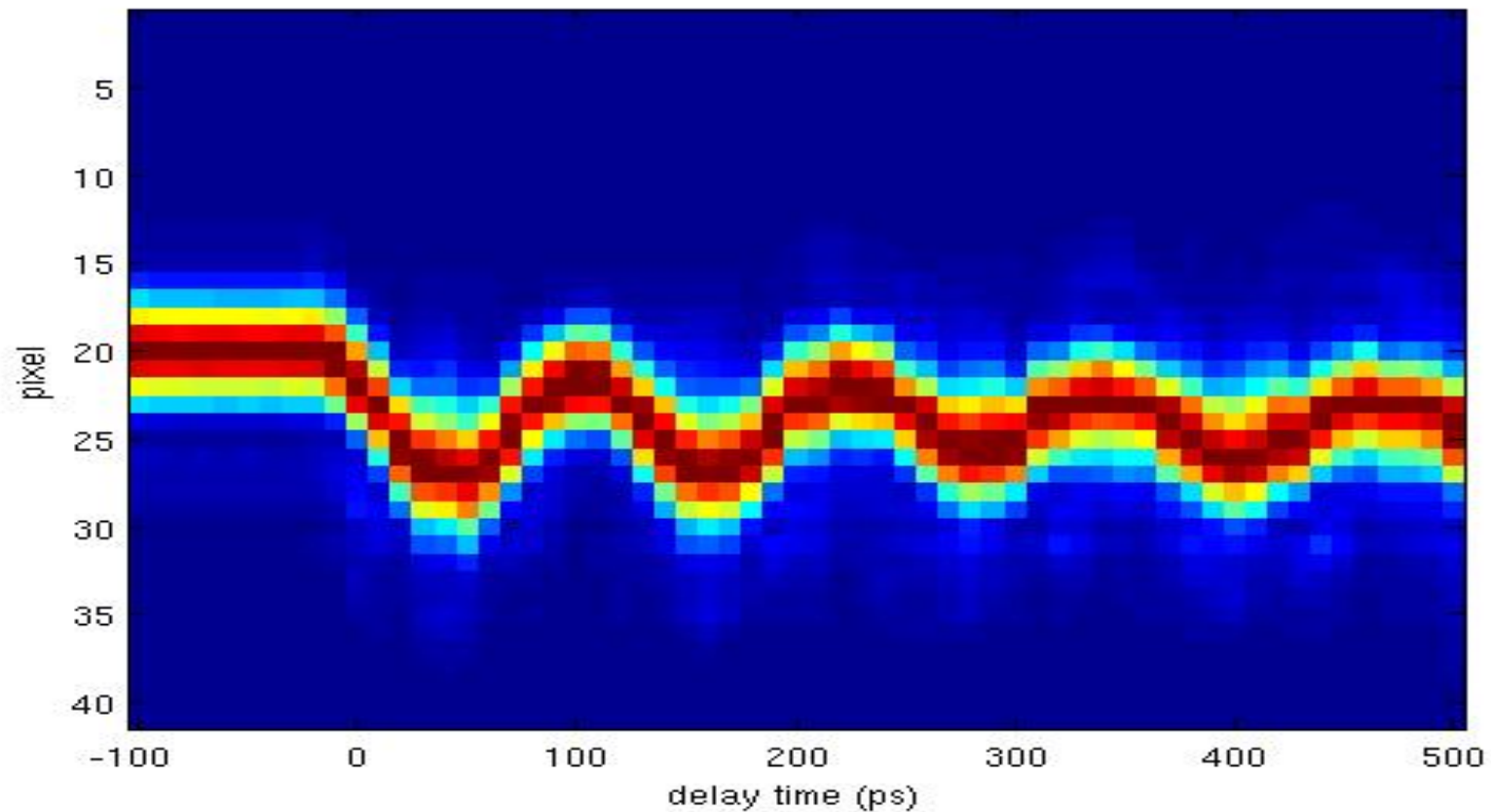


Coherent X-ray Scattering

- I. Coherence
- II. Measuring Coherence
- III. Coherent Imaging Modes
- IV. Ptychography
- V. Experimental methods

Au Pump-probe at LCLS (XPP)

Justin Wark, Loren Beitra, Alexander Korsunsky, Ross Harder, David Fritz ,
Sebastien Boutet, **Jesse Clark**, Garth Williams, Brian Abbey, Andy Higginbotham,
Diling Zhu, Henrick Lemke, Mattieu Chollet, Marc Messerschmidt



“Two-temperature” model

I.K. Robinson et al, Journal of Optics **18** 054007 (2016)

J.K. Chen et al, Int J. Heat Transfer **49** 307 (2006)

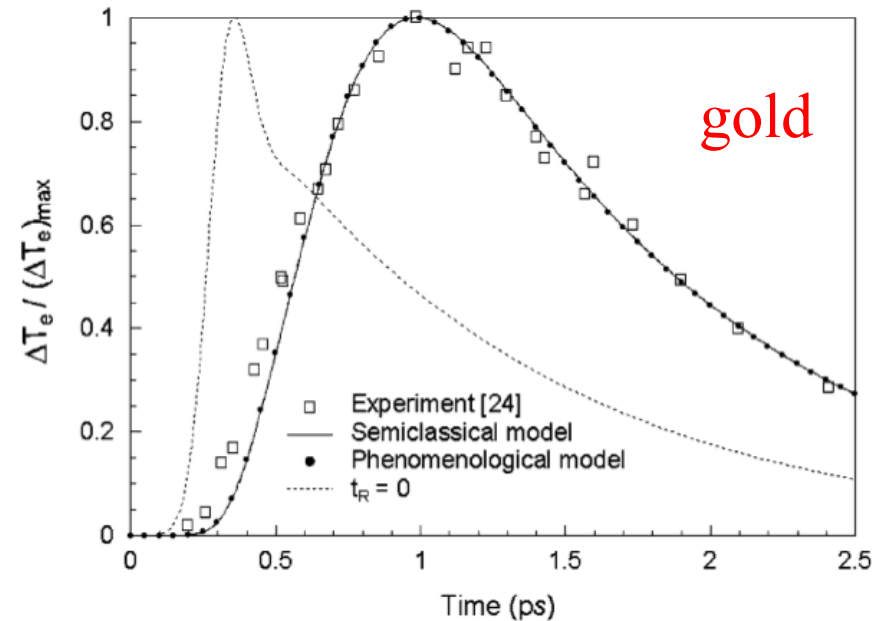
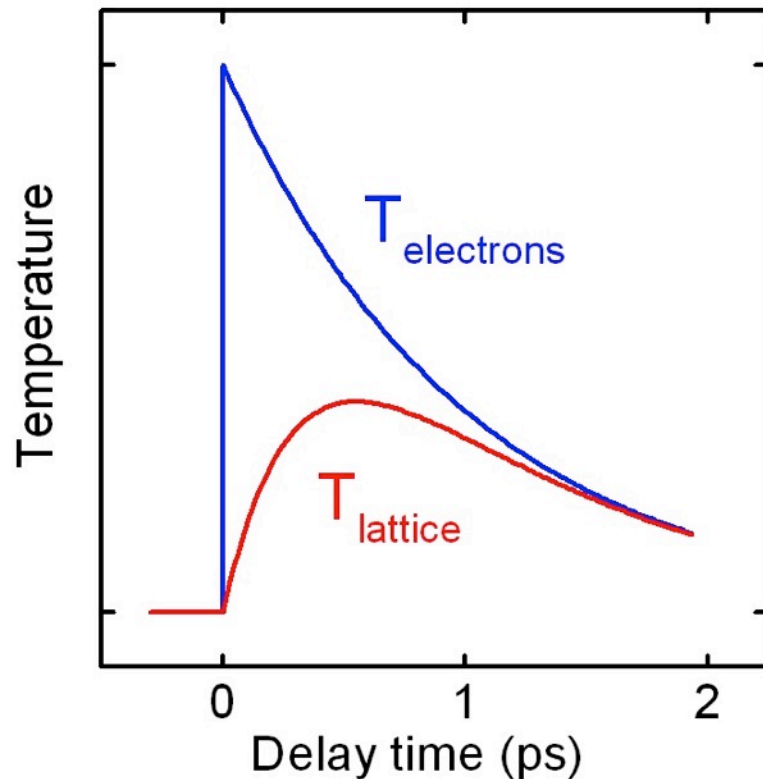
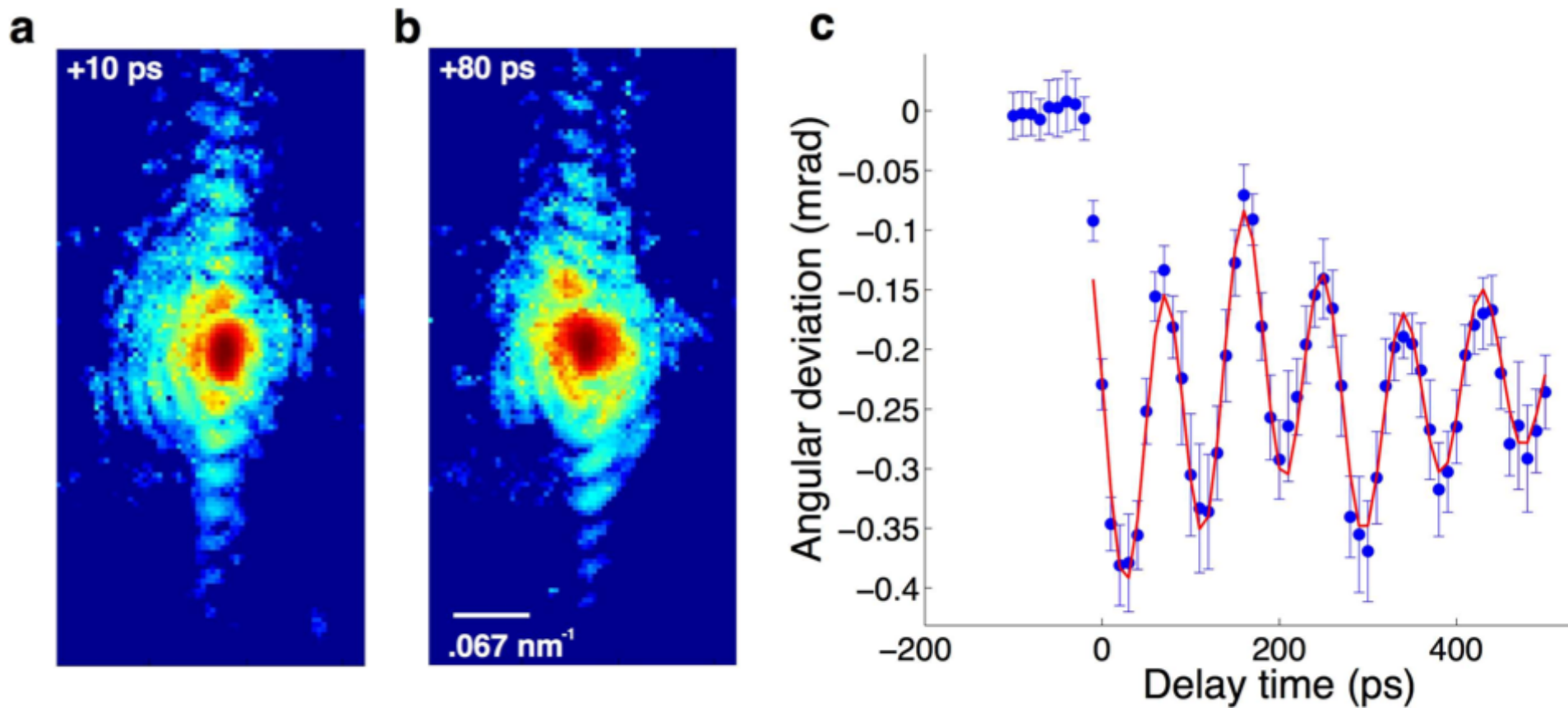


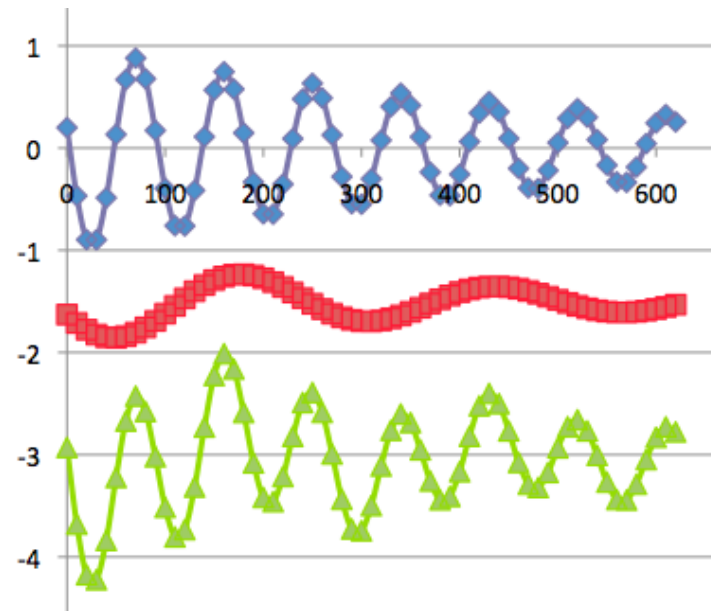
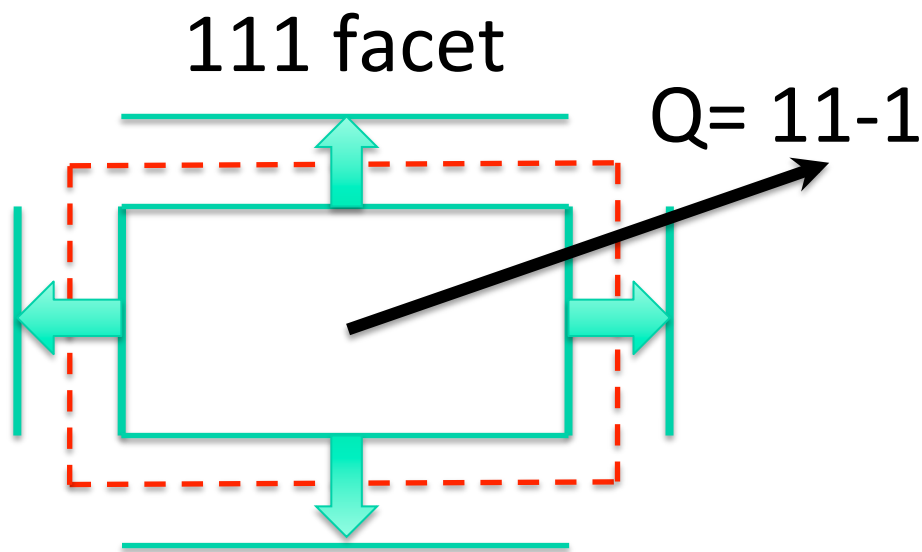
Fig. 2. Comparison of the change in electron temperature at the front surface of an 80-nm gold film irradiated by a 2.8 mJ/cm², 800 nm, 150-fs laser pulse.

Time resolved Bragg peak position



Two Normal Modes of Vibration

$$S(\tau) = \sum_{n=1}^N A_n \exp[-(\tau/\tau_{d,n})^2] \cos(\omega_n \tau + \varphi_{0,n})$$

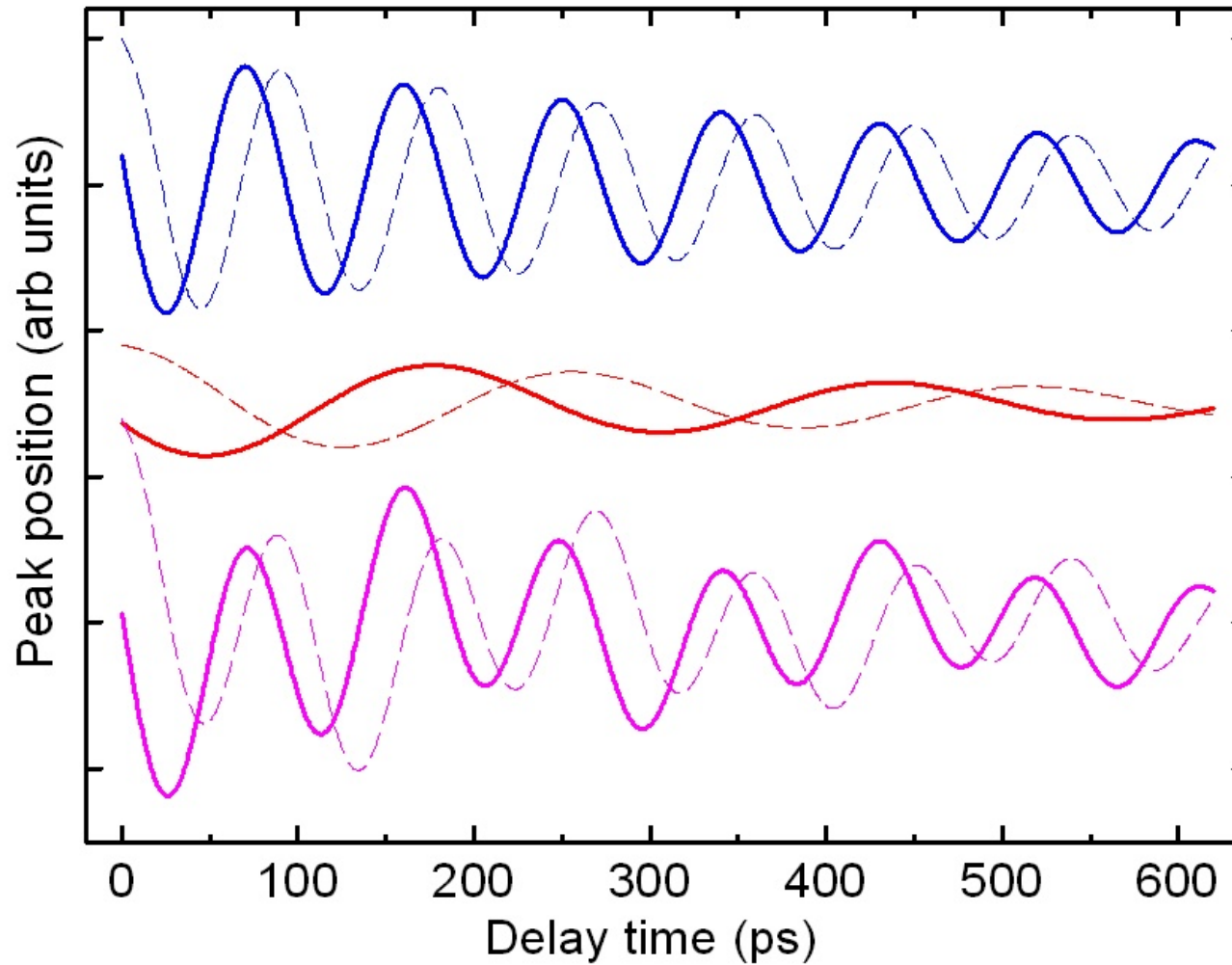


$$T_1 = 90\text{ps} \quad h_1 = 145\text{nm} \quad c_s = 3240\text{ m/s}$$

$$T_2 = 259\text{ps} \quad h_2 = 420\text{nm}$$

Phase Origin of Vibrations

I.K. Robinson et al. Journal of Optics 18 054007 (2016)

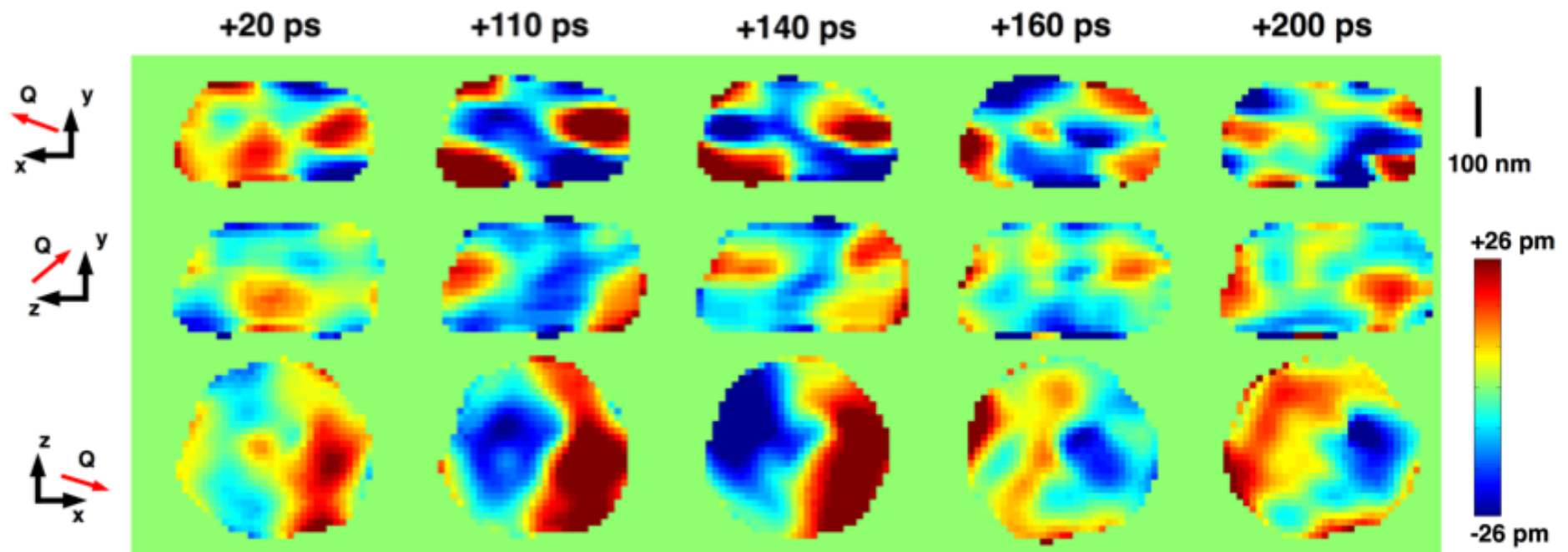


Dynamic imaging of displacements

CDI inversion of 3D diffraction patterns

1000 frames averaged at each point of rocking curve

Jesse Clark et al, Science **341** 56 (2013)

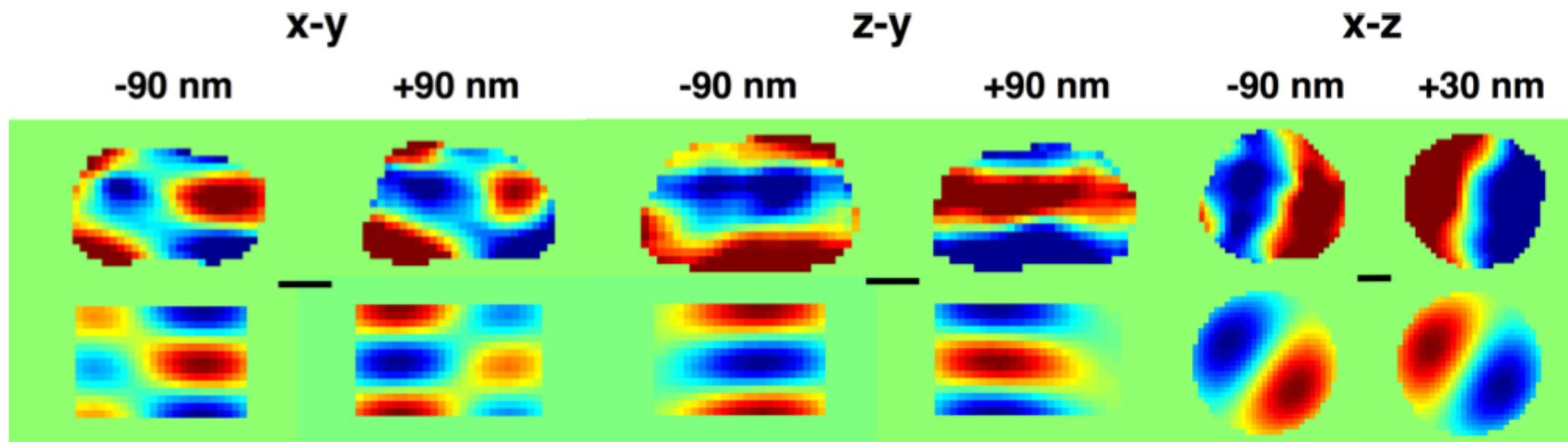


Dynamic imaging of displacements

CDI inversion of 3D diffraction patterns

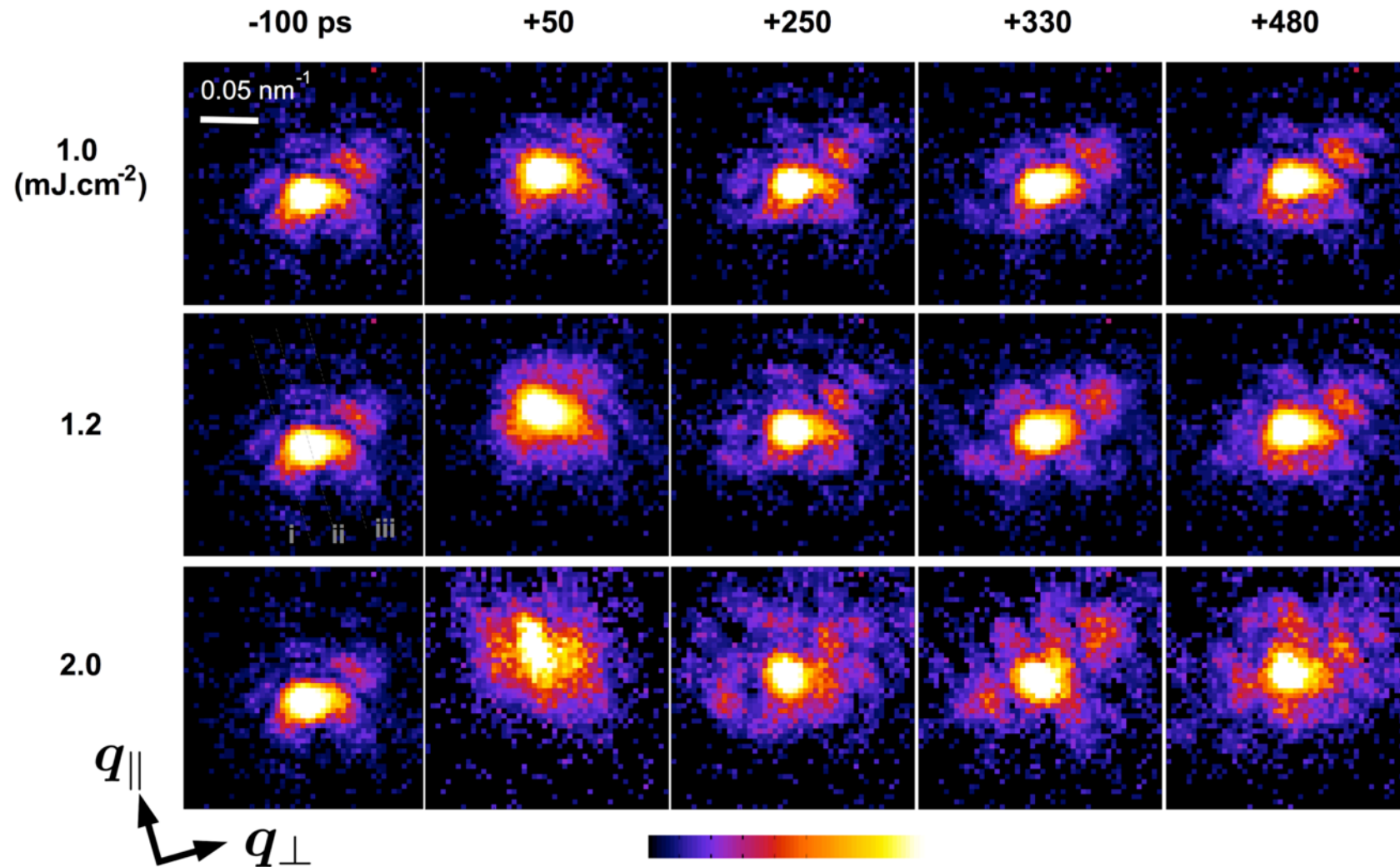
Comparison with (1,1) normal mode of cylinder

Jesse Clark et al, Science **341** 56 (2013)



Dependence on Laser Fluence

Jesse Clark et al, PNAS 112 7444 (2015)



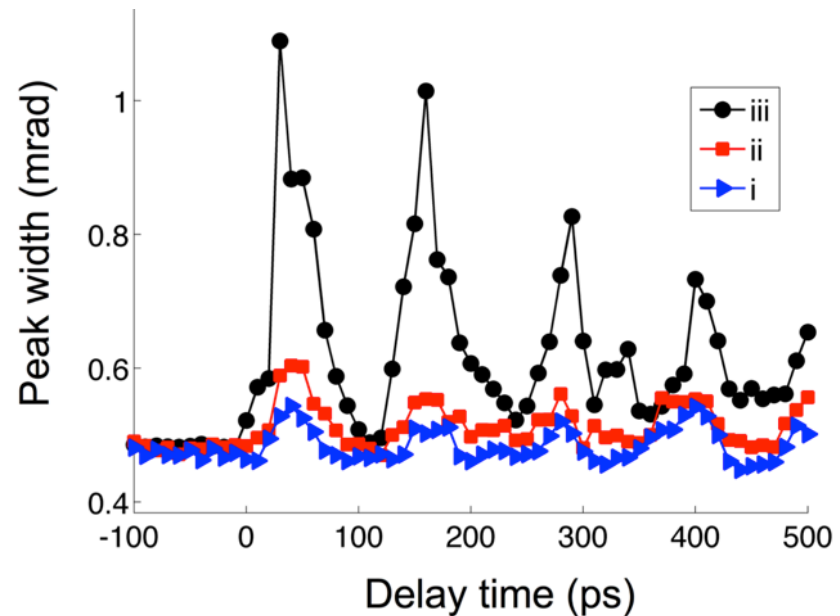
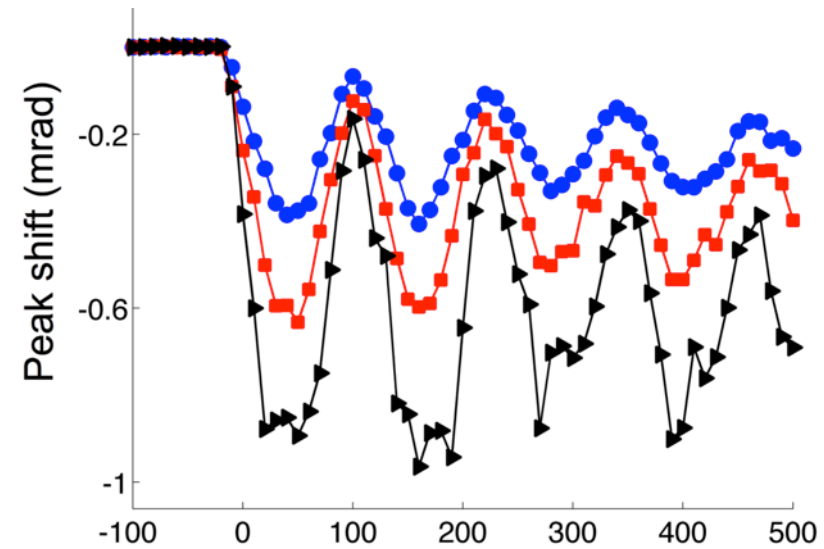
Dependence on Laser Fluence

Jesse Clark et al, PNAS
112 7444 (2015)

1.0 mJ cm⁻²

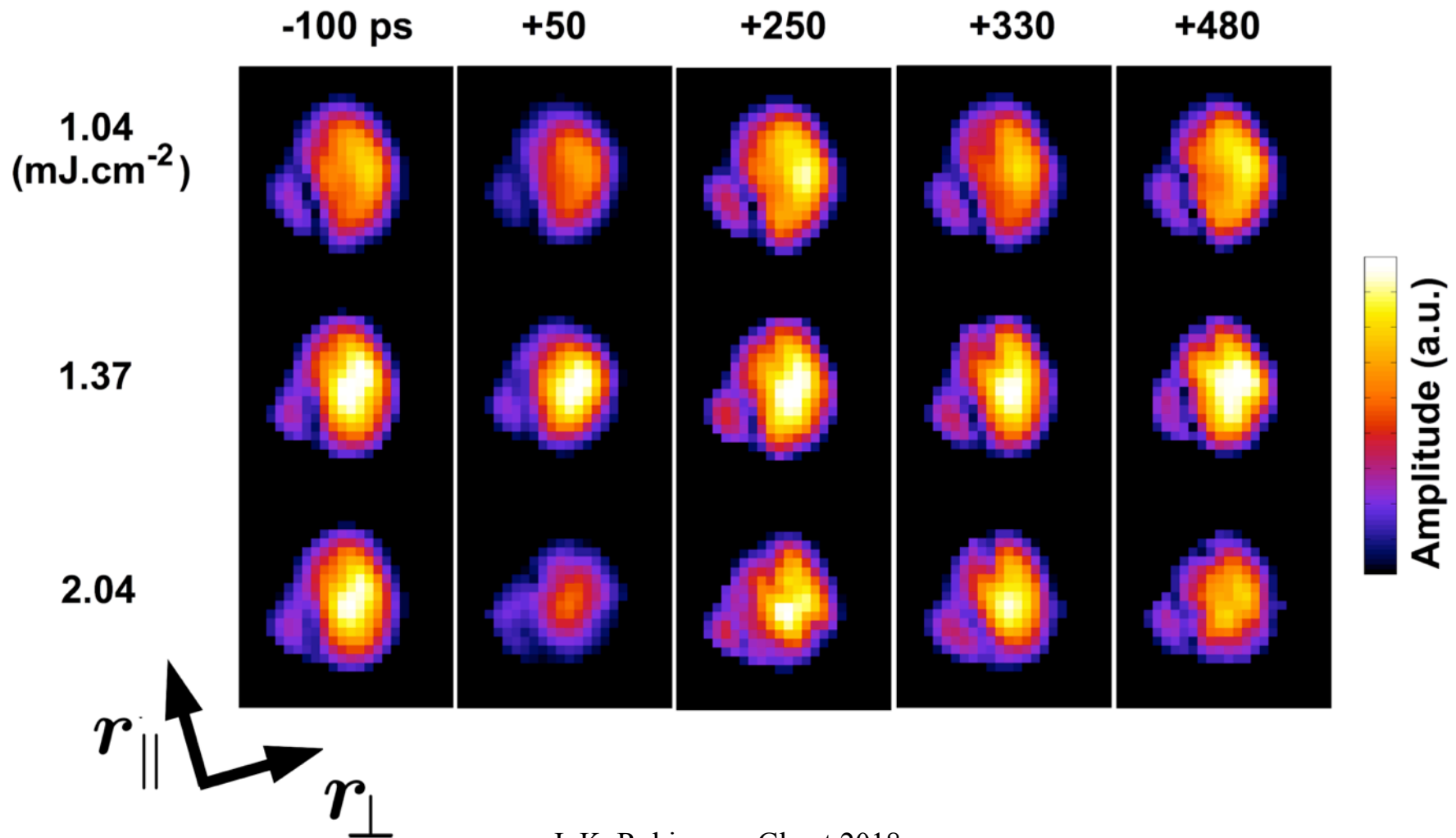
1.4 mJ cm⁻²

2.0 mJ cm⁻²



Dependence on Laser Fluence

Jesse Clark et al, PNAS **112** 7444 (2015)

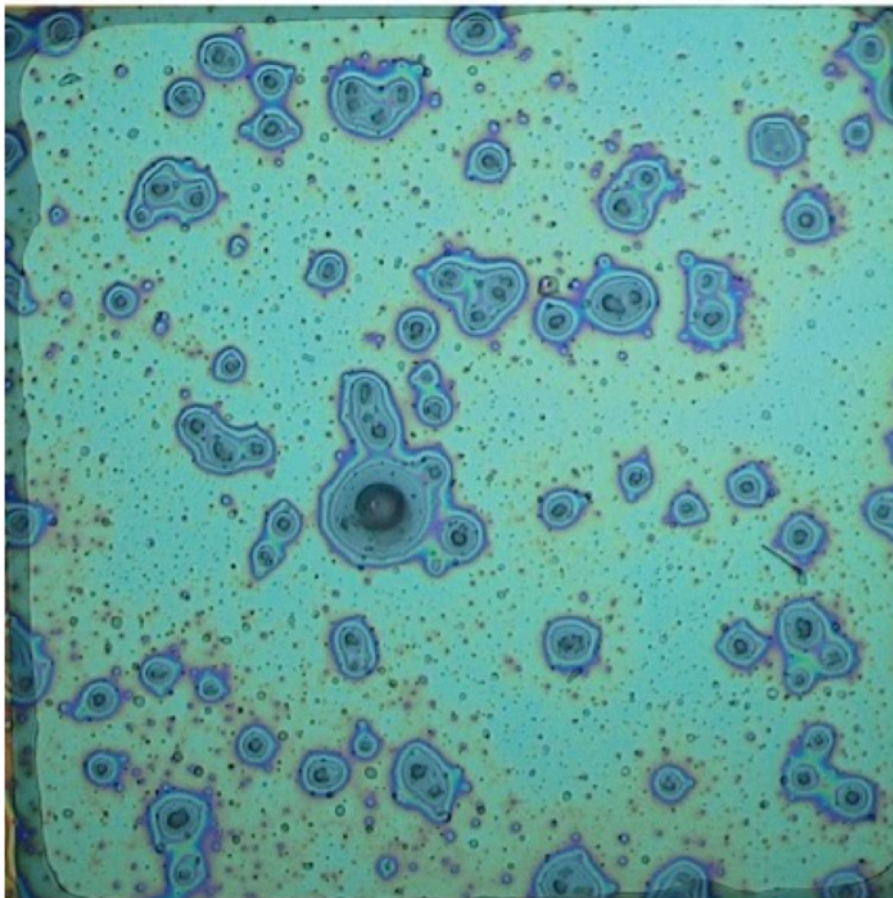


Before and after X-ray exposure

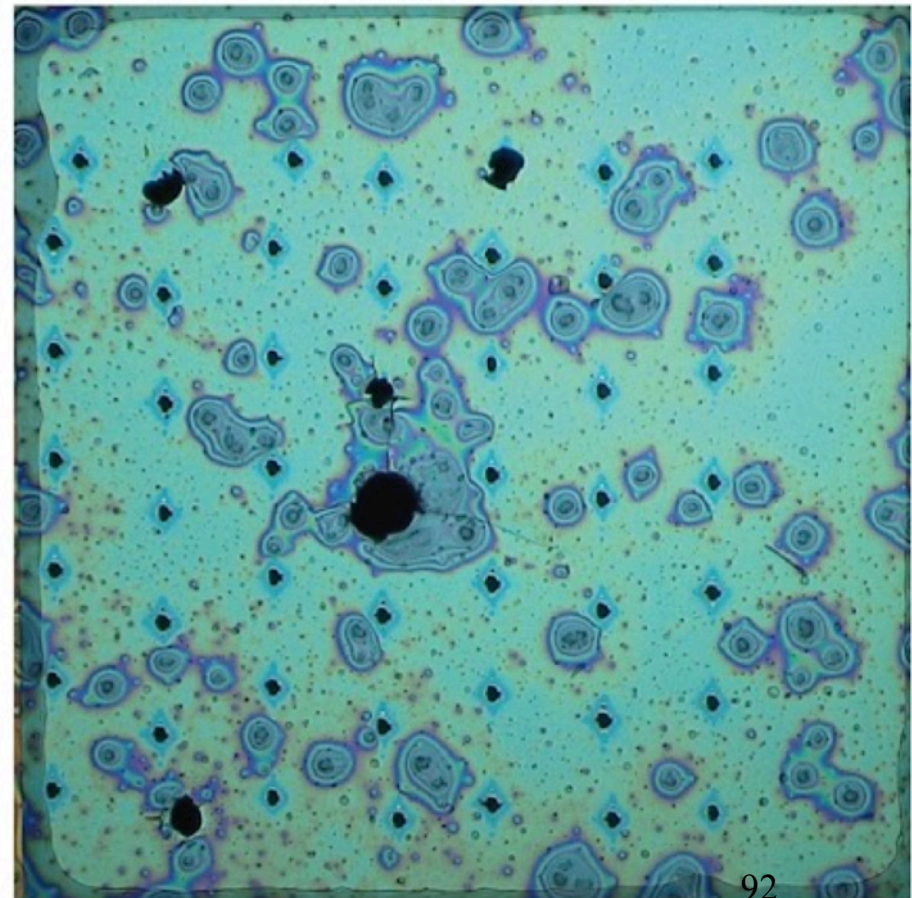
SACLA, June 2015

K4 bl 14-27

Before

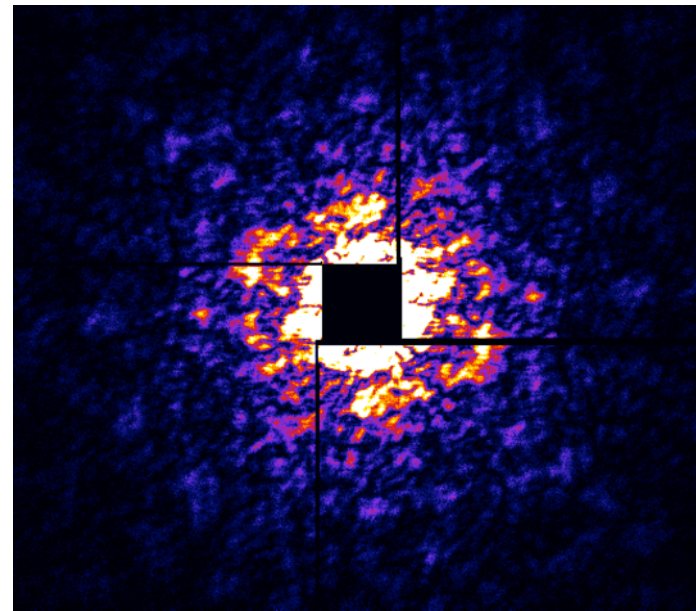
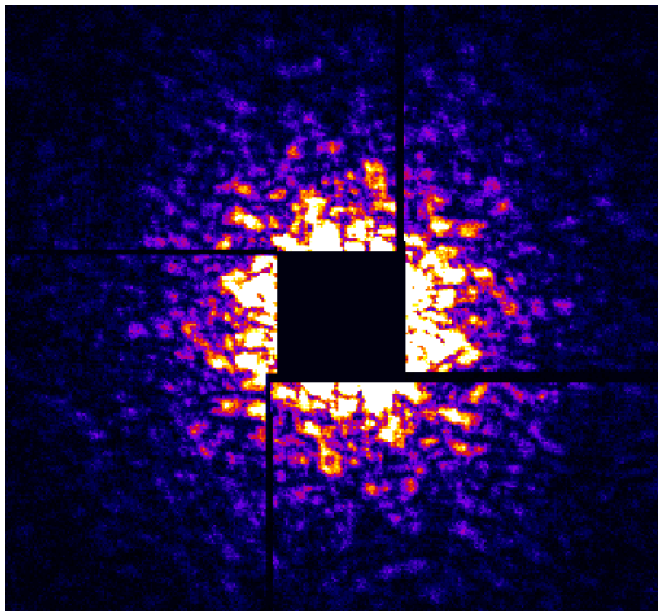


After



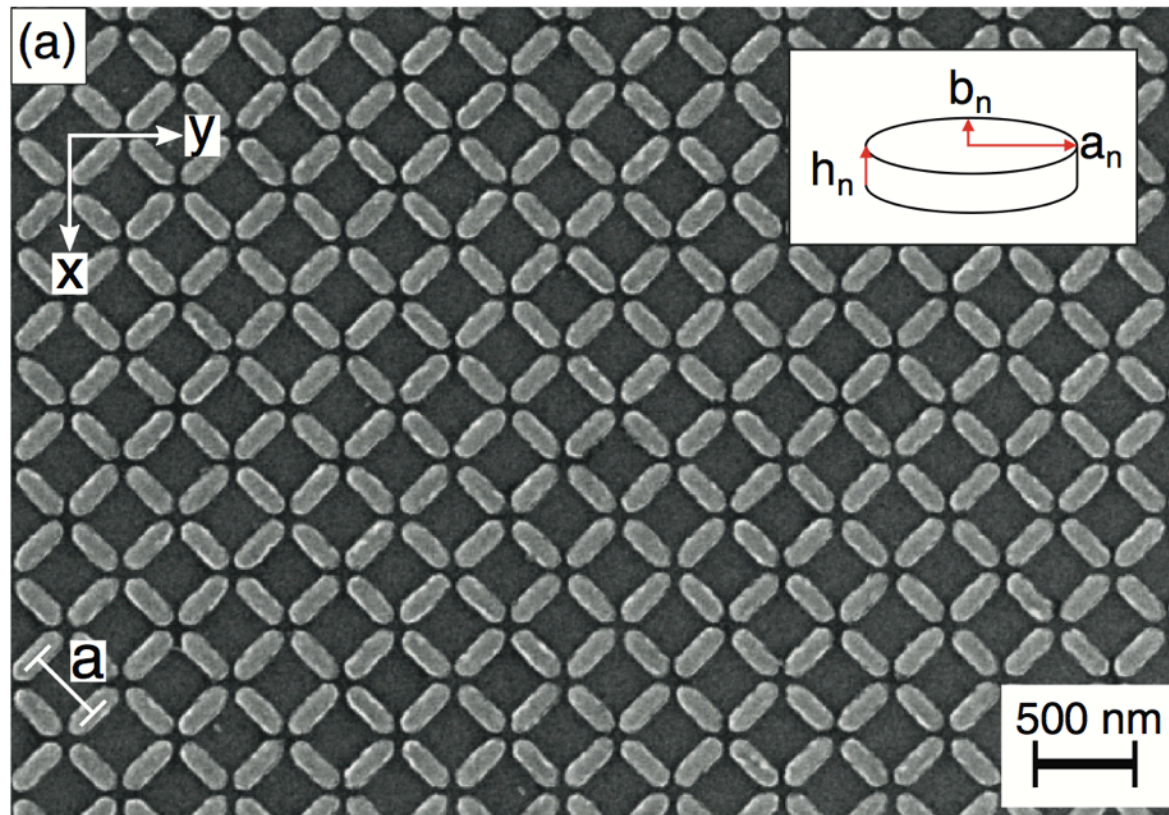
Human Chromosome Sample M2 340600

J. Schwenke, F. Zhang, Y. Mohammed, C. Song, K. Fukui, SACLA



Artificial Spin Ice using HHG?

Perron et al PHYSICAL REVIEW B **88**, 214424 (2013)



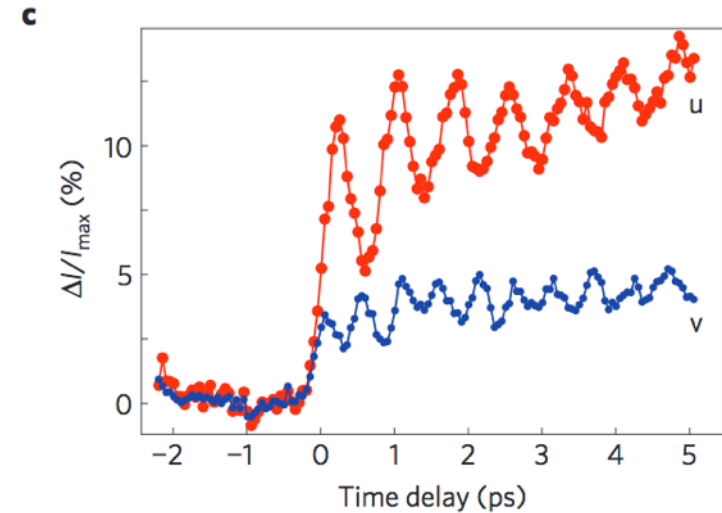
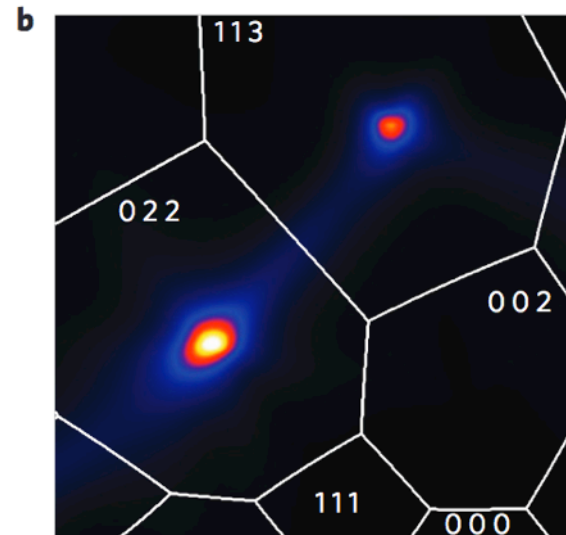
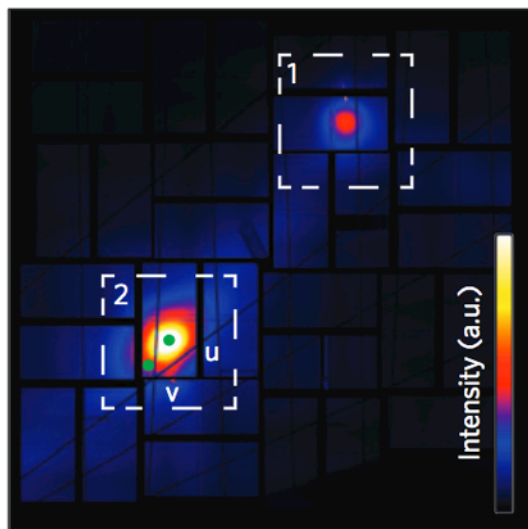
Artificial Spin Ice using HHG?

- Fe M-edge at 62eV
- Resonant coupling to d-orbitals
- Polarisation sensitive to magnetism
- Ultrafast magnetisation dynamics

Phonons mapped in time domain

M. Trigo et. al. Nature Physics **9** 790 (2013)

Ge(001) single crystal



Bragg Coherent Diffraction Imaging

- Complex density can image strain
- Strain associated with nano-shape
- Phase domains in $\text{La}_{0.5}\text{Ca}_{0.5}\text{MnO}_3$
- Collagen and virus imaging
- Ultrafast snapshots of vibrations
- Transient melting of nanoparticles